جامعة الملك سعود
King Saud University

CMSA
المؤتمر السادس لعلوم الرياضيات وتطبيقاتها
The 6th CMSA 2025

6th Conferenceon Mathematical Scienceand Applications

List of Abstracts for 6th-CMSA-2025

King Saud University & SAMS, April 15-17, 2025

Contents

1 Introduction

The **Saudi Association for Mathematical Sciences** (SAMS) hosts a biennial international conference aimed at advancing research in mathematics and its diverse applications within the Kingdom of Saudi Arabia. This event serves as a vital platform to showcase current research, foster collaboration, and promote the exchange of knowledge between local and international scholars. It is designed to provide opportunities for a wide range of researchers, from early-career academics to seasoned experts, to present their work, explore cutting-edge mathematical methodologies, and engage with globally recognized scientists across multiple disciplines.

Over the years, SAMS has successfully organized more than eleven such conferences, each highly praised for its scientific merit and outstanding organizational standards. These conferences have significantly contributed to the development of the mathematical sciences community in the region.

As part of its continued commitment to scientific excellence, SAMS is pleased to organize the **6^{th} International Conference on Mathematical Sciences and Applications** (6^{th}CMSA2025), which will be held at **King Saud University in Riyadh** from April 15 to 17, 2025. This conference aims to further strengthen international cooperation and enrich the academic environment for mathematics in Saudi Arabia and beyond.

1.1 Objectives for 6^{th} CMSA 2025

- Present and discuss recent significant findings in pure and applied mathematics.
- Promote Knowledge Sharing by fostering the exchange of cutting-edge research, innovative methodologies, and novel applications in mathematical sciences among researchers, practitioners, and educators from around the world.
- Encourage Interdisciplinary Collaboration by facilitating collaborations between mathematicians and professionals from diverse fields such as engineering, physics, computer science, actuarial science, finance, and biology to solve complex real-world problems.
- Highlight the latest trends, advancements, and future directions in various branches of mathematical sciences, including applied mathematics, theoretical mathematics, and computational mathematics.
- Provide a platform for young researchers and graduate students to present their work, receive constructive feedback, and network with established experts in the field.
- Explore the role of mathematical sciences in addressing global challenges such as climate change, healthcare, and sustainable development, and promote the development of mathematical models and solutions to these issues.
- Build and strengthen professional networks among attendees, fostering long-term relationships that can lead to future research collaborations, joint projects, and academic exchanges.
- Promote partnerships between academia and industry to ensure that mathematical research is aligned with industry needs and can be effectively translated into practical applications.
- Provide a platform for the dissemination of high-quality research findings through keynote speeches, panel discussions, paper presentations, and poster sessions.

1.2 Steering Committee

- Prof. Dr. Bandar Almohsen, King Saud University (Chair)
- Dr. Reem Alhefthi, King Saud University
- Prof. Dr. Obaid Algahtani, King Saud University
- Prof. Dr. Mhamed Eddahbi, King Saud University
- Mr. Ahmed Ameri, Riyadh Education Administration.

1.3 Organizing Committee

- Dr. Reem Alhefthi, King Saud University (Chair)
- Prof. Dr. Mansoor Alshehri, King Saud University
- Prof. Dr. Nabil Ourimi, King Saud University
- Prof. Dr. Mhamed Eddahbi, King Saud University
- Dr. Wedad Albalawi, Princess Nourah bint Abdulrahman University
- Dr. Zehor Aljehani, Jeddah Education Administration
- Dr. Abdulrahman Alzahrani, King Saud University
- Ms. Amjaad Mousa Alfaifi, King Saud University

1.4 Scientific Committee

- Prof. Dr. Mhamed Eddahbi, King Saud University (Chair)
- Dr. Fawzi Al-Thukair, King Saud University
- Prof. Dr. Souhail Chebbi, King Saud University
- Dr. Hocine Guediri, King Saud University
- Dr. Malik Talbi, King Saud University
- Prof. Dr. Diogo Gomes, King Abdullah University of Science and Technology
- Prof. Dr. Jinchao Xu, King Abdullah University of Science and Technology
- Prof. Dr. Ahmad M. Alghamdi, Umm Al-Qura University
- Dr. Brahim Mezerdi, King Fahd University of Petroleum and Minerals
- Dr. Najla Altwaijry, King Saud University
- Prof. Dr. Fairouz Tchier, King Saud University
- Dr. Liana Topan, King Saud University

1.5 Media Committee

- Dr. Reem Alhefthi, King Saud University (Chair)
- Prof. Dr. Mohammed AbaOud, Imam Mohammad Ibn Saud Islamic University (IMSIU)
- Dr. Khalid Alsharif, King Saud University
- Dr. Maha Alammari, King Saud University
- Ms. Wlaa Hussein Aljroudi
- Ms. Munirah Alshalan, King Saud University

2 Abstracts of Keynote Speakers

2.1 Youssef Ouknine: Optimal Stopping Under Model Uncertainty in a General Setting

Youssef Ouknine*
Mohammed VI Polytechnic University, Africa Business School, Ben Guerir,
and Department of Mathematics, Faculty of Sciences Semlalia, Cadi Ayyad University, B.P. 2390, Marrakesh, Morocco.
Joint work with **Ihsan Arharas**[1], **Siham Bouhadou**[2], **Astrid Hilbert**[1]

Abstract

We consider the optimal stopping time problem under model uncertainty

$$R(v) = \operatorname*{ess\,sup}_{\mathbb{P}\in\mathcal{P}} \operatorname*{ess\,sup}_{\tau\in\mathcal{S}_v} E^{\mathbb{P}}[Y(\tau)|\mathcal{F}_v],$$

for every stopping time v, set in the framework of families of random variables indexed by stopping times. This setting is more general than the classical setup of stochastic processes, and particularly allows for general payoff processes that are not necessarily right-continuous. Under weaker integrability, and regularity assumptions on the reward family $Y = (Y(v), v \in S)$, we show the existence of an optimal stopping time. We then proceed to find sufficient conditions for the existence of an optimal model. For this purpose, we present a universal optional decomposition for the generalized Snell envelope family associated with Y. This decomposition is then employed to prove the existence of an optimal probability model and study its properties[3].

* **Lead presenter**

Result 1: Existence of optimal stopping times

Let $v \in \mathcal{S}$ and $\lambda_1, \lambda_2 \in (0,1)$ such that $\lambda_1 \leq \lambda_2$, then clearly $U^{\lambda_1}(v) \leq U^{\lambda_2}(v)$ a.s. Accordingly, the map $\alpha \to U^{\alpha}(v)$ is non-decreasing on $(0,1)$, and so we define the stopping time

$$U^*(v) := \lim_{\lambda\uparrow 1} U^{\alpha}(v) \quad \text{a.s.} \tag{2.1.1}$$

The stopping time $U^*(v)$ appears to be a good nominee for optimal stopping time for $R(v)$. We state the main existence result of an optimal stopping time in the following theorem.

[1]Department of Mathematics, Linnaeus University, Vejdesplats 7, SE-351 95 Vaxjo, Sweden
[2]Department of Mathematics, Faculty of Sciences Semlalia, Cadi Ayyad University, B.P. 2390, Marrakesh, Morocco
[3]This work has been accepted and is forthcoming in Probability, Uncertainty and Quantitative Risk.

Theorem 2.1.1 *Under additional assumptions on the reward family, we have: For every $v \in \mathcal{S}$, the stopping time $U^*(v)$ (defined by (2.1.1)) is an optimal stopping time for $R(v)$, that is,*

$$R(v) = \operatorname*{ess\,sup}_{\mathbb{P}\in\mathcal{P}} E^{\mathbb{P}}[Y(U^*(v))|\mathcal{F}_v]. \tag{2.1.2}$$

Additionally, $U^*(v) = \mathcal{U}(v) := \operatorname{ess\,inf}\{\tau \in \mathcal{S}_v, R(\tau) = Y(\tau) \quad a.s.\}$ a.s.

Result 2: Existence of optimal probability models

We now consider the question of under which conditions on the family $\mathcal{P}$ there exists an optimal probability model for our problem. The objective is to characterize an optimal probability model using a "universal" optional decomposition for our Snell envelope family $\mathcal{R} = (R(v), v \in \mathcal{S})$ in the sense that it holds simultaneously for all $\mathbb{P} \in \mathcal{P}$. This is our Theorem 2.1.2 below.

Theorem 2.1.2 *Under suitable conditions on the family $\mathcal{P}$ and integrability condition, there exists a probability measure $\mathbb{P}^* \in \mathcal{P}$ such that, for every $v \in \mathcal{S}$,*

$$E^{\mathbb{P}^*}\left[Y(U^*(v))\middle|\mathcal{F}_v\right] = R(v) = \operatorname*{ess\,sup}_{\mathbb{P}\in\mathcal{P}} E^{\mathbb{P}}\left[Y(U^*(v))\middle|\mathcal{F}_v\right] \quad a.s. \tag{2.1.3}$$

Moreover, any model $\mathbb{P} \in \mathcal{P}$ is then optimal.

References

[1] Kobylanski, M. and Quenez, M.-C. (2012). Optimal stopping time problem in a general framework, Electr. J. Prob. 17(72), 1–28.

[2] Krätschmer, V., Ladkau, M., Laeven, R.J.A., Schoenmakers, J.G.M. and Stadje, M. (2018). Optimal stopping under uncertainty in drift and jump intensity. Mathematics of Operations Research 43, 1177-1209.

[3] Riedel, F. (2009). Optimal stopping with multiple priors, Econometrica, 77, 857-908.

[4] Treviño-Aguilar, E. (2012). Optimal stopping under model uncertainty and the regularity of lower Snell envelopes, Quantitative Finance, 12:6, 865-871.

[5] Zamfirescu, I.-M. (2003). Optimal Stopping under Model Uncertainty, Ph.D. thesis, Columbia University.

2.2 Christian G. Boehmer: Dynamical systems in cosmology

Christian G. Boehmer
Department of Mathematics, University College London,
Gower Street, London WC1E 6BT, United Kingdom.

Abstract

The talk begins with a general overview of dynamical systems, a well-known field of applied mathematics with a wide range of applications ranging from epidemiology to cosmology. These techniques can be used for studying the time evolution of infectious diseases or for studying the time evolution of the Universe. First, I give an overview of the various techniques that exist to study dynamical system, starting with linear stability theory. This is followed by Lyapunov stability. Finally, the talk introduces Kosambi-Cartan-Chern (KCC) or Jacobi stability theory, an approach that is based on a geometrical construction. All techniques are then applied to a dynamical system motivated by cosmology. In passing, it will become clear that cosmological dynamical systems offer a rich mathematical structure with many intriguing models.

Result 1 We introduce a novel, model-independent approach to studying cosmological dynamical systems in modified gravity theories with second-order field equations. By using standard cosmological matter variables and a dynamical variable tied to the Hubble function, we construct a framework applicable to any second-order theory. The dimensionality of the dynamical system is determined by the number of matter sources, enabling a general analysis of two-fluid cosmologies.

Result 2 We explore models derived from variational principles, especially Brown's fluid approach, introducing new coupling terms, including boundary term couplings not previously studied in this context. This leads to surprisingly complicated models, showing a much richer structure than seen in other models of similar type.

References

[1] C. G. Boehmer and A. d'Alfonso del Sordo: Cosmological fluids with boundary term couplings, *General Relativity and Gravitation*, **56** (2024) 75.

[2] C. G. Boehmer, E. Jensko and R. Lazkoz: Cosmological dynamical systems in modified gravity, *European Physical Journal*, **C82** (2022) 500.

[3] S. Bahamonde, C. G. Boehmer, S. Carloni, E. J. Copeland, W. Fang and N. Tamanini: Dynamical systems applied to cosmology: dark energy and modified gravity, *Physics Reports*, **775-777** (2018) 1-122.

[4] C. G. Boehmer, T. Harko and S. V. Sabau: Jacobi stability analysis of dynamical systems – applications in gravitation and cosmology, *Advances in Theoretical and Mathematical Physics*, **16** (2012) 1145-1196.

2.3 Daniel Lesnic: Inverse modelling of biological tissues

Daniel Lesnic (joint work with M. Alosaimi)
University of Leeds, Department of Applied Mathematics, Leeds LS2 9JT, United Kingdom D.Lesnic@leeds.ac.uk.

Abstract

Knowledge of the properties of biological tissues is essential in monitoring abnormalities that may be forming and have a major impact on organs malfunctioning. Therefore, these disorders must be detected and treated early to save lives and improve the general health. Several therapeutic interventions guided by medical imaging are available at present to successfully detect, characterise and treat abnormalities within biological tissues by understanding that cancer can be interpreted as a tissue anomaly [6]. For instance, in hyperthermia, tumours are destroyed by increasing their temperature to about $42° - 46°C$, while keeping the neighbouring healthy tissues undamaged [2]. Therefore, understanding the heat transfer in biological tissues and, in particular, the determination of tissue's properties and the blood perfusion rate are important yet difficult tasks. When mathematically modelling such applications, care should be taken to include the underlying processes that are taking place such as heat conduction, convection, blood perfusion and heat generation due to metabolism.

Steady-state models for the elliptic modified Helmholtz equation (obtained by dropping out the terms involving time-derivatives in eqn.(1) below), such as those encountered in diffusive optical tomography [1], require an infinite amount of measurements (the knowledge of the Dirichlet-to-Neumann map) to be performed in theory, or a very large amount in practice, to determine the potential - in the biological context being represented by the blood perfusion coefficient. In such a situation, improved practically-feasible models based on evolutionary (parabolic or hyperbolic equations) equations provide the extra time-dimension that encodes more information about the unknown blood/tissue properties, as well as about an unknown static or moving anomaly, defect or flaw concealed in the body under investigation. One formulation that takes into account the transient mechanisms of heat transfer in biological tissues is based on the Pennes' parabolic reaction-diffusion equation (obtained by taking $\tau = 0$ in eqn.(1) below), which was proposed to model the temperature evolution during cancer hyperthermia treatment [7], the thermal radiation from cellular phones [8] and the ablation of afflicted tissues [3], among others. However, although still widely used, the Pennes parabolic model of heat transfer implies infinite speed of thermal propagation. This characteristic contradicts the physical reality that biological bodies, along with a number of other common materials, exhibit a relatively long thermal relaxation (or lag) time τ (typically between 15 to 30 seconds), [5]. This contradiction is resolved by the thermal-wave model of bio-heat transfer given by the Maxwell-Cattaneo hyperbolic equation [4], which in a bounded domain D over a time duration $T > 0$ reads as

$$\begin{aligned} C(\tau u_{tt} + u_t) + C_b \tau (wu)_t = \nabla \cdot (\kappa \nabla u) - C_b w(u - u_a) \\ + Q_m + Q_e + \tau \partial_t (Q_m + Q_e) \quad \text{in } D \times (0, T), \end{aligned} \tag{2.3.1}$$

where C and C_b are the heat capacities of the tissue and blood, respectively, κ is the thermal conductivity of the tissue, u is the tissue temperature, w is the blood perfusion rate, u_a is the (arterial) blood temperature, and Q_m and Q_e are the heat generations due to metabolism and external heating, respectively. Associated to eqn.(1) there are the initial conditions

$$u(\cdot, 0) = u_0, \quad u_t(\cdot, 0) = 0 \quad \text{in } D, \tag{2.3.2}$$

and a boundary condition of Robin convective type

$$(\kappa \nabla u) \cdot \nu = \sigma(u_\infty - u) \quad \text{on } \partial D \times (0, T) \tag{2.3.3}$$

is appropriate, where ν is the outward unit normal to the boundary ∂D, u_∞ is the ambient temperature and σ is the heat transfer coefficient. The physical inverse problem of interest in this study is to determine the blood perfusion rate w in the model (1)-(3) from extra (noisy) measurements of the temperature u on a portion Γ of the boundary ∂D, namely,

$$u = f, \quad \text{on } \Gamma \times [0, T]. \tag{2.3.4}$$

References

[1] S.R. Arridge and W.R. Lionheart: Non-uniqueness in diffusion-based optical tomography, *Optical Letters*, **23** (1998), 882-884.

[2] M. Baghban and M.B. Ayani: Source term prediction in a multilayer tissue during hyperthermia, *Journal of Thermal Biology*, **52** (2015), 187-191.

[3] A. Jalali, M.-B. Ayani and M. Baghban: Simultaneous estimation of controllable parameters in a living tissue during thermal therapy, *Journal of Thermal Biology*, **45** (2014), 37-42.

[4] J. Liu, X. Chen and L. Xu: New thermal wave aspects on burn evaluation of skin subjected to instantaneous heating, *IEEE Transactions on Biomedical Engineering*, **46** (1999), 420-428.

[5] K. Mitra, A. Kumar, A. Vedevarz and M. Moallemi: Experimental evidence of hyperbolic heat conduction in processed meat, *Journal of Heat Transfer*, **117** (1995), 568-573.

[6] T.P. Quinn, T. Nguyen, S.C. Lee and S. Venkatesh: Cancer as a tissue anomaly, *Frontiers in Genetics*, **10** (2019), Article ID 599.

[7] Z.P. Ren, J. Liu, C.C. Wang and P.X. Jiang: Boundary element method (BEM) for solving normal or inverse bio-heat transfer problem of biological bodies with complex shape, *Journal of Thermal Science*, **4** (1995), 117-124.

[8] P. Wainwright: Thermal effects of radiation from cellular telephones, *Physics in Medicine & Biology*, **45** (2000), Article ID 2363.

2.4 Hervé Gaussier: The Poincaré metric and some generalizations in hyperbolic geometry

Hervé Gaussier
Institut Fourier, Université Grenoble Alpes / CNRS, France

Abstract

The fifth postulate of Euclid is one of the most renowned axioms in the history of mathematics. It asserts that through a point not on a given line, there is exactly one line parallel to the given line in a plane. Alongside Euclid's other postulates, it forms the foundation of Euclidean geometry, which dominated mathematical thought for centuries.

However, the fifth postulate stands out among Euclid's axioms. Unlike the first four, which are straightforward and self-evident, the fifth postulate is less intuitive, as it predicts the infinite behavior of physical objects observed locally. Over time, mathematicians questioned whether it was truly necessary or if it could be derived from the other postulates. Efforts to prove the fifth postulate from the others led to the discovery of non-Euclidean geometries, including hyperbolic geometry.

Hyperbolic geometry emerged in the 19th century as an alternative to Euclidean geometry. In this framework, the fifth postulate is replaced with a new statement: through a point not on a given line, there are infinitely many lines parallel to the given line. This change results in a geometry with constant negative curvature, fundamentally different from the flat space of Euclidean geometry. The discovery of hyperbolic geometry by mathematicians such as Carl Friedrich Gauss, János Bolyai, Nikolai Lobachevsky and H. Poincaré opened new ways in mathematical research, showing that consistent geometries could exist without satisfying Euclid's fifth postulate. This challenged the long-held belief that Euclidean geometry was the sole description of space.

In physics, the concept of a curved space-time is essential for understanding phenomena such as the bending of starlight around massive objects and the expansion of the universe. The mathematical framework of hyperbolic geometry and its generalizations provide the tools necessary to describe these effects, which are not possible within the flat space of Euclidean geometry.

The Poincaré metric, introduced by Henri Poincaré for the upper half-plane and the unit disk in the complex plane, is one of the first examples of a metric with constant negative curvature. It is a cornerstone in the study of complex and Riemannian manifolds, serving as a canonical model in the Uniformization Theorem: the universal cover of every Riemann surface is conformally equivalent to either the projective line, the complex line, or the unit disk.

Extended to higher-dimensional complex manifolds and Riemannian manifolds, the Poincaré metric has paved the way for the study of hyperbolic spaces, still governed by the principles of the Uniformization Theorem.

In complex manifolds, classical invariant metrics provide insights into the geometric and analytic properties of these manifolds. The Kobayashi metric, defined using holomorphic mappings, offers a measure of hyperbolicity and encodes the geometric and analytic properties of complex manifolds. In the case of compact complex manifolds, famous conjectures address the hyperbolicity of sufficiently high-degree hypersurfaces in complex projective space or of their complements (the Kobayashi conjecture), as well as the locus of entire holomorphic maps in projective varieties of general type (the Green-Griffiths-Lang conjecture), see [4] by S. Kobayashi for an overview on the subject. Invariant metrics on non-compact manifolds are also of significant interest and have been the subject of intensive study; see, for example, the remarkable recent result by D. Wu and S.-T. Yau [5].

After introducing the Poincaré model and reviewing some key results in hyperbolic geometry, we will investigate how the Kobayashi metric can be defined within the framework of Riemannian manifolds (see [3], [1]). We will then explore potential connections with classical properties of Riemannian geometry (see [2]) and propose new questions arising in this context.

References

[1] H. Gaussier, A. Sukhov: On the Kobayashi metrics in Riemannian manifolds, *Proc. Amer. Math. Soc.*, **153** (2025), 1993-2006.

[2] H. Gaussier, A. Sukhov: Kobayashi hyperbolicity in Riemannian manifolds, *arXiv:2407.15976*.

[3] M. Gromov: Metric structures for Riemannian and non-Riemannian spaces. In LaFontaine, J. and Pansu, P., editors. Modern Birkhäuser Classics.

[4] S. Kobayashi: Hyperbolic complex spaces. Grundlehren der Mathematischen Wissenschaften. 318. Berlin: Springer. xiii, 471 p. (1998).

[5] D. Wu, S.T. Yau: Invariant metrics on negatively pinched complete Kähler manifolds. *J. Am. Math. Soc.*, **33** (2020), 103-133.

2.5 Mohammed Seaid: On time-stepping methods for computational fluid dynamics: Application to Newtonian and non-Newtonian flows

Mohammed Seaid
Department of Engineering, University of Durham, South Road, Durham DH1 3LE, UK.

Abstract

We present recent advances on fractional-step methods for the numerical solution of unsteady incompressible Navier–Stokes equations for both Newtonian and non-Newtonian fluids. The proposed class of methods is based on a viscosity-splitting approach, and it consists of four uncoupled steps where the convection and diffusion terms of flow solutions are uncoupled while a viscosity term is kept in the correction step at all times. This fractional-step method maintains the same boundary conditions imposed in the original problem for the corrected velocity solution, and it eliminates all inconsistencies related to boundary conditions for the treatment of the pressure solution. In addition, the method is unconditionally stable, and it allows the temperature to be transported by a non-divergence-free velocity field. Two pressure-correction strategies including the scalar auxiliary variable approach are proposed to enhance the accuracy of the method. A rigorous stability analysis is also carried out in this study for the considered strategies. In the case of thermal non-Newtonian fluids, we introduce a methodology to handle the subtle temperature convection term in the error analysis and establish full second-order error estimates for the velocity and the temperature solutions and first-order estimates for the pressure solution in their appropriate norms. Several numerical examples are presented to demonstrate the theoretical results and examine the performance of the proposed method for solving unsteady incompressible Navier–Stokes equations in non-Newtonian fluids. The computational results obtained for the considered examples confirm the convergence, accuracy, and applicability of the proposed time fractional-step method for unsteady incompressible Navier–Stokes equations in non-Newtonian fluids.

Special attention is given in this study on computational fluid dynamics for those fluids with transitory regimes changing from standard Newtonian to complex non-Newtonian fluids. These generalized Newtonian fluids are challenging to solve using the standard projection or fractional-step methods which split the diffusion term from the incompressibility constraint during the time integration process. Most of this class numerical methods already suffer from some inconsistencies, even in the Newtonian case, due to unphysical pressure boundary conditions which deteriorate the quality of approximations especially when open boundary conditions are prescribed in the problem under study. The current work proposes an improved viscosity-splitting approach for solving the generalized Newtonian fluids in which the viscosity follows a nonlinear generic rheological law. This method consists of decoupling the convective effects from the incompressibility while keeping a diffusion term in the last step allowing to enforce consistent boundary conditions. We provide a full algorithmic description of the method accounting for both Dirichlet and Neumann boundary conditions. To evaluate the computational performance of the proposed viscosity-splitting algorithm, we present numerical results for a series of problems from Ocean circulation and from molten salt reactors. Most of the results presented in this contribution have been subject of recent publications including [1–5] among others.

References

[1] A. Obbadi, M. El-Amrani, M. Seaid, D. Yakoubi: A stable second-order splitting method for incompressible Navier–Stokes equations using the scalar auxiliary variable approach, *Computer Methods in Applied Mechanics and Engineering*, **437** (2025), 117801.

[2] M. El-Amrani, A. Obbadi, M. Seaid, D. Yakoubi: A fractional time-stepping method for unsteady thermal convection in non-Newtonian fluids, *Communications in Nonlinear Science and Numerical Simulation*, **140** (2025), 108350.

[3] M. El-Amrani, A. Obbadi, M. Seaid, D. Yakoubi: A time viscosity-splitting method for incompressible flows with temperature-dependent viscosity and thermal conductivity, *Computer Methods in Applied Mechanics and Engineering*, **429** (2024), 117103.

[4] A. Obbadi, M. El-Amrani, M. Seaid, D. Yakoubi: An improved splitting algorithm for unsteady generalized Newtonian fluid flow problems with natural boundary conditions, *Computers & Mathematics with Applications*, **167** (2024), 92-109.

[5] M. El-Amrani, A. Obbadi, M. Seaid, D. Yakoubi: Error estimates for a viscosity-splitting scheme in time applied to non-Newtonian fluid flows, *Computer Methods in Applied Mechanics and Engineering*, **419** (2024), 116639.

2.6 Alexander Schied: Exploring Roughness in Stochastic Processes: From Weierstrass Bridges to Volatility Estimation

Xiyue Han[1] , **Alexander Schied**[1,*] , and **Zhenyuan Zhang**[2]
[1]Department of Statistics and Actuarial Science, University of Waterloo, Canada
[2]Department of Mathematics Stanford University, USA

Abstract

Motivated by the recent success of rough volatility models, we introduce the notion of a roughness exponent to quantify the roughness of trajectories. It can be computed in a straightforward manner for many stochastic processes and fractal functions and also inspired the introduction of a new class of stochastic processes, the so-called Weierstrass bridges. After taking a look at Weierstrass bridges and their sample path properties, we discuss the relations between the roughness exponent and other roughness measures, such as the Hurst index, weighted quadratic variation, and Besov regularity. We show furthermore that the roughness exponent can be statistically estimated in a model-free manner from direct observations of a trajectory but also from discrete observations of an antiderivative—a situation that corresponds to estimating the roughness of volatility from observations of the realized variance. As a consequence, we obtain strong consistency theorems in the context of several rough volatility models.

* **Lead presenter**

The Hurst parameter was originally defined by as a measure of the autocorrelation of a time series. But it is well known that it can also determine a degree of 'roughness' of the trajectories of certain stochastic processes, such as fractional Brownian motion. However, Gneiting and Schlather [1] constructed a class of stationary Gaussian processes for which the Hurst parameter and its roughness decouple completely, if roughness is quantified in terms of fractal dimension. It is therefore necessary to distinguish between the classical, autocorrelation-based Hurst parameter and a suitable index for the roughness of a trajectory. In this talk, we study such a roughness index, which is based on the p^{th} variation of a continuous real-valued function. More precisely, motivated by pathwise stochastic calculus, we say that continuous real-valued function x admits the *roughness exponent* R if the p^{th} variation of x converges to zero for $p > 1/R$ and to infinity for $p < 1/R$. Intuitively, the smaller R, the rougher the trajectory x will look. For instance, if x is continuously differentiable, then it has $R = 1$, if x is a typical sample path of a continuous semimartingale such as Brownian motion, then $R = 1/2$, and if x is a typical sample path of fractional Brownian motion, then R is equal to its classical Hurst parameter. If x is a classical Weierstrass function, which, for $\alpha \in (0, 1)$ and $b \in \{2, 3, \dots\}$, is defined as

$$x(t) = \sum_{n=0}^{\infty} \alpha^n \cos(2\pi b^n t), \qquad t \in [0, 1], \tag{2.6.1}$$

then $R = -\log_b \alpha$. This fact provided the motivation for introducing a new class of stochastic processes, which provide a synthesis between fractional Gaussian processes and fractal geometry. These processes are obtained by replacing the cosine function in (2.6.1) by the trajectories of a fractional Brownian bridge B_H with Hurst parameter H. More precisely, the *fractional Wiener–Weierstrass bridge* with parameters $\alpha \in (0, 1)$, $b \in \{2, 3, \dots\}$, and $H \in (0, 1)$ is defined as the stochastic process

$$Y(t) := \sum_{n=0}^{\infty} \alpha^n B_H(\{b^n t\}), \qquad 0 \le t \le 1,$$

where $\{x\}$ is the fractional part of $x \ge 0$. Although Y remains a Gaussian process, it displays a number of intriguing sample path properties, which will be discussed during this talk, based on [4, 5].

Returning to the general setting, where x is any continuous function on $[0, 1]$, we provide a mild condition on the Faber–Schauder coefficients of x under which the roughness exponent exists and is given as the limit of the classical Gladyshev estimates. This result can be viewed as a strong consistency result for the Gladyshev estimators in an entirely model-free setting, because no assumption whatsoever is made on the possible dynamics of the trajectory x. Nonetheless, our proof is probabilistic and relies on a martingale hidden in the Faber–Schauder expansion of x. We show that the condition of our main result is satisfied for the typical sample paths of fractional Brownian motion with drift, and we provide almost-sure convergence rates for the corresponding Gladyshev estimates. We also discuss the connections between the roughness exponent and the related concepts of Besov regularity and weighted quadratic variation. Since the Gladyshev estimators are not scale-invariant, we construct several scale-invariant estimators. This part of the talk is based on [2].

Based on [3], we then consider the problem of estimating the roughness of the volatility process in a stochastic volatility model that arises as a nonlinear function of fractional Brownian motion with drift. To this end, we introduce a new estimator that measures the so-called roughness exponent of a continuous trajectory, based on discrete observations of its antiderivative. The estimator has a very simple form and can be computed with great efficiency on large data sets. It is not derived from distributional assumptions but from strictly pathwise considerations. We provide conditions on the underlying trajectory under which our estimator converges in a strictly pathwise sense. Then we verify that these conditions are satisfied by almost every sample path of fractional Brownian motion (with drift). As a consequence, we obtain strong consistency theorems in the context of a large class of rough volatility models, such as the rough fractional volatility model and the rough Bergomi model. We also demonstrate that our estimator is robust with respect to proxy errors between the integrated and realized variance, and that it can be applied to estimate the roughness exponent directly from the price trajectory. Numerical simulations show that our estimation procedure performs well after passing to a scale-invariant modification of our estimator.

References

[1] Gneiting, Tilmann, and Martin Schlather. Stochastic models that separate fractal dimension and the Hurst effect. SIAM Review 46, no. 2 (2004): 269-282.

[2] Han, Xiyue, and Alexander Schied. The roughness exponent and its model-free estimation. To appear in the Annals of Applied Probability (2025).

[3] Han, Xiyue, and Alexander Schied. Estimating the roughness exponent of stochastic volatility from discrete observations of the realized variance. arXiv:2307.02582 (2023).

[4] Schied, Alexander, and Zhenyuan Zhang. Weierstrass bridges. Transactions of the American Mathematical Society 377, no. 04 (2024): 2947-2989.

[5] Schied, Alexander, and Zhenyuan Zhang. Sample Path Properties of the Fractional Wiener–Weierstrass Bridge. arXiv:2411.05204 (2024).

2.7 Manuel Morales: Building an university-based knowledge transfer network for the financial sector: The case of Fin-ML

Manuel Morales
University of Montreal, Canada

Abstract

In 2017, the Fin-ML Network was created within the Université de Montréal with the goal of training the next generation of applied mathematicians and statisticians working at the intersection of data-science, machine learning, quantitative finance and business intelligence. In the past five years, it has become a knowledge transfer center fostering collaboration between industry and academia around data-centric value creation for businesses in the financial sector. This collaboration is now international as we have started partnering with the innovation ecosystem in two Mexican states. This talk will narrate this success story while showcasing some of the applied projects our researchers have been working on.

* **Lead presenter**

In 2017, the Fin-ML Network was established at the Université de Montréal with a mission to train the next generation of professionals adept in applied mathematics, statistics, data science, machine learning, quantitative finance, and business intelligence. Over the past eight years, Fin-ML has evolved into a pivotal knowledge transfer center, fostering robust collaborations between academia and industry to drive data-centric value creation in the financial sector.

Genesis and Objectives of Fin-ML

The inception of Fin-ML was driven by the recognition of a significant skills gap in the financial industry, particularly in the application of advanced machine learning techniques to complex financial problems. Supported by the Natural Sciences and Engineering Research Council of Canada (NSERC) through the Collaborative Research and Training Experience (CREATE) Program, Fin-ML set out to bridge this gap by offering a multidisciplinary training program. This initiative brought together six Canadian institutions: Université de Montréal, HEC Montréal, Concordia University, University of Waterloo, Queen's University, and University of Calgary. The program's core objective is to equip students with the expertise required to meet the modeling and implementation needs of Canada's quantitative finance sector, thereby enhancing its global competitiveness.

Academic-Industry Synergy

Central to Fin-ML's success is its emphasis on fostering symbiotic relationships between academic researchers and industry practitioners. By collaborating with major financial institutions–including the Autorité des marchés financiers, Bourse de Montréal, BNP Paribas, CIBC Asset Management, Desjardins, National Bank of Canada, and RBC–Fin-ML ensures that its training programs are aligned with real-world industry needs. This alignment is further strengthened through partnerships with the Institute for Data Valorization (IVADO), facilitating the translation of cutting-edge research into practical applications.

International Expansion and Collaborative Ventures

Recognizing the universal applicability of its model, Fin-ML has extended its collaborative framework beyond Canadian borders. In recent years, the network has initiated partnerships with the innovation ecosystems in two Mexican states. These collaborations aim to address shared challenges in the financial sectors of both countries, particularly in areas such as financial fraud prevention and anti-money laundering efforts. By leveraging collective intelligence and knowledge-sharing platforms, Fin-ML and its Mexican partners strive to enhance the robustness of financial systems against illicit activities.

Showcase of Applied Research Projects

Fin-ML's collaborative efforts have yielded numerous applied research projects that exemplify the network's impact:

- Machine Learning Use Cases in Finance: In partnership with IVADO and Université de Montréal, Fin-ML developed a comprehensive course titled "Machine Learning Use Cases in Finance." This course equips industry professionals and academics with practical knowledge on applying machine learning models to financial contexts, covering topics such as graph neural networks for financial markets and reinforcement learning for portfolio optimization.

- Financial Fraud Detection Initiatives: Collaborating with Mexican financial institutions, Fin-ML has contributed to projects focused on enhancing fraud detection capabilities. By sharing information about fraudsters' methods and attacks, these initiatives create robust collaboration networks that strengthen the financial sector's resilience against fraudulent activities.

- AI-Driven Anti-Money Laundering Systems: Fin-ML has been involved in the development of AI systems designed to combat financial crime. These systems utilize advanced machine learning algorithms to detect suspicious activities with greater accuracy, thereby reducing false positives and improving the efficiency of compliance operations.

Conclusion

The Fin-ML Network stands as a testament to the transformative potential of academia-industry partnerships. By bridging the gap between theoretical research and practical application, Fin-ML not only addresses the evolving needs of the financial sector but also cultivates a new generation of professionals equipped to navigate and shape the future of finance.

References

[1] Fin-ML Network: Training the Next Generation of Finance Professionals. Available at: `https://fin-ml.ca`

[2] Université de Montréal receives NSERC CREATE Program Funding. IVADO, March 20, 2019. Available at: `https://ivado.ca/en/2019/03/20/universite-de-montreal-receives-nserc-create-program-funding/`

3 Abstracts of Invited Speakers

3.1 Ahmad Alghamdi: Dynamical Systems and Algebra

Ahmad Mohammed Ahmad Alghamdi
Mathematics Department, Faculty of Sciences, Umm Al-Qura University, Makkah, Saudi Arabia. Email: amghamdi@uqu.edu.sa.

Abstract

Dynamical system theory has its own AMS classification. That is 37-xx. But it is linked to many other areas of mathematics. The aim of the talk is to introduce our understanding of the relationship between the two concepts of dynamical system and algebra. In particular with the concept of group action. We shall discuss and explain some points such as semigroups and groups action as a dynamical systems. Then Dynamical systems and some disciplines in mathematics id discussed. We present some recent results with are devoted to ring terminology on algebraic structures on smooth vector fields.

This is a survey and a representable article of the relationship between dynamical systems [4] and algebra [2]. In particular we shall discuss and explain the following points:

- **Semi-groups and dynamical systems**: A semigroup $(G, \star)$ is a non-empty set G and a binary operation $\star$ on which we can add two elements of G together and where the associativity law $x \star (y \star z) = (x \star y) \star z$ holds for all choices $x, y, z \in G$. This means that the action is defined and indexed by a collection of maps on certain X such that $T_t : X \to X$ for which we assume that $T_t \circ T_s = T_{ts}$. Does such certain X receive or carry any mathematical structure? That is very important to intimate new theory in this direction. A group $(G, \star)$ is a non-empty set G and a binary operation $\star$ on which we can add two elements of G together and where the associativity law $x \star (y \star z) = (x \star y) \star z$ holds for all choices $x, y, z \in G$ and there is an identity element in G (natural element) and each element has an inverse in G with respect to this binary operation. So each group action is a dynamical system. We mean by that G acts on the non-empty set X if for each $g \in G$ and each $x \in X$ there corresponds a unique element xg in X such that, for all $x \in X$ and $g_1, g_2 \in G$ we have: $(xg_1)g_2 = x(g_1g_2)$ and $x1_G = x$. Group Action is very important subject in mathematics. Let us mention some applications and topics in this regards:

  1. Group acts on a non-empty set G-sets and permutation groups: Permutation representation.
  2. Group G acts on a module or a vector space G-module (Linear representation theory)
  3. Group acts on a ring: G-ring (Ring Theory)
  4. Group acts of a topological space: Topological group.
  5. Group acts on an algebra: G-algebra theory
  6. Group acts on group (nilpotent, solvable and poly-cyclic groups)
  7. Group acts on its subgroups: (series of subgroups)
  8. Group acts on itself (Conjugacy classes and conjugation action)

- **Dynamical systems and some disciplines in mathematics**: Here we shall mention without further details the relationships with some core subject of mathematics with dynamical system:

  1. **Relation with algebra**: As we mention above, group theorists investigates and look at the action of the group in itself. In fact, the action of the group on vector spaces define a very important field in mathematics called representation theory.

2. **Relation with measure theory**: In ergodic theory, they study a map measure space.
3. **Relation with analysis**: the study of partial differential equations, functional analysis, complex analysis and potential theory.
4. **Relation with topology**: Such as Poincare Conjecture and the so called Ricci Flow.
5. **Relation with geometry**: Some people try to classify geometrises by using its Symmetry groups. This approach is called Kleins Erlanger Program.
6. **Relation with probability theory**: Sequences of independent random variables can be obtained using dynamical systems
7. **Relation with logic and complexity** : Every computation by the so called Turing Machines can be realized as a dynamical system.
8. **Relation with number theory**: Diophantine Approximations can be seen as problems in dynamical systems.
9. **Relation with category theory**: A category of mathematical objects has a semigroup of homomorphisms acting on it; such as sets have usual maps, topological spaces have continuous maps, measurable spaces have measurable maps, groups, rings, fields and algebras have homomorphisms. One can view these categories as a dynamical system.

Some results on algebraic structures on smooth vector fields with my PhD student Amenah A Alkenani [1]:

Let n and m be two non-negative integers. A C^∞**-ring** is a non-empty set C together with operations $C_f : C^n \longrightarrow C$ for all smooth functions $f : \mathbb{R}^n \longrightarrow \mathbb{R}$. Here, the function f is an element of $C^\infty(\mathbb{R}^n)$ with the following conditions:

1. If $\pi_i : \mathbb{R}^n \longrightarrow \mathbb{R}$ is the projection given by $\pi_i(x_1, \cdots, x_n) = x_i$ for all $(x_1, \cdots, x_n) \in \mathbb{R}^n$, then $C_{\pi_i}(c_1, \cdots, c_n) = c_i$ for all $(c_1, \cdots, c_n) \in C^n$.

2. If f is an element of $C^\infty(\mathbb{R}^n)$ and g_i is an element of $C^\infty(\mathbb{R}^m)$ where $g_i : \mathbb{R}^m \longrightarrow \mathbb{R}$ with $h(x_1, \cdots, x_m) = f(\ g_1(x_1, \cdots, x_m), \cdots, g_n(x_1, \cdots, x_m)\ )$ is an element of $C^\infty(\mathbb{R}^m)$ where $i = 1, \cdots, n$, then

$$C_h(c_1, \cdots, c_m) = C_f(\ C_{g_1}(c_1, \cdots, c_m), \cdots, C_{g_n}(c_1, \cdots, c_m)\ )$$

   for all $c_1, \cdots, c_m \in C$.

The most important example of C^∞-ring is $C^\infty(L)$, where L is a smooth manifold and

$$C^\infty(L) =: \{f : L \longrightarrow \mathbb{R} \mid f \text{ is a smooth function}\}.$$

Recall that the smooth vector field can be defined as: X on L is a linear map $X : C^\infty(L) \longrightarrow C^\infty(L)$ such that X is a derivation. That is $X(fg) = fX(g) + X(f)g$ for all $f, g \in C^\infty(L)$. In fact, we can define the operations of vector fields addition and scalar multiplication.

The link between analysis and algebra in this setting and in our work is the following results:

1. **Theorem**: Let L be a connected smooth manifold with real algebra structure of smooth functions. Then there is an isomorphism between the module of smooth vector fields $L^\infty(TL)$ and the finitely projective $C^\infty(L)$-modules. Here, $L^\infty(TL)$ is a module consisting of certain derivations.

2. **Theorem**: Let $M = L^\infty(TL)$ be the $C^\infty(L)$-module. If L is a manifold of positive dimension, then M is not semi-simple module.

3. **Corollary**: The socle of the $C^\infty(L)$-module $L^\infty(TL)$ is a proper submodule.

4. **Corollary**: The Jacobson radical of the $C^\infty(L)$-module $L^\infty(TL)$ is not the zero submodule.

5. **Corollary**: The $C^\infty(L)$-module $L^\infty(TL)$ has a non-trivial proper essential submodule.

The proof of the above results depend on construction of some category with preserve both ring structure and smoothness structure. In particular, we focus on the ring of smooth functions and its modules see [1] and [3].

Let me mention in this summery the following topic which is also can be regarded somewhat a relationship between algebra and dynamical system: There is a paper which was written by G. R. Robinson with Marco Thiel with the title " Recurrences determine dynamics ". It was in AIP Publishing 2009. From the abstract of that paper, we mention: They show in that paper that under suitable assumptions, Poincaré recurrences of a dynamical system determine its topology in phase space. Therefore, dynamical systems with the same recurrences are dynamically equivalent. The main theorem to get such result states that: the recurrence matrix determines the topology of closed sets. The theorem states that if a set of points M is mapped onto another set N, such that two points in N are closer than some prescribed fixed distance if and only if the corresponding points in M are closer than some, in general different, prescribed fixed distance, then both sets are homeomorphic. We are trying to understand more in this direction.

References

[1] A. A. Alkinani and A. M. Alghamdi: Algebraic Structures on Smooth Vector Fields. *Symmetry 2023, 15, 2150. https://doi.org/10.3390/sym15122150.*

[2] D. Dummit and R. Foote: Abstract Algebra. Publisher: Wiley; 3 edition (July 14, 2003) Language: English ISBN-10: 0471433349 ISBN-13: 978-0471433347

[3] D. Joyce: Algebraic Geometry over C^∞-Rings. American Mathematical Society: Providence, RI, USA, 2019.

[4] Viacheslav Z. Grines , Timur V. Medvedev , Olga V. Pochinka, Dynamical Systems on 2- and 3-Manifolds, Springer. Berlin Heidelberg 2016.

3.2 Abdelkarim Boua: Right homoderivations in rings and near-rings

Abdelkarim Boua
Department of Mathematics, Polydisciplinary Faculty, LSI, Taza, Sidi Mohammed Ben Abdellah University, Fez, Morocco

Abstract

In this article, we studied the commutativity of rings and near-rings with a new type of mappings, which we called right homoderivations. Our findings led to significant and valuable results that contribute to advancing research in this area.

An additive mapping $d : \mathcal{N} \longrightarrow \mathcal{N}$ satisfying $d(xy) = d(x)y + d(y)x$ for all for all $x, y \in \mathcal{N}$, They obtained intriguing results regarding the commutativity of a 3-prime near-ring $\mathcal{N}$ involving right derivations that satisfy certain algebraic identities [5]. Similar to the tactic taken by El Sofiand Boua regarding homoderivation, the idea of this article is to combine both homomorphism and right derivation into one concept which is called "right homomorphism" on a rings and near-rings.

Definition: Let h be an additive mapping from a ring $\mathcal{R}$ into itself.

1- h is called a right homoderivation on $\mathcal{R}$, if $h(xy) = h(x)h(y) + h(x)y + xh(y)$ for all $x, y \in \mathcal{R}$.

2- h is called a Jordan right homoderivation, if $h(x^2) = h(x)h(x) + 2h(x)x$ for all $x \in \mathcal{R}$.

Result 1 Let $\mathcal{N}$ be a 2-torsion free 3-prime zero-symmetric near-ring and $\mathcal{I}$ be a nonzero Lie right ideal. If $\mathcal{N}$ admits a non-zero right homoderivation h such that $h(\mathcal{I}) \subseteq Z(\mathcal{N})$, then $\mathcal{N}$ is abelian.
Idea of the proof: If $\{0\} \neq h(\mathcal{I}) \subseteq Z(\mathcal{N})$, then there exists $i \in \mathcal{I}$ such that $h(i) \in Z(\mathcal{N}) setminus \{0\}$. Since $h(i) + h(i) = h(i + i) \in Z(\mathcal{N})$, $(\mathcal{N}, +)$ is abelian and the 2-torsion freeness of $\mathcal{N}$. Now suppose that $h(i) = 0$ for all $i \in \mathcal{I}$. Replacing i by $[n, i]$, where $n \in \mathcal{N}$, and using the last equation, we get

$$h(n)i = ih(n) \quad \text{for all} \quad i \in \mathcal{I}, n \in \mathcal{N}. \tag{3.2.1}$$

Substituting $h(n)t$ for n in (3.2.1) and applying (3.2.1), we give

$$h^2(n)ti = ih^2(n)t \quad \text{for all} \quad i \in \mathcal{I}, n, t \in \mathcal{N}. \tag{3.2.2}$$

Putting tm instead of t in (3.2.2) and using (3.2.2), we have

$$\begin{aligned} h^2(n)tmi &= ih^2(n)tm \\ &= h^2(n)tim \quad \text{for all} \quad i \in \mathcal{I}, m, n, t \in \mathcal{N}. \end{aligned}$$

The last expression implies that $h^2(n)\mathcal{N}[i, m] = \{0\}$ for all $i \in \mathcal{I}, n, m \in \mathcal{N}$. By the 3-primeness of $\mathcal{N}$, we arrive at

$$h^2(\mathcal{N}) = \{0\} \text{ or } \mathcal{I} \subseteq Z(\mathcal{N}).$$

If $h^2(\mathcal{N}) = \{0\}$, then we get $h = 0$; a contradiction. So, $\mathcal{I} \subseteq Z(\mathcal{N})$, and $\mathcal{N}$ is abelian.

Result 2 If $\mathcal{R}$ is commutative and $Char(\mathcal{R}) \neq 2$, then every Jordan right homoderivation is a right homoderivation.
Idea of the proof:Let h be a Jordan right homoderivation on $\mathcal{R}$, then $h(x^2) = h(x)h(x) + h(x)x + h(x)x$ for all $x \in \mathcal{R}$. Replace x with $x + y$ in the last relation to get $h((x + y)^2) = h(x + y)h(x + y) + h(x + y)(x + y) + h(x + y)(x + y)$ for all $x \in \mathcal{R}$. Hence, $h(x^2) + h(y^2) + 2h(xy) = h(x)h(x) + h(x)x + h(x)x + h(y)h(y) + h(y)y + h(y)y + 2(h(x)h(y) + h(x)y + h(y)x)$, Since $\mathcal{R}$ is commutative and 2-torsion free, then $h(xy) = h(x)h(y) + h(x)y + h(y)x$, so h is a right homoderivation.

References

[1] A. Al-Kenani, A. Melaibari & N. Muthana, Homoderivations and commutativity of $*$-prime rings, East-West J. of Mathematics: Vol. 17, No 2 (2015) pp. 117-126.

[2] Bell H. E. 1997. On Derivations in Near-Rings II. Near-rings, Near-fields and k-loops. Kluwer Academic Publishers. Dordrecht. 426: 191-197.

[3] A. Boua, Homoderivations and Jordan right ideals in 3-prime near-rings, AIP Conference Proceedings 2074, 020010 (2019).

[4] A. Boua & E. Farhan, generalized homoderivations on near-rings, Indian journal of mathematics, vol.63, No.2,2021,229-242.

[5] A. Majeed & E. Farhan. Right n-derivations in prime Near-Rings. Journal Al-Qadisiyah / Pure Sciences. 2016, 2(3): 31-41.

[6] S. Mouhssine & A. Boua. Homoderivation and semigroup ideals in 3-prime near-rings, Algebraic Structures and Their Applications Vol. 8 No. 2 (2021), pp 177-194.

[7] El Sofy. M, (2000), Rings with some kinds of mappings. M. Sc. Thesis, Cairo University, Branch of Fayoum, Cairo, Egypt.

[8] G. Pilz, Near-rings, second edition, North-Holland Mathematics Studies, 23, North Holland Publishing Co., Amsterdam, 1983.

3.3 Abderrahmane Raji: Commutativity of 3-prime near-rings with certain special maps

Abderrahmane Raji
LMACS Laboratory, Faculty of Sciences and Technology, Sultan Moulay Slimane University, Beni Mellal, Morocco.

Abstract

Numerous research in rings and near-rings theory have demonstrated that certain prime rings and 3-prime near-rings must be commutative under certain conditions. In this context, the commutativity of 3-prime near-rings with derivation was initiated by Bell and Mason in [4]. Over the last two decades, a lot of work has been done on this subject. Recently, in [1], Ashraf and Siddeeque deőned the following notations: An additive mapping $d : \mathcal{N} \to \mathcal{N}$ is called a $*$-derivation if there exists an involution $* : \mathcal{N} \to \mathcal{N}$ such that $d(xy) = d(x)y^* + xd(y)$, for all $x, y \in \mathcal{N}$. An additive mapping $F : \mathcal{N} \to \mathcal{N}$ is called a left $*$-multiplier if $F(xy) = F(x)y^*$ hold for all $x, y \in \mathcal{N}$. Motivated by these concepts, we introduce the concepts of $*$-generalized derivation in near-rings as follows: An additive mapping $F : \mathcal{N} \to \mathcal{N}$ is called a $*$-generalized derivation if there exist a $*$-derivation d of $\mathcal{N}$ such that $F(xy) = F(x)y^* + xd(y)$ for all $x, y \in \mathcal{N}$.

In the present paper, we investigate some properties involving that of $*$-generalized derivation of a $*$-prime near-ring $\mathcal{N}$ which forces$\mathcal{N}$ to be a commutative ring. Some properties of generalized semiderivations and multiplicative derivations have also been given in the context of 3- prime near-rings. Consequently, some well known results have been generalized. Furthermore, we will give examples to demonstrate that the restrictions imposed on the hypothesis of various results cannot be marginalized.

References

[1] M. Ashraf and M. A. Siddeeque: On $*$-derivations in near-rings with involution, *J. Adv. Res. Pure Math.*, **6** (2) (2014), 1-12.

[2] H. E. Bell: On derivations in near-rings II, *Kluwer Academic Publishers Netherlands*, **1997**, 191-197.

[3] Z. Bedir and O. Gölbaşi: Notes on prime near-rings with multiplicative derivation, *Cumhuriyet Univ. Fac. Sci., Sci. J. (CSJ)*, **38** (2) (2017), 355-363.

[4] H. E. Bell and G. Mason: On derivations in near-rings, *North-Holland Math. Studies*, **137** (1987), 31-35.

[5] A. Boua, G. S. Sandhu and A. Y. Abdelwanis: Jordan ideals and (α, β)-derivations on 3-prime near-rings and rings, *Ann. Univ. Ferrara*, **70** (2) (2024), 479-491.

[6] A. Boua, A. Raji and A. En-guady: On Jordan ideals with generalized left derivations in 3-prime near-rings, *Note Mat.*, **43** (2) (2023), 1-12.

[7] A. Boua, A. Raji: Several algebraic inequalities on a 3-prime near-ring, *JP J. Algebra Number Theory Appl.*, **39** (1) (2017), 105-113.

[8] A. Boua, L. Oukhtite and A. Raji: On generalized semiderivations in 3-prime near-rings, *Asian-Eur. J. Math.*, **9** (21) (2016), 1650036 (11 pages).

[9] A. Boua, A. Raji, A. Asma and A. Farhat: On generalized semiderivations of prime near-rings, *Int. J. Math. Math. Sci.*, **2015** (1) (2015), 867923.

[10] A. Boua, L. Oukhtite and A. Raji: Jordan ideals and derivations in prime near-rings, *Comment. Math. Univ. Carolin.*, **55** (2) (2014), 131-139.

[11] M. N. Daif: When is a multiplicative derivation additive?, *Int. J. Math. Math. Sci.*, **14** (3) (1991), 615-618.

[12] A. En-guady, A. Boua and A. Raji: Some algebraic identities in 3-prime near-rings, *Adv. Pure Appl. Math.*, **15** (1) (2024), 18-28.

[13] H. Goldmann and P. Sěmrl: Multiplicative derivations on $C(X)$, *Monatshefte Math.*, **121** (1996), 189-197.

[14] A. M. Kamal and K. H. Al-Shaalan: Existence of derivations on near-rings, *Math. Slovaca*, **63** (3) (2013), 431-438.

[15] L. Oukhtite and A. Raji: On two-sided α-n-derivation in 3-prime near-rings, *Acta Math. Hungar.*, **157** (2) (2019), 465-477.

3.4 Abdellatif Laradji: The nucleus of a block of a p-solvable group

Abdellatif Laradji
King Saud University, College of Science, Department of Mathematics, P.O. Box 2455, Riyadh 11451, Saudi Arabia.

Abstract

Let G be a finite p-solvable group. For a given p-block B of G, we define a canonical pair (K, A), referred to as a nucleus for B, where K is a subgroup of G and A is a block of K of maximal defect, defined uniquely by B up to G-conjugacy. The irreducible characters (ordinary or modular) associated with B are closely related to those associated with A. Also, not surprisingly, (K, A) is just (G, B) in case B is of maximal defect. Given a normal subgroup N of G and a block b of N, we show that there exist a nucleus $(\widehat{N}, \widehat{b})$ for b and a subgroup $\widehat{G}$ of G containing $\widehat{N}$ as a normal subgroup such that the blocks of G covering b behave quite analogously to those of $\widehat{G}$ covering $\widehat{b}$.

3.5 Abdul Wahab: Multipolar Source Reconstruction Using Sparse Far-Field Data

Abdul Wahab[1,*], **Shujaat Khan**[2], **Yukun Guo**[3] and **Xianchao Wang**[3]
[1]Department of Mathematics, Sultan Qaboos University, Oman.
[2]Department of Computer Engineering, King Fahd University of Petroleum and Minerals, Saudi Arabia.
[3]School of Mathematics, Harbin Institute of Technology, China.

Abstract

We present an algorithm to reconstruct multipolar electromagnetic sources from sparse multi-frequency far-field signatures of the electromagnetic waves generated by geometrically sparse unknown sources. We use a two-stage strategy. First, we enrich the sparse data, and then we use a Fourier algorithm to reconstruct the sources from the enriched data. We link the data enrichment problem to the recovery of the missing spectrum of a signal having a finite rate of innovations. The missing spectrum problem is subsequently converted to a constraint optimization problem for matrix completion subject to a low-rankness constraint.

* **Lead presenter**

The recovery of multipolar acoustic or electromagnetic sources from their far-field signatures is important for many scientific and engineering applications, particularly in the fields of biomedical imaging [1, 2], non-destructive testing [3], and telecommunication [4]. For example, these inverse source problems are employed in electromagnetic media to manufacture conformal antennas [4]. Inverse source problems have also been used for expressing neuron responses in intracranial recordings and electroencephalography (EEG) [1, 2]. The use of inverse source problems also appears in *magnetoencephalography* (MEG) [5].

To solve these inverse source problems, an array of algorithms has been proposed. These methods necessitate the acquisition of dense multi-frequency data at the Nyquist sampling rate. Unfortunately, most real-world inverse source problems and imaging setups offer only limited multi-frequency discrete observations of the radiated waves. This limitation hinders the use of most of these mathematical algorithms. On the other hand, the null space of the inverse source-to-data operator is strongly affected by the availability of only sub-sampled grid measurements of the far-field signature. This causes noticeable artifacts in the reconstructed images. Therefore, either more information about the source is required or the application of regularization techniques is needed.

We present a novel two-stage approach for multipolar source reconstruction from sub-sampled sparse data, taking advantage of the physical domain sparsity of the sources. The data is recovered at the Nyquist sampling rate by first enriching the subsampled data. After that, a standard inversion algorithm is used to reconstruct the sources. The data recovery problem is linked to a spectrum recovery problem for the signal with the finite rate of innovations (FIR) [6]. Next, a structured Hankel matrix completion optimization problem with a low-rankness constraint is related to the data recovery and missing spectrum problems. An *annihilating filter-based low-rank Hankel matrix completion approach* (ALOHA) [7, 8] is then used to deal with the constraint optimization problem. Lastly, the sources are reconstructed from the enriched data using a Fourier technique in the second stage.

According to numerical data, the suggested approach betters the traditional regularization-based inversion techniques in terms of computational cost, peak-signal-to-noise ratio (PSNR), and structural similarity index measure (SSIM).

References

[1] B. J. Thio, A. S. Aberra, G. E. Dessert and W. M. Grill: Ideal current dipoles are appropriate source representations for simulating neurons for intracranial recordings, *Clinical Neurophysiology*, **145** (2023), 26-35.

[2] L. Beltrachini, N.von Ellenrieder, R. Eichardt, and J. Haueisen: Optimal design of on-scalp electromagnetic sensor arrays for brain source localisation, *Human Brain Mapping*, **42** (2021), 4869-4879.

[3] S. Takahashi, K. Suzuki, T. Hanabusa, and S. Kidera: Optimal design of on-scalp electromagnetic sensor arrays for brain source localisation, *IEEE Transactions on Antennas and Propagation*, **70** (2022), 11009-11023.

[4] G. Leone, M. A. Maisto, and R. Pierri: Application of inverse source reconstruction to conformal antennas synthesis, *IEEE Transactions on Antennas and Propagation*, **66** (2018), 1436-1445.

[5] K. Jerbi, S. Baillet, J.C. Mosher, G. Nolte, L. Garnero, and R.M. Leahy: Localization of realistic cortical activity in MEG using current multipoles, *NeuroImage*, **22** (2004), 779-793.

[6] M. Vetterli, P. Marziliano, and T. Blu: Sampling signals with finite rate of innovation, *IEEE Transactions on Signal Processing*, **50** (2002), 1417-1428.

[7] K. H. Jin and J. C. Ye: Annihilating filter-based low-rank Hankel matrix approach for image inpainting, *IEEE Transactions on Image Processing*, **24** (2015), 3498-3511.

[8] J. C. Ye, J. M. Kim, K. H. Jin, and K. Lee: Compressive sampling using annihilating filter-based low-rank interpolation, *IEEE Transactions on Information Theory*, **63** (2017), 777-801.

3.6 Hocine Guediri: Analytic structure in the maximal ideal space of some function algebra

Hocine Guediri
Department of Mathematics, College of Science, King Saud University, Riyadh, Saudi Arabia. Email: hguediri@ksu.edu.sa

Abstract

We investigate the existence of an analytic structure in the maximal ideal space of the Banach algebra of bounded analytic functions over the half-plane. We outline connections with Carleson corona theorem, and characterize analytic disks in the fibers. We explore the impact of the pseudohyperbolic distance on analytic properties of the maximal ideal space, especially on the characterization of their Gleason parts and on the construction of Hoffman type maps. Moreover, we discuss applications to Toeplitz operators with symbols that are continuous on this maximal ideal space.

3.6.1 Main results

In the setting of the Bergman space of the upper half-plane $\mathbb{C}^+$, we are currently interested in investigating various properties of Toeplitz operators with symbols that are either continuous, harmonic, vertical, or angular. In this connection, we have been led to consider Toeplitz operators with symbols that are continuous on the maximal ideal space $\mathcal{M}$ of the Banach algebra $H^\infty(\mathbb{C}^+)$ of bounded analytic functions on $\mathbb{C}^+$. This will enable us to explore Banach algebra techniques in the light of the leading work of S. Axler, P. Gorkin, R. Mortini, D. Suárez, R. Douglas, G. McDonald, C. Sundberg, D. Zheng, K. Stroethoff, Ž. Čučković, and many others. The paper of I.J. Schark [7] and the deep work of K. Hoffman [4] represent the cornerstone in this direction. The book of J. Garnett [2] provide a systematic exposition of these results and further developments, while the papers of T. Gamelin [1] and S. Krantz [5] gave some extra momentum to the theme. The celebrated corona problem has been always one of the crucial questions in the theory of bounded analytic functions and in operator theory. In this connection, we refer to the book of J. Garnett [2] for a good exposition of its famous solution due to L. Carleson. For its applications in operator theory, see for instance G. McDonald and C. Sundberg [6] and K. Stroethoff [8]. In order to achieve our goal, first we have to shed some light on the analytic structure of the maximal ideal space $\mathcal{M}$ of the algebra of bounded analytic functions on $\mathbb{C}^+$ and on its associated class of symbols, as well as on its connection with Carleson corona theorem. Further, we study Gleason parts and construct Hoffman type maps, and discuss applications to Toeplitz operators. skip

We regard $\mathbb{C}^+$ as an open subset of the extended complex plane $\mathbb{C}_\infty$, and let $\widehat{\mathbb{C}^+} := \overline{\mathbb{C}^+} \cup \{\infty\}$ denote its one-point compactification, and $\partial_\infty \mathbb{C}^+ := \partial\widehat{\mathbb{C}^+} = \widehat{\mathbb{C}^+} \setminus \mathbb{C}^+$. Let $H^\infty(\mathbb{C}^+)$ be the algebra of bounded analytic functions on $\mathbb{C}^+$. Denote by $\mathcal{M}$ the family of all non-zero multiplicative linear functionals $\{m : H^\infty(\mathbb{C}^+) \longrightarrow \mathbb{C}\}$. This collection $\mathcal{M}$ endowed with the Gelfand topology constitutes the maximal ideal space of $H^\infty(\mathbb{C}^+)$. Identifying the uniform algebra $H^\infty(\mathbb{C}^+)$ with its Gelfand transform, we can think of $H^\infty(\mathbb{C}^+)$ as a subalgebra of $\mathscr{C}(\mathcal{M})$, the algebra of continuous complex-valued functions on $\mathcal{M}$. Let ρ be the mapping of $\mathcal{M}$ into $\widehat{\mathbb{C}^+}$ defined by $\rho : \mathcal{M} \ni m \longrightarrow \rho(m) = \lambda \in \widehat{\mathbb{C}^+}$, where λ is the unique point of $\widehat{\mathbb{C}^+}$ such that $m(f) = f(\lambda)$, $f \in H^\infty(\mathbb{C}^+)$, and f is analytic near λ. For those $\lambda \in \partial_\infty\mathbb{C}^+$, there are points $m \in \mathcal{M}$ such that $\rho(m) = \lambda$. The fiber of λ in $\mathcal{M}$ is defined to be the set $\mathcal{M}_\lambda = \rho^{-1}(\{\lambda\}) = \{m \in \mathcal{M},\ \rho(m) = \lambda\}$. We can identify $\mathbb{C}^+$ with $\rho^{-1}(\mathbb{C}^+)$, and we can thus write $\mathbb{C}^+ = \{m \in \mathcal{M},\ \ \mathrm{Im}\,(\rho(m)) > 0\}$. All fibers $\mathcal{M}_\lambda$ are non-empty and mutually homeomorphic, and can be viewed as large compact spaces lying above points of $\widehat{\mathbb{C}^+}$. If Ω is a domain of the Riemann sphere which supports nonconstant bounded analytic functions and each point in $\partial\Omega$ is essential for $H^\infty(\Omega)$, then, the set $\mathfrak{C} := \mathcal{M} \setminus \overline{\Omega}$ is called the corona, and we say that the corona theorem is true if the corona $\mathfrak{C} := \mathcal{M} \setminus \overline{\Omega}$ is empty. Carleson's Corona theorem is valid for simply connected domains [2], thus in particular, the corona theorem is true for the upper half-plane $\mathbb{C}^+$. Now, denote by $\Xi^+ := \{\xi,\ \mathrm{Im}(\xi) > 0\}$, then we construct a non-constant map $L: \Xi^+ \longrightarrow \mathcal{M}$ satisfying $L(\mathbb{C}^+) \subset \mathcal{M}_0$, the fiber of $\mathcal{M}$ over $z = 0$, and $f \circ L(\xi)$ is analytic on Ξ^+, $\forall f \in H^\infty(\mathbb{C}^+)$. Further, we introduce the following pseudohyperbolic distance on $\mathcal{M}$: $\vartheta(m_1, m_2) = \sup\left\{|f(m_2)| : f \in \overline{\mathcal{B}_1}\left(H^\infty(\mathbb{C}^+)\right),\ \text{and } f(m_1) = 0\right\}$. The restriction of ϑ to $\mathbb{C}^+$ coincides with its usual Möbius invariant pseudohyperbolic distance $\vartheta_{\mathbb{C}^+}(z, w) = \left|\frac{z-w}{z-\overline{w}}\right|$, for $z, w \in \mathbb{C}^+$, which gives rise to the equivalence relation $m_1 \sim m_2$ if and only if $\vartheta(m_1, m_2) < 1$, yielding Gleason parts $G(m) = \{m' \in \mathcal{M} : \vartheta(m, m') < 1\}$. They satisfy: $G(m) \neq \emptyset$, as $m \in G(m)$, for all $m \in \mathcal{M}$, for any $w \in \mathbb{C}^+$, we have $G(w) = \mathbb{C}^+$, and two Gleason parts $G(m)$ and $G(m')$ are either identical or disjoint, also observe that Gleason parts form a partition of $\mathcal{M}$.

References

[1] Gamelin, T.W.: *Localization of the corona problem.* Pacific J. Math., 34 (1), (1970), 73–81.

[2] Garnett, J.: *Bounded analytic functions.* Pure and Applied Mathematic, 96, Academic Press, Inc., New York-London, 1981.

[3] Gleason, A.: *Function Algebras.* In Seminars on Analytic Functions, Vol. II, Institute for Advanced Study, Princeton, 1957, pp. 213-216.

[4] Hoffman, K.: *Bounded analytic functions and Gleason parts.* Ann. of Math., 86 (1967), 74–111.

[5] Krantz, S.: *Homage to A.M. Gleason and I.J. Schark.* Complex Var. Elliptic Equat. 60 (3), (2015), 310–322.

[6] McDonald, G. and Sundberg, C.: *Toeplitz operators on the disc.* Indiana Univ. Math. J., 28 (4), (1979), 595–611.

[7] Schark, I.J.: *Maximal ideals in an algebra of bounded analytic functions.* Journal of Mathematics and Mechanics, 10 (5), (1961), 735–746.

[8] Stroethoff, K.: *Essentially commuting Toeplitz operators with harmonic symbols.* Can. J. Math., 45 (5), (1993), 1080–1093.

3.7 Malik Talbi: Difference sets, Symmetric designs and the love problem

Malik Talbi
King Saud University, College of Science, Department of Mathematics, P.O. Box 2455, Riyadh 11451, Saudi Arabia

Abstract

A symmetric $(v,k,\lambda)-$design is an incidence structure consisting on v points and v blocks, such that any point is contained in k blocks, any two points are contained in λ common blocks, any block contains k points and any two blocks intersect in λ points. It is known that the last two conditions are superfluous and can be deduced from the first two ones. Symmetric designs are closely connected to groups with difference sets. Any difference set defines a symmetric design and the reciprocal is true under certain conditions. In graph theory, doubly regular tournaments and the love problem for regular digraphs define symmetric designs. The aim of this talk, is to present a topic where combinatorics, group theory, incidence geometry and number theory interact. We will discuss what happens if in the definition of symmetric designs we keep the second condition and drop the other three ones.

In this talk, we will present a topic where combinatorics, group theory, incidence geometry and number theory interact. We will start by introducing difference sets for finite groups. Then, we will talk about symmetric designs which appear very naturally. After this, we will connect them to the love problem for digraphs. Finally, we will discuss regularity conditions in the definition to present our results.

Definition 1: A difference set D in a finite group G is a proper nonempty subset of G such that any non-identity element of G can be written in exactly λ ways as $d_1d_2^{-1}$, where d_1 and d_2 are in D.

As examples, $\{1,2,4\}$ is a difference set in $\mathbb{Z}_7$ with $\lambda = 1$. $\{1,3,4,5,9\}$ is a difference set in $\mathbb{Z}_{11}$ with $\lambda = 2$. In fact, there are infinitely many examples of groups with difference sets, even for $\lambda = 1$.

Definition 2: A symmetric $(v,k,\lambda)-$design is an incidence structure $(\mathcal{P},\mathcal{B})$, where $\mathcal{P}$ is a set of v points, $\mathcal{B}$ is a set of v subsets of $\mathcal{P}$ called blocks, such that

1. any point is element of k blocks;
2. any two points are elements of λ common blocks;
3. any block contains k points;
4. any two blocks intersect in λ points.

Any group G with difference set D defines a symmetric design as follows: The points are the elements of G, the blocks are the subsets gD, where $g \in G$. A group structure is something "very regular" and so, their corresponding symmetric designs are "very regular". One needs to add more conditions on a symmetric design to make it corresponding to a group with difference set.

It is well known that axioms 3 and 4 in the definition of symmetric designs are superfluous and can be deduced from axioms 1 and 2. A question arises naturally: What happens if we keep the second axiom and drop the three others? This leads us to talk about a third structure studied in graph theory.

Definition 3: We say that a directed graph $\mathcal{G}$ has the $\lambda-$love property, if any two different vertices of $\mathcal{G}$ dominate exactly λ common vertices.

This definition corresponds to axiom 2 in the definition of symmetric designs, where blocks are the sets of vertices dominated by a vertex. Conversely, except for some special cases, to any incidence structure satisfying axiom 2, we can associate a directed graph with the $\lambda-$love property.

The love problem was first studied for tournaments, known as "Doubly regular tournaments". These are very connected to skew-symmetric Hadamard matrices. Then, the study of the love property was generalized to digraphs.

For the case $\lambda = 1$, we obtained the following results:

Result 1: Let $(\mathcal{P}, \mathcal{B})$ be an incidence structure that satisfies axiom 2 of Definition 2 with $\lambda = 1$. If none of the blocks is the whole set $\mathcal{P}$, then axiom 4 is satisfied and there exists a bijection $\phi : \mathcal{P} \rightarrow \mathcal{B}$ such that for all $p \in \mathcal{P}$, $p \notin \phi(p)$.

This result allows us to associate a directed graph that has the love property with such an incidence structure, where the set of vertices is $\mathcal{P}$ and the arcs are $\vec{pq}$ with $p \in \phi(q)$.

Result 2: Let $(\mathcal{P}, \mathcal{B})$ be an incidence structure that satisfies axiom 2 of Definition 2 with $\lambda = 1$. If all blocks have cardinality less than $v - 1$, then $(\mathcal{P}, \mathcal{B})$ is a symmetric design.

Result 3: A complete characterization of the incidence structure is given when there is a block with $v - 1$ points.

References

[1] Moore, E.H., Pollatsek, H.S. Difference sets. Connecting algebra, combinatorics, and geometry. In: Student Mathematical Library, vol. 67, American Mathematical Society, Providence (2013)·

[2] Reid, K. B., E. Brown 1972. Doubly regular tournaments are equivalent to skew-Hadamard matrices. J. Comb. Theory A 12: 332–338.

[3] John M. Hammersley. The friendship theorem and the love problem. In *Surveys in combinatorics (Southampton, 1983)*, volume 82 of *London Math. Soc. Lecture Note Ser.*, pages 31–54.

[4] Malik Talbi. Alternative proofs of a theorem of Bose and Dowling for strongly regular graphs. To appear in Journal of Multiple-Valued Logic and Soft Computing.

[5] Malik Talbi. Symmetric designs and the love problem. In preparation.

3.8 Mario Lefebvre: First-passage problems for jump-diffusion processes

Mario Lefebvre
Department of Mathematics and Industrial Engineering Polytechnique Montréal, Canada

Abstract

Let $\{X(t), t \geq 0\}$ be a diffusion process with jumps according to a Poisson process, and let $\tau(x)$ be the first time that the process, starting from $X(0) = x$, leaves the interval (a, b). Various problems for which the continuous part of the process is a Wiener, Ornstein-Uhlenbeck or Bessel process are considered. The jumps are distributed uniformly and are x-dependent. Exact and explicit expressions are obtained by solving integro-differential equations, subject to the appropriate boundary conditions.

We consider the stochastic process $\{X(t), t \geq 0\}$ defined by

$$X(t) = X(0) + \int_0^t f[X(s)]\mathrm{d}s + \int_0^t \{v[X(s)]\}^{1/2}\,\mathrm{d}B(s) + \sum_{i=0}^{N(t)} Y_i,$$

where $f(\cdot)$ is a real function, $v(\cdot) > 0$, $\{B(t), t \geq 0\}$ is a standard Brownian motion, $\{N(t), t \geq 0\}$ is a Poisson process with rate λ (which is independent of $\{B(t), t \geq 0\}$) and $Y_1, Y_2, \ldots$ are independent and identically distributed random variables. Moreover, we assume that $f(\cdot)$ and $v(\cdot)$ are such that $\{X(t), t \geq 0\}$ is a jump-diffusion process.

We define the first-passage time

$$\tau(x) = \inf\{t > 0 : X(t) \leq a \text{ or } X(t) \geq b \mid X(0) = x \in (a, b)\}.$$

Let

$$M(x;\alpha) := E\left[e^{-\alpha\tau(x)}\right],$$

where $\alpha > 0$. We can show that the function M satisfies the integro-differential equation [writing $M(x;\alpha)$ as $M(x)$]

$$\frac{1}{2}v(x)M''(x) + f(x)M'(x) + \lambda\left\{\int_{-\infty}^{\infty} M(x+y)f_Y(y)\mathrm{d}y - M(x)\right\} = \alpha M(x), \tag{3.8.1}$$

where Y is distributed as the Y_i's. The boundary conditions are $M(x) = 1$ if $x \leq a$ and $M(x) = 1$ if $x \geq b$.

Similarly, to obtain the functions $m(x) := E[\tau(x)]$ and $p(x) := P[X(\tau(x)) \leq a]$, we need to solve the following equations:

$$\frac{1}{2}v(x)m''(x) + f(x)m'(x) + \lambda\left\{\int_{-\infty}^{\infty} m(x+y)f_Y(y)\mathrm{d}y - m(x)\right\} = -1, \tag{3.8.2}$$

subject to $m(x) = 0$ if $x \leq a$ or $x \geq b$, and

$$\frac{1}{2}v(x)p''(x) + f(x)p'(x) + \lambda\left\{\int_{-\infty}^{\infty} p(x+y)f_Y(y)\mathrm{d}y - p(x)\right\} = 0, \tag{3.8.3}$$

subject to $p(x) = 1$ if $x \leq a$ and $p(x) = 0$ if $x \geq b$.

The above equations are solved explicitly in particular cases when the random variable Y has a uniform distribution on the interval $(-2x, 0)$, for $x > 0$, and on the interval $(0, -2x)$, for $x < 0$. The integro-differential equations (IDEs) are first transformed into third-order linear ordinary differential equations (ODEs). Then, the solutions to these ODEs are substituted into the IDEs to determine the constants in the solutions.

References

[1] M. Abundo: On the first-passage area of a one-dimensional jump-diffusion process, *Methodology and Computing in Applied Probability*, **15(1)** (2013), 85–103. DOI: 10.1007/s11009-011-9223-1

[2] M. Lefebvre: Exit problems for jump-diffusion processes with uniform jumps, *Journal of Stochastic Analysis*, **1(1)** (2020), Article 5. DOI: 10.31390/josa.1.1.05

[3] M. Lefebvre: Exact solutions to first-passage problems for jump-diffusion processes, *Bulletin of the Polish Academy of Sciences − Mathematics*, **72** (2024), 81–95. DOI: 10.4064/ba190812-11-6

3.9 Samir Ben Hariz: Change-point for random design regression derivative with non-stationary errors.

Samir Ben Hariz,
Laboratoire Manceau de Mathématiques. Université du Maine. Av. Olivier Messiaen. 72085 Le Mans, France.

Abstract

We consider the regression model

$$Y_i = g(X_i) + \sigma(X_i)\varepsilon_i, \quad i = 0, 1, 2..., n,$$

where the regression function derivative has a jump point at an unknown position θ. We propose a non-parametric Kernel-based estimator of the jump location θ. We prove a rate of convergence of the estimator, for a wide class of errors. This includes short-range dependent errors as well as long-range dependent and even non-stationary errors.

Key words: Change-point; Kink estimation; Non-parametric regression.

3.9.1 Introduction and main result

Change point problems are an important and active research topic in Statistics and Econometrics. It is important since structural breaks induce changes in the underlying model and therefore violates the assumptions and the conclusions are misleading. For example, in pharmacology, we are interested in the minimum effective dose. Typically the regression function $g(x)$ is the response at dose-level x, and hence we are looking for the threshold of the first raising of g from its baseline value. In economy, Y is an economic variable of interest, X is a covariate and g is the link function. Researchers often assume stability of the model governing Y. However markets are periodically subject to large shocks that can cause abrupt breaks in the model (change in policy, severe crisis, etc...). Hence, whenever there is a break, it is important to detect and locate such singularities. We also need a robust method and almost model-free to locate structural breaks. This is the main task of the the current work.

Assume that we observe n pairs of couples of variables (X_i, Y_i) following the model:

$$Y_i = g(X_i) + \sigma(X_i)\varepsilon_i \quad i = 0, 1, 2, ..., n \tag{3.9.1}$$

We assume that the function is continuous with a jump in the first derivative at θ and we seek for a robust method to estimate the change point position.

Let K be a one-sided kernel with a compact support $[0, 1]$. We define $K^*(u) = K(u)a(u - b)$, where $b = \int_0^1 vK(v)\,dv$ and $a^{-1} = \int_0^1 K(v)(v - b)v dv$. For $t \in T = \{t = k/n,\ k \quad \text{integer}, 0 \leq k/n \leq 1\}$ we define the kernel transform of Y as

$$TY(t, h) = \frac{1}{nh^2}\sum_{i=1}^{n}\left(K^*\left(\frac{X_i - t}{h}\right) + K^*\left(\frac{t - X_i}{h}\right)\right)Y_i,$$

and we estimate θ by

$$\hat{\theta} = \hat{\theta_n} = \arg\max\left\{|TY(t, h)|, h < t < 1 - h, t \in T\right\}. \tag{3.9.2}$$

The kernel transform could be written as a sum a mean part denoted $m(t)$ and a random part denoted $Z(t)$. The absolute value of the mean part achieves his maximum at $t = \theta$ and the random part will converges uniformly to zero. These two facts allow us to prove the following :

Theorem 3.9.1 *Let (X_i, Y_i) be a sequence given by (3.9.1). Under very general conditions including SRD and LRD, non-stationnary errors, we have*

$$\lim_{n\to+\infty}\mathbb{P}\left(\left|\hat{\theta_n} - \theta\right| > h\right) = 0. \tag{3.9.3}$$

3.9.2 Monte Carlo Experiments

We investigate finite sample properties of our method and we compare it to the Cheng and Raimondo's one [2]. We consider the model (3.9.1) the design variables are i.i.d uniform on $[0, 1]$. The errors are generated from an $I(d)$ sequence: $\varepsilon_i = (1 - L)^{-d}\xi_i$, where ξ_i is an i.i.d. sequence with $N(0, \sigma^2)$ law and L is the backshift operator. The sequence (ε_i) is correlated with a covariance structure of the form $Cov\,(\varepsilon_i, \varepsilon_j) \sim (1 + |i - j|)^{-\rho}$, where $\rho = 0.3, 0.7$ and ∞. The smaller is the value of ρ, the stronger is the dependence.

We run $Nsim = 10000$ simulations. For each sample, we estimate θ for different values of the window h. Then, we evaluate the mean absolute error. $MAE(n, h)$. We do the same with the Cheng and Raimondo's method.

From this small study, we can make the following comments. The two approaches behave quite similarly. It is surprising to notice that the estimator is almost insensitive to the dependence of the errors. This is in deep contrast with the fixed design regression where the rate is slower when the error's dependence is stronger.

References

[1] Samir Ben Hariz. J. Wylie. Q. Zhang. "Optimal rate of convergence for nonparametric change-point estimators for nonstationary sequences." Ann. Statist. 35 (4) 1802 - 1826.

[2] Cheng M. Y.; Raimondo M. Kernel Methods for Optimal Change-Points Estimation in Derivatives. Journal of Computational and Graphical Statistics, (2008), no. 17,56-75.

[3] Loader, C. R. Change point estimation using nonparametric regression. Ann. Statist. 24 (1996), no. 4, 1667–1678.

3.10 Mogtaba Mohammed: Homogenization of a nonlinear stochastic model for reactive flows with a noise boundary

Mogtaba Mohammed
Department of Mathematics, College of Science Majmaah University Al-Majmaah 11952, Saudi Arabia.

Abstract

In this talk, we examine the nonlinear stochastic convection and diffusion of a solute within a porous medium, accounting for a linear chemical reaction of adsorption and desorption occurring on the pore surfaces. The mathematical model consists of two coupled nonlinear stochastic convection-diffusion equations: one governing the bulk of the saturated fluid flowing through the porous medium, and the other describing the pore surface at the interface with the solid part of the medium. The two equations are coupled via a linear reaction term that represents the exchange of mass between the bulk concentration and the surface concentration. By employing the method of two-scale convergence with drift and utilizing probabilistic compactness, we derive the homogenized problem within a moving domain.

* **Mogtaba Mohammed**

Model's description:
Concentration of the solute in the Fluid Phase. In the fluid phase D^ϵ, the concentration c_f^ϵ of the solute evolves according to a nonlinear stochastic convection-diffusion equation:

$$dc_f^\epsilon + \frac{1}{\epsilon}\mathbf{v}_f^\epsilon \cdot \nabla c_f^\epsilon dt - \operatorname{div}(\kappa_f^\epsilon \nabla c_f^\epsilon)dt = \beta_f(c_f^\epsilon, \nabla c_f^\epsilon)dt + \alpha_f(c_f^\epsilon)dW_1 \text{ in } D^\epsilon \times (0,T). \tag{3.10.1}$$

Concentration of the adsorbed solutes on the surface. On the surface ∂D^ϵ, the concentration c_s^ϵ of the solute evolves according to a nonlinear stochastic convection-diffusion-reaction equation:

$$dc_s^\epsilon + \frac{1}{\epsilon}\mathbf{v}_s^\epsilon \cdot \nabla_s c_s^\epsilon dt - \operatorname{div}_s(\kappa_s^\epsilon \nabla c_s^\epsilon)dt = \frac{\eta}{\epsilon^2}\left(c_f^\epsilon - \frac{c_s^\epsilon}{\lambda}\right)dt + \alpha_s(c_s^\epsilon)dW_2 \text{ on } \partial D^\epsilon \times (0,T). \tag{3.10.2}$$

We apply the following Neumann boundary condition for the solute concentration c_f^ϵ

$$-\frac{\kappa_f^\epsilon}{\epsilon}\nabla c_f^\epsilon \cdot \mathbf{n} = \frac{\eta}{\epsilon^2}\left(c_f^\epsilon - c_s^\epsilon/\lambda\right) \text{ on } \partial D^\epsilon \times (0,T). \tag{3.10.3}$$

The initial concentrations

$$c_f^\epsilon(x,0) = c_f^0(x) \text{ in } D^\epsilon, \quad c_s^\epsilon(x,0) = c_s^0(x) \text{ on } \partial D^\epsilon, \tag{3.10.4}$$

where

- $c_f^\epsilon(x,t)$ and $c_s^\epsilon(x,t)$ are the solute concentration in the the fluid and the skeleton's surface phases,
- $\mathbf{v}_f^\epsilon(x)$ and $\mathbf{v}_s^\epsilon(x)$ are given vector functions representing the velocity fields of the fluid in the fluid and the skeleton's surface phases,
- $\kappa_f^\epsilon(x)$ and $\kappa_s^\epsilon(x)$ are the diffusion coefficient in the fluid concentrations in the fluid and the skeleton's surface phases,
- $\beta_f(t, c_f^\epsilon, \nabla c_f^\epsilon)$ is a nonlinear function that represent an external force depends on the solute concentration in the fluid phase and its diffusion,

- $\eta/\epsilon^2 \left(c_f^\epsilon - c_s^\epsilon/\lambda\right)$ is a reaction term coupling the concentrations on the fluid and on the skeleton's surface phases, where $\eta \in (0,1)$ is the rate of the adsorption in the fluid and $\lambda \in (0,1)$ is the constant of adsorption equilibrium.

- $\alpha_f(t, c_f^\epsilon)$ and $\alpha_s(t, c_s^\epsilon)$: These functions represent the strength and nature of the random forces in the fluid and the skeleton's surface phases. They allow the random fluctuations to depend on the local concentrations of the solute in both phases, meaning that areas of high solute concentration could experience more intense or different random forcing than areas with lower concentrations.

- $W_1(t)$ and $W_2(t)$ are independent standard Wiener processes associated with the fluid and the skeleton's surface phases, respectively.

Main result Homogenization results for this model. i.e., studying the asymptotic behavior of the model when ϵ goes to zero.

Idea of the proof:

- We will start by obtaining bounds estimates of various norms of the solutions of our original problems in appropriate probabilistic evolution spaces.

- We have to prove the tightness of probability measures generated by the perturbed problems.

- We will use the Prokhorov and Skorokhod's probabilistic compactness results to reduce the original problem into a new perturbed problem; in which the noise will depends on the perturbation parameter.

- The passage to the limits is more challenging because of the existence of the convection term, the dependence of the noise on the perturbation parameter, and the nonlinearity of the noise.

References

[1] G. Allaire and H. Hutridurga, Homogenization of reactive flows in porous media and competition between bulk and surface diffusion, IMA J. Appl. Math., 77 (2012), 788-815.

[2] H Bessaih, M Mohammed, IM Tayel, Homogenization and corrector results for a stochastic coupled thermoelastic model, Discrete and Continuous Dynamical Systems 45 (7), 2349-2380, 2025.

[3] M Eddahbi, M Mohammed, H El-Otman, Well-posedness of a nonlinear stochastic model for a chemical reaction in porous media and applications, AIMS Mathematics 9 (9), 24860-24886, 2024.

[4] M Mohammed, Homogenization of a nonlinear stochastic model with nonlinear random forces for chemical reactive flows in porous media.Discrete and Continuous Dynamical Systems-Series B 28 (8) 2023.

3.11 Rafik Aguech: Gaussian fluctuations of the elephant random walk with gradually increasing memory

Rafik Aguech (raguech@ksu.edu.sa)

College of Science, King Saud university.

6th Conference on Mathematical Science and Applications.

The elephant random walk (ERW) is a discrete-time random walk introduced by Schütz and Trimper (2004) in order to investigate how long-range memory affects the behavior of the random walk. Its particularity is that the next step of the walker depends on its whole past through a parameter $p \in [0, 1]$. In this work, we investigate the validity of the central limit theorem of the ERW when the walker has only a gradually increasing memory. Our contribution provides a positive answer to a conjecture raised in a recent work by Gut and Stadtmüller (2022 Stat. Probab. Lett. 189 109598).
Joint work with Mohamed El Machkouri, University of Rouen Normandie, France.

References

[1] Rafik Aguech, Mohamed El Machkouri (2024), *Gaussian fluctuations of the elephant random walk with gradually increasing memory*,
J. Phys. A: Math. Theor. 57 06520.

[2] Rafik Aguech, Mohamed El Machkouri (2024), *Corrigendum: Gaussian fluctuations of the elephant random walk with gradually increasing memory*,
J. Phys. A: Math. Theor. 57 349501

3.12 Mohamed El Machkouri: On a class of unbalanced step-reinforced random walks

R. Aguech[1], **S. Ben Hariz**[2], **M. El Machkouri**[3,*], and **Y. Faouzi**[4]
[1] Department of Statistics and Operations Research,
King Saud University, Riyadh, Saudi Arabia.
[2] Department of Mathematics, Le Mans University, France.
[3,4] EMINES - School of Industrial Management, UM6P - University Mohammed VI Polytechnic, Benguerir, Morocco.

Abstract

A step-reinforced random walk is a discrete-time stochastic process with long-range dependence. At each step, with a fixed probability $\alpha \in [0,1]$, the so-called positively step-reinforced random walk repeats one of its previous steps, chosen randomly and uniformly from its entire history. Alternatively, with probability $1-\alpha$, it makes an independent move. For the so-called negatively step-reinforced random walk, the process is similar, but any repeated step is taken with its direction reversed. These random walks have been introduced respectively by Simon [8] and Bertoin [4] and are sometimes referred to the self-confident step-reinforced random walk and the counterbalanced step-reinforced random walk respectively. In this work, we introduce a new class of unbalanced step-reinforced random walks for which we prove the strong law of large numbers and the central limit theorem. In particular, our work provides a unified treatment of the famous elephant random walk introduced by Schütz and Trimper [7] and the positively and negatively step-reinforced random walks.

* **Lead presenter**

The most famous example of step-reinforced random walk is the so-called elephant random walk (ERW) on $\mathbb{Z}$ introduced by Schütz and Trimper [7]. Its name is motivated by the well-known idea that elephants have excellent memories and are able to remember at any time all the places they have visited. At time $n = 0$, the elephant is at position $Z_0 = 0$. At time $n = 1$, the elephant moves toward 1 (i.e. "one step to the right") with probability s and toward -1 (i.e. "one step to the left") with probability $1 - s$ where $s \in [0,1]$ is a fixed parameter. Thus, the position of the elephant at time $n = 1$ is given by Z_1 where Z_1 is a Rademacher random variable satisfying $\mathbb{P}(Z_1 = 1) = 1 - \mathbb{P}(Z_1 = -1) = s$. Let $n \geqslant 1$ be a fixed integer and U_n be an integer chosen uniformly at random from the set $\{1, 2, \ldots, n\}$. Then, the $(n+1)$th step Z_{n+1} of the elephant is defined by

$$Z_{n+1} = \begin{cases} Z_{U_n} & \text{with probability } p, \\ -Z_{U_n} & \text{with probability } 1-p. \end{cases}$$

where $p \in [0,1]$ is the memory parameter of the ERW model. Thus, for $n \geq 2$, the position of the elephant at time n is $\sum_{i=1}^{n} Z_i$. The description of the asymptotic behavior of the ERW has motivated a great deal of work in recent years. In particular, it has been shown (see [7]) that the dynamics of the ERW is a function of the value of the memory parameter p. More precisely, the ERW exhibits three different regimes called *diffusive*, *critical* and *superdiffusive* depending on whether $p < 3/4$, $p = 3/4$ or $p > 3/4$ respectively. It is not possible to give an exhaustive list of the results obtained to date on the ERW. However, one can recall that by establishing an elegant connection of the ERW model with Pólya-type urns, Baur and Bertoin [1] obtained an invariance principle (functional central limit theorem) and Bercu [2] proposed a powerful approach based on martingale theory allowing to establish many limit theorems for the ERW. A step-reinforced random walk is an extension of the ERW by allowing the law of its first step Z_1 to be no longer the Rademacher law. More precisely, let $(\xi_n)_{n\geqslant 1}$ be a sequence of i.i.d. real random variables and $\alpha \in [0,1]$, a positively step-reinforced sequence $(Y_n)_{n\geqslant 1}$ is defined in the following way: $Y_1 = \xi_1$ a.s. and for any integer $n \geqslant 2$, with probability α, the nth step Y_n equals one of the previous steps $Y_1, Y_2,...,Y_{n-1}$ chosen uniformly and with probability $1-\alpha$, Y_n is defined as an independent step ξ_n. Similarly, the sequence $(Y_n)_{n\geqslant 1}$ is called a negatively step-reinforced sequence if $Y_1 = \xi_1$ and for any integer $n \geqslant 2$, with probability α, the nth step Y_n equals the opposite of one of the previous steps $Y_1, Y_2,...,Y_{n-1}$ chosen uniformly and Y_n equals an independent step ξ_n with probability $1-\alpha$. The concept of positively random walks goes back to a basic linear reinforcement algorithm which was introduced a long time ago by H. A. Simon [8] to explain the occurrence of certain heavy tailed distributions in a variety of empirical data. However, the negatively step-reinforced random walk was introduced recently by Bertoin [4] for which he investigated the law of large numbers and the central limit theorem (see also Hu and Zhang [6] and Hu [5]). In this work, we introduce a new class of step-reinforced random walks in order to provide an unified analysis of the ERW and the positively and negatively step-reinforced random walks. More precisely, if $(p,\alpha) \in [0,1]^2$ is fixed then the unbalanced step-reinforced random walk $(X_n)_{n\geqslant 1}$ with parameter (p,α) is defined by $X_1 = \xi_1$ and for any integer $n \geqslant 1$,

$$X_{n+1} = \begin{cases} X_{U_n} & \text{with probability} \quad p\alpha \\ -X_{U_n} & \text{with probability} \quad (1-p)\alpha \\ \xi_{n+1} & \text{with probability} \quad 1-\alpha \end{cases} \tag{3.12.1}$$

where $(U_n)_{n\geqslant 1}$ is a sequence of i.i.d. random variables uniformly distributed on $\{1,...,n\}$. One can notice that $(X_n)_{n\geqslant 1}$ reduces to a positively or negatively step-reinforced random walk as soon as $p=1$ or $p=0$ respectively. Moreover, if $\alpha = 1$ and $\mathbb{P}(\xi_1 = 1) = 1 - \mathbb{P}(\xi_1 = -1) = s$ with $s \in [0,1]$ then $(X_n)_{n\geqslant 1}$ reduces to the ERW introduced in Schütz and Trimper [7]. In the sequel, $T_n := \sum_{k=1}^n X_k$ denotes the position of the unbalanced step-reinforced walker at time $n \geqslant 1$. Our first result is the following strong law of large numbers.

Result 1. *If* $\mathbb{E}[|\xi_1|] < +\infty$ *then* $\frac{T_n}{n} \xrightarrow[n\to+\infty]{a.s.} \frac{(1-\alpha)\mu_1}{1-a}$.

If ξ_1 is square-integrable then the central limit theorem holds.

Result 2. *Assume that* $\mathbb{E}[\xi_1^2] < +\infty$ *and denote* $\sigma^2 = \mu_2 - \frac{(1-\alpha)^2\mu_1^2}{(1-a)^2}$ *with* $a = (2p-1)\alpha$ *and* $\mu_\ell = \mathbb{E}[\xi_1^\ell]$ *for any* $\ell \in \{1,2\}$.

i) *If* $-1 \leqslant a < 1/2$ *then* $\sqrt{n}\left(\frac{T_n}{n} - \frac{\mu_1(1-\alpha)}{1-a}\right) \xrightarrow[n\to+\infty]{\text{Law}} \mathcal{N}\left(0, \frac{\sigma^2}{1-2a}\right)$.

ii) *If* $a = 1/2$ *then* $\frac{\sqrt{n}}{\sqrt{\log n}}\left(\frac{T_n}{n} - 2\mu_1(1-\alpha)\right) \xrightarrow[n\to+\infty]{\text{Law}} \mathcal{N}\left(0, \mu_2 - 4\mu_1^2(1-\alpha)^2\right)$.

iii) *If* $1/2 < a < 1$ *then* $\sqrt{n^{2a-1}}\left(n^{1-a}\left(\frac{T_n}{n} - \frac{\mu_1(1-\alpha)}{1-a}\right) - L\right) \xrightarrow[n\to+\infty]{\text{Law}} \mathcal{N}\left(0, \frac{\sigma^2}{2a-1}\right)$ *where* L *is a non-gaussian square-integrable random variable.*

Ideas of the proofs: truncation techniques and martingale limit theory.

References

[1] Baur, E.. and Bertoin, J.: *Elephant random walks and their connection to Pólya-type urns*, Physical review., E 94, 052134, 2016.

[2] Bercu, B.: *A martingale approach for the elephant random walk*, J. Phys. A, Journal of Physics. A. Mathematical and Theoretical, 51, 2018, 1, 015201, 16.

[3] Bercu, B. and Laulin, L.: *On the multi-dimensional elephant random walk*, J. Stat. Phys., Journal of Statistical Physics, 175, 2019, 6, 1146–1163.

[4] Bertoin, J.: *Counterbalancing steps at random in a random walk*, J. Eur. Math. Soc. 26, 2655–2677 (2024).

[5] Hu, Z.: *Berry-Esseen bounds for step-reinforced random walks*, arXiv:2504.02502v1.

[6] Hu, Z and Zhang, Y.: *Strong limit theorems for step-reinforced random walks*, Stochastic Process. Appl., 178, Paper No. 104484, 16 pages, 2024.

[7] Schütz, G. M. and Trimper, S.: *Elephants can always remember: Exact long-range memory effects in a non-Markovian random walk*, Phys. Rev., E 70, 045101, 2004.

[8] Simon, H.A.: *On a class of skew distributions functions*, Biometrika, 42, 425-440, 1955.

3.13 Wissem Jedidi: Advances in Generalized Stieltjes Transforms and Their Implications for Infinite Divisibility

Wissem Jedidi
Department of STAT & OR, College of Science, Kind Saud University, Saudi Arabia.

Abstract

The investigation of infinitely divisible distributions occupies a central position in the probabilistic analysis of limit theorems for stochastic processes. These distributions, distinguished by their decomposability into an infinite convolution of independent and identically distributed random variables, constitute a cornerstone of modern probability theory. This work focuses on the class of ID laws supported on the non-negative real half-line $\mathbb{R}_+$, examined through the lens of their Lévy–Khintchine representation in terms of Bernstein functions. By systematically studying the functional transformations of these Bernstein functions, we elucidate their implications for the associated probability measures, thereby establishing connections to both probabilistic modeling and analytical techniques in mathematical statistics. A principal contribution lies in the detailed examination of three hierarchically nested subclasses of Bernstein functions, indexed by a shape parameter, which arise naturally in the context of generalized Stieltjes transforms. This analysis yields novel insights into the deep structural relationships between analytic function theory and the theory of infinite divisibility.

References

[1] D. Karp and E. Prilepkina: Generalized Stieltjes functions and their exact order, *J. Class. Anal.* **1**(1)(2012) , 53-74.

[2] Schilling, R.L.; Song, R.; Vondraček, Z.: *Bernstein functions. Theory and applications.* Second edition. de Gruyter Studies in Mathematics, 37. Walter de Gruyter & Co., Berlin 2012.

[3] Steutel, F.W., Van Harn, K.: *Infinite divisibility of probability distributions on the real line.* Marcel Dekker 2004.

[4] Widder, D.V.: *The Laplace Transform*, Princeton Univ. Press, Princeton 1941.

3.14 Mofdi El-Amrani: Enhancing modelling of fish population dynamics in the Mediterranean Sea using stochastic PDEs

Mofdi El-Amrani[1,*] **Nafea Lachhab[1]** **Nabil El Moçayd**[2] and **Mohammed Seaid[3]**
[1]Laboratory of Mathematics and Applications, FSTT, Abdelmalek Essaadi University, Tangier, Morocco
[2]College of Agriculture and Environmental Sciences, University Mohammed VI Polytechnic, Benguerir, Morocco
[3]Department of Engineering, University of Durham, South Road, Durham DH1 3LE, UK.

Abstract

In this study, we investigate the implementation of a class of stochastic partial differential equations for the mathematical modelling and numerical simulation of fish population dynamics. The considered model consists of a system of stochastic differential equations for transport and dispersion of fish population based on an empirical equations for habitat index. The hydrodynamics is also accounted for in this study by solving a barotropic ocean model with friction terms, bathymetric forces, Coriolis and wind stresses. As a numerical solver, we propose a high-order stochastic Runge-Kutta scheme coupled with a multilevel adaptive semi-Lagrangian finite element method that combines various techniques, including the modified method of characteristics, finite element discretization, coupled projection scheme based on a rotational pressure correction algorithm, and an adaptive L^2-projection. The method is fast, highly accurate and can be used for both slowly and rapidly hydrodynamics simulations. The approach also employs the gradient of the concentration as an error indicator for enrichment adaptations and increasing the number of quadrature points where needed without refining the mesh. The method is shown to provide accurate and efficient simulations for fish population dynamics subject to different scenarios. The proposed approach distinguishes itself from the well-established adaptive finite element methods for incompressible viscous flows by retaining the same structure and dimension of linear systems during the adaptation process. Numerical results are shown for several test examples including a problem of fish population dynamics in the Mediterranean Sea. The results demonstrate the robustness of the stochastic partial differential equations compared to the standard Monte-Carlo simulations. The results presented in this study suggest that the use of high-order stochastic Runge-Kutta methods may also save a considerable amount of the necessary computational cost for all the considered cases.

* **Lead presenter**

References

[1] M. El-Amrani, A. Ouardghi, M. Seaid: Modeling and simulation of pollution transport in the Mediterranean Sea using enriched finite element method, *Mathematics and Computers in Simulation*, **223** (2024), 565-587.

[2] M. El-Amrani, A. Ouardghi, M. Seaid: A fast and accurate method for transport and dispersion of phosphogypsum in coastal zones: Application to Jorf Lasfar, *International Journal for Numerical Methods in Fluids*, **96** (2024), 336-363.

[3] M. El-Amrani, A. Ouardghi, M. Seaid: Enriched Galerkin-Characteristics Finite Element Method for Incompressible Navier–Stokes Equations, *SIAM Journal on Scientific Computing*, **43** (2021), A1336-A1361.

3.15 Mourad Ben Slimane: On anisotropic and directional regularity

Mourad Ben Slimane
King Saud University, College of Science, Department of Mathematics, P.O. Box 2455, Riyadh 11451, Saudi Arabia

Abstract

Many mathematical objects, as well as many multivariate signals and images need to distinguish local directional behaviors. We obtain criteria of directional and anisotropic regularities by decay conditions on anisotropic wavelet coefficients.

The classical pointwise Hölder regularity of a multi-variate function is uniform in all directions. However many classes of functions are images exhibiting singularities in many directions (sattelite images of clouds, X-ray of bones, medical images, see [1]).

Usual isotropic wavelets do not deal with directional regularity efficiently.

Using some results of Jaffard and Triebel, we obtain criteria of directional and anisotropic regularities by decay conditions on Triebel anisotropic wavelet coefficients.

Result 1 Using some results of Jaffard and Triebel [2,3], we obtain criteria of anisotropic regularity by decay conditions on Triebel anisotropic wavelet coefficients.

Idea of the proof: The proof is based on the regularity and cancellation of anisotropic wavelets.

Result 2 We characterize pointwise directional regularity by highly oriented multi-scaled wavelet coefficients

Idea of the proof: The proof is based on the link between directional and multi-anisotropic regularities.

References

[1] Arneodo, A., Audit, B., Decoster, N., Muzy, J.-F. and Vaillant, C. (2002). Wavelet-based multifractal formalism: applications to DNA sequences, satellite images of the cloud structure and stock market data, in *The Science of Disasters*, A. Bunde, J. Kropp, H. J. Schellnhuber eds., Springer, 27–102.

[2] S. Jaffard: Pointwise and directional regularity of nonharmonic Fourier series, *Appl. Comput. Harmon. Anal.*, **28**, (2010), 251–266.

[3] H. Triebel, Theory of Function Spaces III, Monographs in Mathematics, **78**, Birkhäuser, Basel 2006.

3.16 Nasser-eddine Tatar: Control of structures under large amplitudes

Nasser-eddine Tatar
King Fahd University of Petroleum and Minerals, Department of Mathematics, Dhahran, Saudi Arabia.
Email: tatarn@kfupm.edu.sa

Abstract

The long-time behavior of a one-dimensional viscoelastic porous-elastic system with large amplitude is considered in the present paper. We prove an exponential decay result under the weak dissipation produced by the viscoelasticity in the first equation and the other one acting in the second equation. The major difficulty encountered in the analysis stems from the non-applicability of the energy method at least in the usual way. This is due to the large deformation.

We consider the model

$$\begin{cases} \rho u_{tt} - \left[\left(1+\frac{1}{\sqrt{1+|u_x|^2}}\right)u_x\right]_x + \int_0^t g(t-s)\left[\left(1+\frac{1}{\sqrt{1+|u_x|^2}}\right)u_x\right]_x ds - b\phi_x = 0, \\ J\phi_{tt} - \delta\phi_{xx} + bu_x + \xi\phi + \tau\phi_t = 0, \end{cases} \tag{3.16.1}$$

with the boundary conditions

$$\phi(0,t) = \phi(1,t) = u(0,t) = u(1,t) = 0, \tag{3.16.2}$$

and the initial data

$$\begin{cases} u(x,0) = u_0(x),\ u_t(x,0) = u_1(x), \\ \phi(x,0) = \phi_0(x),\ \phi_t(x,0) = \phi_1(x), \end{cases} \tag{3.16.3}$$

where $x \in [0,1]$ and $t \in \mathbb{R}^+$. Here, u is the displacement of the solid elastic material and ϕ is the volume fraction. The system describes materials where the mass at each point is obtained by the product of the mass density of the material matrix by the volume fraction. The importance of such materials comes from the applications in different fields in petroleum industry, material science, soil mechanics, foundation engineering, powder technology, biology and others. For more details, we refer to ([1], [2], [3], [4]) and the references therein.

In contrast to the commonly used models, structures subjected to large amplitude, have not been well-studied. In this case, the spacial derivative u_x is of significant value. Therefore, the standard simplification

$$1 + (u_x)^2 \approx 1$$

is no longer reasonable.

Motivated by the above results, we aim in this work to extend the existing works to the case of large amplitude of u_x.

$$\begin{aligned} E(t) \;=\;& \frac{\rho}{2}||u_t||_2^2 + \frac{J}{2}||\phi_t||_2^2 + \frac{\delta}{2}||\phi_x||_2^2 + \frac{1}{2}\left(1 - \int_0^t g(s)ds\right)||u_x||_2^2 \\ &+ \frac{\xi}{2}||\phi||_2^2 + ||u_{xt}||_2^2 + \frac{1}{2}(g\circ u_x)(t) + \int_0^1 \left(b\phi u_x + \sqrt{1+|u_x|^2} - 1\right)dx \end{aligned} \tag{3.16.4}$$

Result (Exponential Decay) *Let* (u,ϕ) *be a solution of system* (3.16.1) $-$ (4.2.2). *Assume further that the assumptions* $\xi l > b^2$ and $g(0) > 0, \quad 1 - \int_0^\infty g(s)ds =: l > 0$ *are fulfilled. Then, there is a* $g^* > 0$ *such that the solution energy* (3.16.4) *satisfies, for two positive constants* k_1, k_2,

$$E(t) \le k_1 e^{-k_2 t}, \qquad \forall t \ge 0,$$

provided that $\overline{g} \le g^*$*(determined in the proof).*

Idea of the proof: We shall introduce some appropriately chosen Lyapunov functionals in the context of the multiplier technique combined with some properties of positive definite functions.

References

[1] S. Chiriţă, M. Ciarletta, and C. D'Apice, On the theory of thermoelasticity with microtemperatures, J. Math. Anal. Appl. 397 (2013) 349–361.

[2] S. C. Cowin and J. W. Nunziato, Linear elastic materials with voids, J. Elast. 13 (1983) 125–147.

[3] S. C. Cowin, The viscoelastic behavior of linear elastic materials with voids, J. Elast. 15 (1985) 185–191.

[4] A. Magana and R. Quintanilla, On the time decay of solutions in one-dimensional theories of porous materials, Int. J. Solids Struct. 43 (2006) 3414–3427.

3.17 Mohammed Guediri: Characterizing Extrinsic Spheres in Riemannian and Lorentzian Einstein Manifolds

Mohammed Guediri
King Saud University, College of Science, Department of Mathematics, P.O. Box 2455, Riyadh 11451, Saudi Arabia

Abstract

In this talk, we explore rigidity results for compact Riemannian and spacelike hypersurfaces in Einstein Riemannian and Lorentzian manifolds, respectively. The main result asserts that for a compact Riemannian (or spacelike) hypersurface (M, g) in an Einstein Riemannian (or Lorentzian) manifold $(\overline{M}, \overline{g})$ which admits a conformal vector field $\overline{\xi}$ (assumed to be timelike in the Lorentzian case), the hypersurface (M, g) is an extrinsic sphere in $(\overline{M}, \overline{g})$ if and only if the integral of the Ricci curvature of the hypersurface, taken in the direction of the tangential component $\xi^{\top}$ of the restriction ξ of $\overline{\xi}$ to M, satisfies a certain lower bound. As an application of this main result, we investigate compact spacelike hypersurfaces in generalized Robertson-Walker (GRW) spacetimes.

3.18 Reny George: On some dislocated generalized metric spaces and applications

Turki Bin Hussein Bin Sultan Alduwaihi[1] , **Sultan bin Abdullah bin Abdulaziz Al-Solah**[2], **Abdullah bin Saud bin Ibrahim Swailem [3]** and **Reny George[4,*]**
[1,2,3,4]Department of Mathematics, College of Science and Humanities in Alkharj, Prince Sattam bin Abdulaziz University, Alkharj, Saudi Arabia

Abstract

In this paper we introduce the concepts of some dislocated generalized metric spaces such as dislocated quais α_v-controlled metric space, dislocated quasi θ_v-extended b-metric space which are generalisations of $b_v(s)$-metric space, extended b-metric space and controlled metric space and other spaces existing in literature. We further investigate some possible applications of these spaces in fixed point theory. Our claims are supported by proper numerical examples.

* **Lead presenter**

In our first result we introduce α_v-controlled metric space and θ_v-extended metric space from which we deduce several concepts of generalized metric spaces which are either new in literature or are generalizations of some existing concepts.

Definition 3.18.1 *Let X be a nonempty set and $d_\alpha : X \times X \to R$. For all $x, y, \in X$ and distinct $u_1, \cdots, u_v \in X - \{x, y\}$, consider the following axioms:*

$(b_{\alpha-1})$ $d_\alpha(x,y) \geq 0$ *and* $d_\alpha(x,y) = 0$ *implies* $x = y$,

$(b_{\alpha-2})$ $d_\alpha(x,x) = 0$,

$(b_{\alpha-3})$ $d_\alpha(x,y) = d_\alpha(y,x)$,

$(b_{\alpha-4})$ $d_\alpha(x,y) \leq \alpha(x,u_1)d_\alpha(x,u_1)+\alpha(u_1,u_2)d_\alpha(u_1,u_2)+\cdots+\alpha(u_{v-1},u_v)d_\alpha(u_{v-1},u_v)+\alpha(u_v,y)d_\alpha(u_v,y)]$, *for some* $\alpha : X \times X \to [1,\infty)$,

$(b_{\alpha-5})$ $d_\alpha(x,y) \leq \theta(x,y[)d_\alpha(x,u_1)+d_\alpha(u_1,u_2)+\cdots+d_\alpha(u_{v-1},u_v)+d_\alpha(u_v,y)]$, *for some* $\theta : X\times X \to [1,\infty)$

*If d_α satisfy $(b_{\alpha-1})$, $(b_{\alpha-2})$, $(b_{\alpha-3})$ and $(b_{\alpha-4})$ then we say that d_α is an α_v-controlled metric on X and (X, d_α, α) is α_v-**controlled metric space**.*
*If d_α satisfy $(b_{\alpha-1})$, $(b_{\alpha-2})$, $(b_{\alpha-3})$ and $(b_{\alpha-5})$ then we say that d_α is a θ_v-extended metric on X and (X, d_α, θ) is a θ_v-**extended metric space**. If d_α satisfy $(b_{\alpha-1})$, $(b_{\alpha-3})$ and $(b_{\alpha-4})$ then we say that d_α is a dislocated α_v-controlled metric on X and (X, d_α, α) is a **dislocated** α_v-**controlled metric space**. If d_α satisfy $(b_{\alpha-1})$, $(b_{\alpha-3})$ and $(b_{\alpha-5})$ then we say that d_α is a dislocated θ_v-extended metric on X and (X, d_α, θ) is a **dislocated** θ_v-**extended metric space**. If d_α satisfy $(b_{\alpha-1})$, $(b_{\alpha-2})$ and $(b_{\alpha-4})$ then we say that d_α is a quasi α_v-controlled metric on X and (X, d_α, α) is a **quasi** α_v-**controlled metric space**. If d_α satisfy $(b_{\alpha-1})$, $(b_{\alpha-2})$ and $(b_{\alpha-5})$ then we say that d_α is a quasi θ_v-extended metric on X and (X, d_α, θ) is a **quasi** θ_v-**extended metric space**. If d_α satisfy $(b_{\alpha-1})$ and $(b_{\alpha-4})$ then we say that d_α is a dislocated quasi α_v-controlled metric on X and (X, d_α, α) is a **dislocated quasi** α_v-**controlled metric space**. If d_α satisfy $(b_{\alpha-1})$ and $(b_{\alpha-5})$ then we say that d_α is a dislocated quasi θ_v-extended metric on X and (X, d_α, θ) is a **dislocated quasi** θ_v-**extended metric space**.*

Some deductions

Remark 3.18.1

- *For $v = 1$, dislocated α_v-controlled metric space is a dislocated controlled metric space which is a generalization of controlled metric space given in [2].*

- *For $v=1$, dislocated θ_v-extended metric space is a dislocated extended metric space which is a generalization of extended metric space given in [3].*

- *For $v=1$, quasi α_v-controlled metric space is a quasi controlled metric space which is a generalization of controlled metric space given in [2].*

- *For $v=1$, quasi θ_v-extended metric space is a quasi extended metric space which is a generalization of extended metric space given in [3].*

- *For $v=1$, dislocated quasi α_v-controlled metric space is a dislocated quasi controlled metric space which is a generalization of controlled metric space given in [2].*

- *For $v=1$, dislocated quasi θ_v-extended metric space is a dislocated quasi extended metric space which is a generalization of extended metric space given in [3].*

Some remarks

Remark 3.18.2 *By taking $\alpha(x,y)=s$ for all $x,y\in X$ and some $s\geq 1$, α_v-controlled metric space reduces to $b_v(s)$ metric space given in [1]. Thus every $b_v(s)$ metric space is an α_v-controlled metric space with $\alpha(x,y)=s$ for all $x,y\in X$ and some $s\geq 1$. But the converse is not necessarily true.*
By taking $\theta(x,y)=s$ for all $x,y\in X$ and some $s\geq 1$, θ_v-extended metric space reduces to $b_v(s)$ metric space given in [1]. Thus every $b_v(s)$ metric space is a θ_v-extended metric space with $\alpha(x,y)=s$ for all $x,y\in X$ and some $s\geq 1$. But the converse is not necessarily true.
α_v-controlled metric space and θ_v-extended metric space are independent of each other.
For $v=1$, α_v-controlled metric space is a controlled metric space given in [2].
For $v=1$, θ_v-extended metric space is an extended metric space given in [3].
For $v=2$, α_v-controlled metric space is a controlled rectangular metric space given in [4].

In our second result we prove some fixed point theorems in α_v-controlled metric space and θ_v-extended metric space which generalizes many known results in literature.
Let (X,d_α,α) is α_v-controlled metric space and $T:X\to X$. We then say that T is a $(\mathbf{G},\mathbf{d}_\alpha)$-implicit type mapping if there exists $\mathbf{G}\in\mathbf{W}_\alpha$ such that for $x,y\in X$,

$$\mathbf{G}(\alpha(x,y)d_\alpha(Tx,Ty),d_\alpha(x,y),d_\alpha(x,Tx),d_\alpha(y,Ty),d_\alpha(x,Ty))\leq 0.$$

Theorem 3.18.1 *Let (X,d_α,α) be a right (or left) d_α-complete α_v-controlled metric space and $T\colon X\to X$ be a continuous $(\mathbf{G},\mathbf{d}_\alpha)$-implicit type mapping. Then T has a unique fixed point.*

Note: We provide an analytical proof for the above theorem and deduce various known results in fixed point theory as corollary to the above theorem. We also provide proper example in support of our theorem and further investigate its applications in other mathematical problems arising in engineering and science.

References

[1] Zoran Mitrovic and Stojan Radenovic: The Banach and Reich contractions in $b_v(s)$- metric spaces,*Journal of Fixed Point Theory and Applications*, **19** (2017), 3087-3095.

[2] Nabil Mlaiki, Hassen Aydi,Nizar souayah and Thabet Abdeljawad: Controlled metric type spaces and the related contraction principles, *Mathematics*, **6, 194** (2018)

[3] T. Kamran, M. Samreen and O.U Ain, A generalisation of b-metric space and some fixed point theorems, *Mathematics*, **5, 19** (2017)

3.19 Said Mesloub: On a Fractional Nonlinear Singular Quasistatic problem

Said Mesloub, Eman Alhazzani
Mathematics Department, College of Science, King Saud University, P.O. Box 2455, Riyadh 11451, Saudi Arabia.

Abstract

This work deals with the well posedness of a one point initial boundary value problem for a nonlinear fractional singular integro-differential equation, which arises from one-dimensional quasi-static contact problems in nonlinear thermo-elasticity. Our proofs are mainly based on a fixed point theorem and some a priori bounds. The solvability of the problem is proved when the given data are related to a weighted Sobolev space. An additional result allows us to study the regularity of the solution of the posed problem is obtained.

3.19.1 Statement of the Problem

In the rectangle $Q_T = (0,1) \times [0,T]$, where $0 < T < \infty$, we consider the fractional nonlinear singular second order integro-differential equation

$$\partial_t^\sigma \theta - \frac{\partial^2 \theta}{\partial x^2} - \frac{1}{x}\frac{\partial \theta}{\partial x} + \theta = \max\left(\int_0^x \eta\theta(\eta,t)d\eta, 0\right) + \beta(x,t), \tag{3.19.1}$$

where $\partial_t^\sigma \theta$ indicates the right Caputo fractional derivative of order σ, $0 < \sigma \leq 1$ given by

$$\partial_t^\sigma \theta = \frac{1}{\Gamma(1-\sigma)} \int_0^t \frac{\theta_\tau(\tau)}{(t-\tau)^\sigma} d\tau, \quad \forall t \in [0,T].$$

The equation (3.19.1) is supplemented by the initial condition

$$\theta(x,0) = Z(x),\ x \in (0,1), \tag{3.19.2}$$

and the one point boundary condition

$$\theta_x(1,t) = 0, \qquad t \in [0,T], \tag{3.19.3}$$

where $Z(x) \in W^1_{\rho,2}((0,1)$, and $\beta \in L^2(0,T;L^2(0,1)$

3.19.2 Uniqueness of solution

Theorem 3.19.1 *Let $Z \in W^1_{\rho,2}((0,1)$, and $\beta \in L^2(0,T;L^2_\rho(0,1)$. Then the posed problem (3.19.1)-(3.19.3) has at most one solution in $L^2(0,T;H^\sigma_\rho((0,1)$, if it exists.*

3.19.3 Solvability and existence of nontrivial solution

Theorem 3.19.2 *Let $Z \in W^1_{\rho,2}((0,1))$, and $\beta \in L^2(0,T;L^2_\rho(0,1))$ be given and satisfy*

$$\|Z\|^2_{W^1_{\rho,2}((0,1))} + \|\beta\|^2_{L^2(0,T;L^2_\rho(0,1))} \leq C_2, \tag{3.19.4}$$

for $C_2 > 0$ small enough and that

$$\frac{\partial Z(1)}{\partial x} = 0. \tag{3.19.5}$$

Then problem (3.19.1)-(3.19.3) admits a unique solution $\theta \in L^2(0,T;H^\sigma_\rho((0,1))$.

3.19.4 A priori bound and regularity of the solution

Theorem 3.19.3 *Let $L^2(0,T;H^{2,\sigma}_{\gamma}(0,1))$, be a solution of problem(3.19.1)-(3.19.3), then the following a priori estimate is true*

$$\|\theta\|^2_{L^2(0,T;H^{2,\sigma}_{\gamma}(0,1))} \leq D\left(\|Z\|^2_{W^1_{2,\gamma}((0,1))} + \|\beta\|^2_{L^2(0,T;L^2_{\rho}(0,1))}\right), \tag{3.19.6}$$

where

$$D = \max\left\{2, \frac{T^{1-\sigma}}{(1-\sigma)\Gamma(1-\sigma)}\right\}. \tag{3.19.7}$$

References

[1] Miller, R.K.: An integro-differential equation for grid heat conductors with memory. J.Math. Anal. Appl. 66, 313–332 (1978).

[2] Wang, Y., Liu, L.: Uniqueness and existence of positive solutions for the fractional integro-differential equation. Bound. Value Probl. 2017, 12 (2017).

[3] M. Renardy, W. J. Hrusa, J. A. Nohel; Mathematical Problems in Viscoelasticity, Pitman Monogr. Pure Appl. Math., vol. 35, Longman Sci. Tech., Harlow, Essex, 1988.

[4] M. Renardi, W. J. Hrusa, J. A. Nohel; Mathematical problems in viscoelasticity, Pitman Monographs and Surveys Pure Appl. Math. No. 35, Wiley, 1987.

[5] S. Mesloub, F. Aldosari, Well posedness for a singular two dimensional fractional initial boundary value problem with Bessel operator involving boundary integral conditions, AIMS Mathematics, 2021, Volume 6, Issue 9: 9786-9812. doi: 10.3934/math.2021569.

[6] Mesloub, S.: A nonlinear nonlocal mixed problem for a second order parabolic equation. J. Math. Anal. Appl. 316, 189-209 (2006).

[7] M.M. Arjunan and V. Kavitha, Controllability of impulsive fractional evolution integrodifferential equations in Banach spaces, J. KSIAM 15 (2011), 177–190.

[8] B. Ahmed and S. Sivasundaram. Existence of solutions for nonlinear fractional integro-differential equations with three-point nonlocal fractional boundary condi- tions. Advances in Difference Equations, 2010:Article ID 691721, 2020.

3.20 Messaoud Bounkhel: Mathematical Modeling of the motion of nanoparticles in straight Tube

Messaoud Bounkhel
King Saud University, College of Science, Department of Mathematics, P.O. Box 2455, Riyadh 11451, Saudi Arabia.

Abstract

Nanotechnology is a rapidly evolving field with profound implications for science and technology, leading to significant research investments worldwide. While most studies in this domain primarily address chemical, physical, and biological phenomena or their intersections, mathematical modeling remains an underexplored yet highly valuable approach. By leveraging mathematical models, researchers can significantly reduce the time required for experimental validation, thereby optimizing research efficiency and minimizing costs.

In this work, we focus on the mathematical modeling of nanoparticle motion within a viscous fluid confined in a straight tube. Our goal is to illustrate how Nonsmooth Analysis and Multivalued Differential Equations can serve as powerful tools for modeling and simulating complex real-world phenomena. The presentation is divided into two main sections. The first part introduces fundamental theoretical concepts and key results in Nonsmooth Analysis and Multivalued Differential Equations, providing the necessary groundwork for their application. The second part explores their practical implementation, where we integrate the proposed theoretical framework with a differential system to model nanoparticle dynamics effectively.

Furthermore, we present a numerical simulation that visually demonstrates the behavior of nanoparticles in straight tubes, highlighting the accuracy and efficiency of our approach. These simulations offer valuable insights into the movement patterns of nanoparticles in confined environments, which can be crucial for various applications, including biomedical engineering, drug delivery systems, and microfluidics. By bridging the gap between abstract mathematical theory and applied nanotechnology, this work underscores the potential of mathematical modeling as a transformative tool in advancing research in this field.

3.21 Fairouz Tchier: Relational Demonic Fuzzy Refinement and some applications

Fairouz Tchier,
Mathematics department King Saud University Riyadh, Saudi Arabia ftchier@ksu.edu.sa.

Abstract

We use relational algebra to define a refinement fuzzy ordering called (*demonic fuzzy refinement*) and also the associated fuzzy operators which are fuzzy demonic join, fuzzy demonic meet and fuzzy demonic composition. Our definitions and properties are illustrated by some examples using mathematica software (fuzzy logic). We applied our results to irrigation, traffic lights and to diabetics diagnosis.

Fuzzy set theory appeared in 1965 [8]. Since then, it has received increasing attention by the scientific community and applied in almost all the general disciplines known in the world [3]. Fuzzy set theory provides a strict mathematical framework (there is nothing fuzzy about fuzzy set theory) in which vague conceptual phenomena can be precisely and rigorously studied. It can also be considered as a modeling language well suited for situations in which fuzzy relations, criteria, and phenomena exist. It will mean different things, depending on the application area and the way it is measured. In the meantime, numerous authors have contributed to this theory. In 1984 as many as 4000 publications may already exist. The first publications in fuzzy set theory by Zadeh [8] and Goguen [1, 2] show the intention of the authors to generalize the classical notion of a set. Zadeh [8] writes:"The notion of a fuzzy set provides a convenient point of departure for the construction of a conceptual framework which parallels in many respects the framework used in the case of ordinary sets, but is more general than the latter and, potentially, may prove to have a much wider scope of applicability, particularly in the fields of mathematics and computer science (pattern classification and information processing). Fuzzy logic is a superset of conventional logic that has been extended to handle the concept of partial truth-truth values between "completely true" and "completely false". As its name suggests, it is the logic underlying modes of reasoning which are approximate rather than exact. The importance of fuzzy theory derives from the fact that most modes of human reasoning and especially common sense reasoning are approximate in nature.
The calculus of relations has been an important component of the development of logic and algebra since the middle of the nineteenth century [4, 5] The main advantages of the relational formalization are uniformity and modularity. Actually, once problems in these fields are formalized in terms of relational calculus, these problems can be considered by using formulae of relations, that is, we need only calculus of relations in order to solve the problems. In the context of software development, one important approach is that of developing programs from specifications by stepwise refinement, see, e.g. [6, 7]. One point of view is that a specification is a relation constraining the input-output (respectively, argument-result) behaviour of programs.

Result 1 We used previous results in fuzzy theory and in relational algebra to define demonic fuzzy operators and apply them to real-world problems. We used theoretical and software engineering concepts (Mathematica and Phyton) to do illustrate our results

Idea of the proof: The demonic calculus of relations views any relation R from a set A to another set B as specifying those programs that terminate for all $a \in A$ wherever R associates any values from B with a, and then the program may only return values b for which $(a, b) \in R$. Consequently, a relation R refines another relation S if R specifies a larger domain of termination and fewer possibilities for return values. The demonic calculus of relations has the advantage that the demonic operations are defined on top of the conventional relation algebraic operations, and can easily and usefully be mixed with the latter, allowing the application of numerous algebraic properties.

References

[1] Goguen, J. A. . : L-fuzzy sets. *JMAA 18*, 145-174.

[2] Goguen, J. A. . : The logic of inexact concepts. *Synthese 19*, 325-373.

[3] Mamdani, E. H. : "Advances in the Linguistic Syntesis of Fuzzy Controllers In Fuzzy Reasoning and Its Applications", Academic Press, London (1981).

[4] Ströhlein, E.: Vorlesungen über die Algebra der Logik(exacte Logik). Teubner, Leipzig, 1895.Vol.3, Algebra und Logik der Relative, part I,2^{nd}edition published by Chelsea, 1966.

[5] Tarski, A.: On the calculus of relations. *J. Symb. Log. 6*, 3, 1941, 73–89.

[6] Tchier, F.: Demonic semantics by monotypes. *International Arab conference on Information Technology* (Acit2002),University of Qatar, Qatar, 16-19 December 2002.

[7] Tchier, F.: While loop demonic relational semantics monotype/residual style. *2003 International Conference on Software Engineering Research and Practice (SERP'03)*, Las Vegas, Nevada, USA, 23-26, June 2003.

[8] Zadeh, L. A. .: Fuzzy Sets. *Inform and Control 8* 1965, 338–353.

3.22 Alfonso Montes: Hyperbolic Fourier series

Alfonso Montes-Rodríguez
Montes-Rodríguez: Department of Mathematical Analysis University of Sevilla, Sevilla, Spain, amontes@us.es.

Abstract

A pair (Γ, Λ), where $\Gamma \subset \mathbb{R}^2$ is a locally rectifiable curve and $\Lambda \subset \mathbb{R}^2$ is a *Heisenberg uniqueness pair* if an absolutely continuous finite complex-valued Borel measure supported on Γ whose Fourier transform vanishes on Λ necessarily is the zero measure. Here, absolute continuity is with respect to arc length measure. If Γ is the hyperbola $x_1x_2 = M^2/(4\pi^2)$, where $M > 0$ is the mass, and Λ is the lattice-cross $(\alpha\mathbb{Z} \times \{0\}) \cup (\{0\} \times \beta\mathbb{Z})$, where α, β are positive reals, then (Γ, Λ) is a Heisenberg uniqueness pair if and only if $\alpha\beta M^2 \leq 4\pi^2$. The Fourier transform of a measure supported on a hyperbola solves the one-dimensional Klein-Gordon equation, so the theorem supplies discrete uniqueness sets for a class of solutions to this equation. By rescaling, we may assume that the mass equals $M = 2\pi$, and then the above-mentioned theorem is equivalent to the following assertion: *the functions*

$$e^{\mathrm{i}\pi\alpha mt}, \quad e^{-\mathrm{i}\pi\beta n/t}, \qquad m, n \in \mathbb{Z},$$

span a weak-star dense subspace of $L^\infty(\mathbb{R})$ if and only if $0 < \alpha\beta \leq 1$. The proof involved ideas from Ergodic Theory. To be more specific, in the critical regime $\alpha\beta = 1$, the crucial fact was that the Gauss-type map $t \mapsto -1/t$ modulo $2\mathbb{Z}$ on $[-1, 1]$ has an ergodic absolutely continuous invariant measure with infinite total mass.

As for the holomorphic counterpart, *it can be shown that the functions*

$$e^{i\pi\alpha mt}, \quad \mathrm{e}^{-i\pi\beta n/t}, \qquad m, n \in \mathbb{Z}_+ \cup \{0\},$$

span a weak-star dense subspace of $H^\infty_+(\mathbb{R})$ *if and only if* $0 < \alpha\beta \leq 1$. Here, $H^\infty_+(\mathbb{R})$ is the subspace of $L^\infty(\mathbb{R})$ which consists of those functions whose Poisson extensions to the upper half-plane are holomorphic. In the critical regime $\alpha\beta = 1$, the proof relies on the nonexistence of a certain invariant distribution in the predual of real H^∞ for the above mentioned Gauss-type map on the interval $[1, 1]$, which is a new result of dynamical flavor. To attain it, we need a subtle analysis of the iterates of the even Gauss operator

$$(\mathbf{P}f)(x) = \sum_{k \in \mathbb{Z} \setminus \{0\}} \frac{1}{(x + 2k)^2} f\left(\frac{-1}{x + 2k}\right)$$

We have to handle in detail series of powers of the even Gauss operator, a rather intractable problem where even the recent advances by Melbourne and Terhesiu do not apply. More specifically, our approach – which is obtained by combining ideas from Ergodic Theory with ideas from Harmonic Analysis – involves a splitting of the Hilbert kernel, as induced by the transfer operator. The careful analysis of this splitting involves handling the Hurwitz zeta function as well as to the theory of totally positive matrices.

The previous results have been developed with H. Hedenmalm.

Finally, with the aim to delete points of the lattice cross Λ, very recently, with A. Bakan and H. Hedenmalm we have developed a theory on Hyperbolic Fourier series in which certain classes of complex functions f defined on $\mathbb{R}$ can be represented in terms of hyperbolic series

$$f(x) = \sum_{n \in \mathbb{Z} \setminus \{0\}} a_n e^{i\pi nt} + b_n e^{-i\pi nt}$$

where a_n and b_n are complex numbers.

3.23 Nabil Ourimi: Compactness theorems for sequences of holomorphic coverings between domains in almost complex manifolds

Nabil Ourimi
King Saud University, Department of Mathematics, ourimi@ksu.edu.sa.

Abstract

The classical local version of Wong-Rosay theorem states that the unit ball $\mathbb{B}^{n+1}$ in $\mathbb{C}^{n+1}$ is a model for the class of $\mathcal{C}^2$-strongly pseudoconvex domains in $\mathbb{C}^{n+1}$ (or more generally, complex manifolds of dimension $n+1$) at an accumulation point of an automorphism orbit. This local version is valid only in almost complex manifolds of real dimension four and fails in general for higher dimensions; the Siegel half-plane admits an automorphism orbit accumulating at a strongly pseudoconvex boundary point and whose almost complex structure is non-integrable. Our purpose here, is to extend this theorem to unbranching proper holomorphic mappings (pseudo-holomorphic coverings) in almost complex manifolds. We will characterize smooth domains (D, J) and (D', J') in almost complex manifolds of real dimension $2n+2$ with a covering orbit $\{f_k(p)\}$, accumulating at a strongly pseudoconvex boundary point, for some (J, J')-holomorphic coverings $f_k : (D, J) \to (D', J')$ and $p \in D$. It was shown that such domains are both biholomorphic to a model domain, if the source domain (D, J) admits a bounded strongly J-plurisubharmonic exhaustion function. Furthermore, if the target domain (D', J') is strongly pseudoconvex, then both (D, J) and (D', J') are biholomorphic to the unit ball in $\mathbb{C}^{n+1}$ with the standard complex structure. Our results can be considered as compactness theorems for sequences of pseudo-holomorphic coverings. They generalize a result of [E.B.Lin and B.Wong, Curvature and proper holomorphic mappings, between bounded domains in $\mathbb{C}^n$; Rocky Mountain Journal of Mathematics], (1990) and a result of [N. OURIMI, A local version of Wong-Rosay's theorem for proper holomorphic mappings, Proc. A.M.S. (2000)] for relatively compact domains in almost complex manifolds.

3.24 Wedad Albalawi: New Double Integral Inequalities on Time Scales via Positive Operators

Wedad Albalawi
Department of Mathematical Sciences, College of Science, Princess Nourah bint Abdulrahman University, P.O. Box 84428, Riyadh 11671, Saudi Arabia Email: wsalbalawi@pnu.edu.sa.

Abstract

This study improves some nonlinear dynamic inequalities in time scale version, using some positive operators. The study includes several cases on the operators with introducing some restrictions on the nonnegative rd-continuous functions of the operator. The inequalities in the new versions can be tools to solve some types of differential equations and prove the uniqueness of the solution. The results done by time scales analysis and some theorems as Fubini theorem.

Keywords: Time scales, inequality of Hardy and Copson, Fubini's Theorem, Steklov-operator.

Main results: Throughout this paper, $\Omega(t_1, t_2)$ denote to the operator of Copson-Steklov with considering the existence for the integral. The functions φ_l, Λ_l, ϑ_l, ϕ_l in the resultss below are nonnegative rd-continuous functions, Δ-integrable and the integrals are assumed to be exist.

Result 1. Let $a \in [0, \infty)_{\mathbb{T}_l}$, for $l = 1, 2$. Assume there exist $\mu, \lambda \geq 1$ and $\beta = \frac{1}{\lambda+1}$ such that

$$\frac{\varphi_l^{\Delta_l}(t_l)}{\varphi_l^{\sigma}(t_l)} \leq \mu \frac{\Phi_l^{\Delta_l}(t_l)}{\Phi_l(t_l)}, \quad \frac{\vartheta_l^{\Delta_l}(t_l)}{\vartheta_l^{\sigma}(t_l)} \leq \lambda \frac{\Gamma_l^{\Delta_l}(t_1, t_2)}{\Gamma_l(t_1, t_2)} \text{ and } \frac{\vartheta_l^{\sigma}(t_l)}{\vartheta_l(t_l)} \leq \beta \frac{\varphi_l^{\sigma}(t_l)}{\varphi_l(t_l)},$$

where $\Delta_l = \frac{\partial}{\partial t_l}$ for every l. Define $\Phi_l(t_l) = \int_a^{t_l} \phi_l(s_l) \Delta s_l$ with $\Phi_l(\infty) = \infty$, and $\varphi_l(a) = 0$,

$$\Gamma(t_1, t_2) := \int_a^{t_1} \int_a^{t_2} \prod_{l=1}^{2} \frac{1}{\vartheta_l(s_l)} \frac{\phi_l(s_l)}{\Phi_l(s_l)} \Lambda(s_1, s_2) \Delta s_1 \Delta s_2,$$

and the operator

$$\Omega(t_1, t_2) = \prod_{l=1}^{2} \vartheta_l(t_l) \Gamma(t_1, t_2)$$

is a positive Copson-Steklov operator. Then

$$\int_a^{\infty} \int_a^{\infty} \prod_{l=1}^{2} \varphi_l^{\sigma}(t_l) \frac{\phi_l(t_l)}{\Phi_l^{\rho}(t_l)} (\Omega^{\sigma}(t_1.t_2))^p \Delta t_1 \Delta t_2 \leq \Big(\frac{p}{\rho - \mu - 1)}\Big)^p \int_a^{\infty} \int_a^{\infty} \prod_{l=1}^{2} \varphi_l^{\sigma}(t_l) \frac{\phi_l(t_l)}{\Phi_l^{\rho}(t_l)} \Lambda^p(t_1, t_2) \Delta t_1 \Delta t_2,$$

where $p \geq 1$ and $\rho > \mu + 1$.

Idea of the proof: The proof was done with some restrictions on the nonnegative rd-continuous functions of the operator in case $p \geq 1$ and $\rho > \mu + 1$. The concepts in time scale version such as time scales calculus are used to unify and extend many problems from the theories of differential and of difference equations. In addition, we use some properties of multiple integrals on time scales, some theorems of Fubini and the inequality of Hölder.

Result 2. Let $a \in [0, \infty)_{\mathbb{T}_l}$, for $l = 1, 2$. Assume there exist $\lambda, \mu \geq 1$ and $\beta = \frac{1}{1+\lambda}$ such that

$$\frac{\varphi_l^{\Delta_l}(t_l)}{\varphi_l^{\sigma}(t_l)} \geq \mu \frac{\Phi_l^{\Delta_l}(t_l)}{\Phi_l(t_l)}, \quad \frac{\vartheta_l^{\Delta_l}(t_l)}{\vartheta_l^{\sigma}(t_l)} \leq \lambda \frac{\Gamma_l^{\Delta_l}(t_1, t_2)}{\Gamma_l(t_1, t_2)}, \text{ and } \frac{\vartheta_l^{\sigma}(t_l)}{\vartheta_l(t_l)} \leq \beta \frac{\varphi_l^{\sigma}(t_l)}{\varphi_l(t_l)},$$

where $\Gamma^{\Delta_l} = \frac{\partial \Gamma}{\partial t_l}$, for every l. Define

$$\Phi_l(t_l) = \int_a^{t_l} \phi_l(s_l)\Delta s_l, \text{ with } \Phi_l(\infty) = \infty, \text{ and } \varphi_l(a) = 0,$$

$$\Gamma(t_1, t_2) := \int_{t_1}^{\infty} \int_{t_2}^{\infty} \prod_{l=1}^{2} \frac{1}{\vartheta_l(s_l)} \frac{\phi_l(s_l)}{\Phi_l(s_l)} \Lambda(s_1.s_2)\Delta s_1 \Delta s_2,$$

and the operator

$$\Omega(t_1, t_2) = \prod_{l=1}^{2} \vartheta_l(t_l)\Gamma(t_1, t_2) \geq 0$$

is a positive Copson-Steklov operator. Then

$$\int_a^{\infty} \int_a^{\infty} \prod_{l=1}^{2} \varphi_l^{\sigma}(t_l) \frac{\phi_l(t_l)}{\Phi_l^{\rho}(t_l)} (\Omega^{\sigma}(t_1, t_2))^p \Delta t_1 \Delta t_2 \leq \Big(\frac{p}{\mu + 1 - \rho}\Big)^p \int_a^{\infty} \int_a^{\infty} \prod_{l=1}^{2} \varphi_l^{\sigma}(t_l) \frac{\phi_l(t_l)}{\Phi_l^{\rho}(t_l)} \Lambda^p(t_1, t_2)\Delta t_1 \Delta t_2,$$

where $p \geq 1$ and $0 \leq \rho < \mu + 1$.

Result 3. Let $\mathbb{T}_l$ be a time scale with $a \in [0, \infty)_{\mathbb{T}_l}$, for $l = 1, 2$. Further, assume there exist $\lambda, \mu \geq 1$ and $\beta = \frac{1}{\lambda - 1}$ such that

$$\frac{\varphi_l^{\Delta_l}(t_l)}{\varphi_l^{\sigma}(t_l)} \geq \mu \frac{\Phi_l^{\Delta_l}(t_l)}{\Phi_l(t_l)}, \quad \frac{\vartheta_l^{\Delta_l}(t)}{\vartheta_l^{\sigma}(t)} \geq \lambda \frac{\Gamma_l^{\Delta_l}(t_1, t_2)}{\Gamma_l(t_1, t_2)}, \text{and } \frac{\vartheta_l(t_l)}{\vartheta_l^{\sigma}(t_l)} \leq \beta \frac{\varphi_l(t_l)}{\varphi_l^{\sigma}(t_l)}.$$

Define

$$\Phi_l(t_l) = \int_a^{t_l} \phi_l(s_l)\Delta s_l, \text{ with } \Phi_l(\infty) = \infty, \text{ and } \varphi_l(a) = 0,$$

$$\Gamma(t_1, t_2) := \int_{t_1}^{\infty} \int_{t_2}^{\infty} \prod_{l=1}^{2} \vartheta_l(s_l) \frac{\phi_l(s_l)}{\Phi_l(s_l)} \Lambda(s_1, s_2)\Delta s_1 \Delta s_2,$$

$$\Omega(t_1, t_2) := \prod_{l=1}^{2} \frac{1}{\vartheta_l(t_l)} \Gamma(t_1, t_2) \geq 0$$

is a positive Copson-Steklov operator. Then

$$\int_a^{\infty} \int_a^{\infty} \prod_{l=1}^{2} \varphi_l^{\sigma}(t_l) \frac{\phi_l(t_l)}{\Phi_l^{\rho}(t_l)} (\Omega^{\sigma}(t_1, t_2))^p \Delta t_1 \Delta t_2 \leq \Big(\frac{p}{\mu + 1 - \rho}\Big)^p \int_a^{\infty} \int_a^{\infty} \prod_{l=1}^{2} \varphi_l^{\sigma}(t_l) \frac{\phi_l(t_l)}{\Phi_l^{\rho}(t_l)} \Lambda^p(t_1, t_2)\Delta t_1 \Delta t_2,$$

where $p \geq 1$ and $0 \leq \rho < \mu + 1$.

Idea of the proof: We follow the same proof of the first result with considering new restriction on the operator that is consistent with case $p \geq 1$ and $0 \leq \rho < \mu + 1$.

References

[1] G. H. Hardy, "Note on a theorem of Hilbert," Math. Z6, 314-317, 1920.

[2] E. T. Copson, "Some Integral Inequalities," Proceedings of the Royal Society of Edinburgh: Section A Mathematics, 75, no. 2, 157-164, 1976.

[3] W. Albalawi and Z.A. Khan, "Synchronization Analysis of Multiple Integral Inequalities Driven by Steklov Operator," Fractal Fractional, 5, 97, 2021.

[4] W. Albalawi, "Time-Scale Integral Inequalities of Copson with Steklov Operator in High Dimension." Journal of Mathematics, 2022.

[5] M. Bohner and A. Peterson, "Advanced in Dynamic Equations on Time Scales," Birkhuser Boston. Inc.,Boston, MA. 2003.

[6] S. Hilger,"Ein makettenkalkl mit anwendung auf zentrumsmannigfaltigkeiten," Wurzburg Universtat Wurzburg,1988.

[7] L. Y. Chan, "Some extensions of Hardy's inequality," Canadian Mathematical Bulletin, 22 (2), 165-169, 1979.

[8] B. G. Pachpatte, "A note on certain inequalities related to Hardy's inequality," Indian Journal of Pure and Applied Mathematics, 23, 773-776, 1992.

[9] P. Řehák, "Hardy inequality on time scales and its application to half-linear dynamic equations," Journal of Inequalities and Applications 2005, 495-507, 2005.

4 Abstracts of Contributed Talks

4.1 AbdulRahman M. Alharbi: General Monotone Operators for First-Order Separable Mean-Field Games with Mixed Boundary Conditions

AbdulRahman M. Alharbi[1,2,*] and **Diogo Gomes[2]**
[1] The Islamic University of Al-Madinah
[2] King Abdullah University of Science and Technology (KAUST)

Abstract

We establish the existence and (partial) uniqueness of solutions for the variational inequality arising from a stationary mean-field game (MFG) system posed on bounded domains with nonstandard boundary conditions. The MFG system consists of a Hamilton–Jacobi equation coupled with a stationary transport equation via the players' density. The main contributions of the paper are defining the correct monotone operator that incorporates the boundary conditions and addressing the lack of coercivity issue through careful manipulations of the operator's domain. We subsequently apply the Browder–Minty theorem to establish the existence of solutions for the variational inequality associated with the modified operator. Finally, we retract our steps and prove the existence of solutions to the original MFG system via a limiting process.

$*$ **Lead presenter**

Mean-field game (MFG) models describe the interactions of large populations of rational players making individual decisions while collectively influencing the system's dynamics. The model was introduced in 2006-2007 by the independent works of Lasry and Lions [4–6] and Huang, Caines, and Malhamé [2, 3]. Mathematically, a MFG is a coupled system consisting of a Hamilton–Jacobi (H–J) equation, which arises from the underlying control problem, and a transport equation, which governs the evolution of the players' distribution. While standard Dirichlet boundary conditions are well studied, these boundary conditions produce an unrealistic phenomenon where virtual players enter through the exit boundary to satisfy the Dirichlet conditions. To address this issue, we introduce nonstandard constraints that prescribe the inflow of agents on a part of the boundary, denoted Γ_N, and enforce a relaxed Dirichlet condition on the remaining part of the boundary, denoted Γ_D. We further impose a no-entry condition on Γ_D, complemented by contact conditions, which together eliminate the unrealistic entry phenomenon. More precisely, we introduce the following system.

The Separable MFG System Consider an open, bounded, and connected domain $\Omega \subset \mathbb{R}^d$ with a C^1 boundary, denoted by $\Gamma := \partial\Omega$. Let Γ_D and Γ_N be relatively open, smooth $(d-1)$–dimensional manifolds that form a proper partition of Γ (i.e., $\Gamma = \overline{\Gamma_D \cup \Gamma_N}$ and $\Gamma_D \cap \Gamma_N = \emptyset$). Let $H : \Omega \times \mathbb{R}^d \to \mathbb{R}$ be continuous, $g : [0, \infty) \to \mathbb{R}$ be non-decreasing, and $j : \Gamma_N \to [0, \infty)$ be non-vanishing. The first *mean-field game* (MFG) system is defined by:

$$\begin{cases} H(x, Du) = g(m) & \text{in } \Omega, \\ -\operatorname{div}(mD_pH(x, Du)) = 0 & \text{in } \Omega, \end{cases} \tag{4.1.1}$$

subject to the boundary conditions

$$\begin{cases} mD_pH(x, Du) \cdot \nu = j(x) & \text{on } \Gamma_N, \\ mD_pH(x, Du) \cdot \nu \leq 0, \quad u(x) \leq 0 & \text{on } \Gamma_D, \\ u\, mD_pH(x, Du) \cdot \nu = 0 & \text{on } \Gamma_D. \end{cases} \tag{4.1.2}$$

Because these boundary conditions are nonstandard, the above MFG system poses additional challenges, ranging from the functional space of definition to the coercivity of the associated differential operator.

Let $\mathcal{X} := L^{\beta+1}(\Omega) \times W^{1,\gamma}(\Omega) \times L^{\gamma'}(\Gamma_D)$, and let $\mathcal{X}'$ be its topological dual. Let $\mathcal{X}^+ \subset \mathcal{X}$ be the domain that admits nonnegative functions m and h (see below). In this paper, we define a sequence of penalized differential operators $A_\epsilon : \mathcal{X}^+ \to \mathcal{X}'$ that reproduces the MFG system in the limit $\epsilon \to 0^+$. This operator incorporates the Γ_D–boundary conditions via an auxiliary variable h encoding outflow at Γ_D.

$$A_\epsilon \begin{bmatrix} m \\ u \\ h \end{bmatrix} := \begin{bmatrix} -H(x, Du) + g(m) \\ -\operatorname{div}\big(m\, D_pH(x, Du)\big) + \big(m\, D_pH(x, Du) \cdot \nu\, \chi_\Gamma - j\, \chi_{\Gamma_N} + h\, \chi_{\Gamma_D}\big)\mathcal{H}^{d-1} \\ \big(-u + \epsilon^{\gamma'} h^{\gamma'-1}\big)\chi_{\Gamma_D}\mathcal{H}^{d-1} \end{bmatrix}, \tag{4.1.3}$$

where χ_S denotes the characteristic function of a set S and $\mathcal{H}^{d-1}(\cdot)$ is the $(d-1)$–dimensional Hausdorff measure. The space $\mathcal{X}^+$ has the appropriate regularity and convexity properties for the well-definedness of the boundary conditions and the application of monotone operator theory. Indeed, the operator A_ϵ exhibits monotonicity and hemicontinuity properties for functions in this domain.

The main results of the presentations establish the existence of solutions to the Separable MFG System in the weak sense, which is formulated as a variational inequality.

Result 1 Under some appropriate growth and regularity assumptions on the data, there exists a triplet

$$(m, u, h) \in L^{\beta+1}(\Omega) \times W^{1,\gamma}(\Omega) \times W^{1-\frac{1}{\gamma},\gamma'}(\Gamma_D)$$

such that

$$\left\langle A_0 \begin{bmatrix} m \\ u \\ h \end{bmatrix}, \begin{bmatrix} \mu - m \\ v \\ k - h \end{bmatrix} \right\rangle \geq 0 \qquad \forall (\mu, v, k) \in \mathcal{X}^+.$$

Idea of the proof: We establish this by taking the limit of the solutions of the penalized variational inequalities as $\epsilon \to 0^+$. We provide a series of intermediate theorems and lemmas that aid this approach. In particular, we prove the following existence result for the variational inequality associated with the penalized operator.

Result 2 Let $\epsilon > 0$. Under some appropriate growth and regularity assumptions on the data, there exists a triplet $(m, u, h) \in \mathcal{X}^+$ such that

$$\left\langle A_\epsilon \begin{bmatrix} m \\ u \\ h \end{bmatrix}, \begin{bmatrix} \mu - m \\ v \\ k - h \end{bmatrix} \right\rangle \geq 0.$$

for all $(\mu, v, k) \in \mathcal{X}^+$.

Idea of the proof: We first prove the well-definedness of the operator A, followed by its monotonicity and continuity, which are straightforward given our assumptions and the dominated convergence theorem. To exploit the Minty-Browder theorem, we circumvent the issue of lack of coercivity by restricting the operator to the a priori known set where solutions reside, then taking the quotient of the space by the subspace of constant functions. This partially eliminates the issue of lack of coercivity.

We use this partial resolution to further restrict the domain of the operator into a smaller domain and properly redefine the operator on the quotient space as a single-valued operator rather than the direct method of defining it as a set-valued operator. The choice is made optimally to ensure the uniqueness and existence of solutions. Finally, we establish that the obtained solution for the quotient-space monotone operator corresponds to a solution for the original perturbed operator. Taking the limit as $\epsilon \to 0^+$ provides the proof of Result 1.

.

References

[1] A. M. Alharbi, Y. Ashrafyan, and D. Gomes: A First-Order Mean-Field Game on a Bounded Domain with Mixed Boundary Conditions, *arXiv preprint*, 2025.

[2] M. Huang, R. Malhamé, and P. Caines: Large Population Stochastic Dynamic Games: Closed-Loop McKean-Vlasov Systems and the Nash Certainty Equivalence Principle, *Communications in Information and Systems*, **6**(3), 221–251, 2006.

[3] M. Huang, P. Caines, and R. Malhamé: Large-population cost-coupled LQG problems with non-uniform agents: individual-mass behavior and decentralized ϵ-Nash equilibria, *IEEE Transactions on Automatic Control*, **52**(9), 1560–1571, 2007.

[4] J.-M. Lasry and P.-L. Lions: Jeux á Champ Moyen. I. Le Cas Stationnaire, *Comptes Rendus Mathématique*, **343**(9), 619–625, 2006.

[5] J.-M. Lasry and P.-L. Lions: Jeux á champ moyen. II – Horizon fini et contrôle optimal, *Comptes Rendus Mathématique*, **343**(10), 679–684, 2006.

[6] J.-M. Lasry and P.-L. Lions: Mean Field Games, *Japanese Journal of Mathematics*, **2**(1), 229–260, 2007.

4.2 Aisha Alshaery: Analytical and Numerical Study of Cubic-Quartic Solitons in Birefringent Fibers Using the New Kudryashov Method and Improved Adomian Decomposition

Afrah M. Almalki[1,*], A. A. Alshaery[1], H. O. Bakodah[1]
[1]Department of Mathematics and Statistics, Faculty of Science, University of Jeddah, Jeddah, Saudi Arabia.

Abstract

This study examines cubic-quartic solitons in birefringent fibers described by the cubic-quartic nonlinear Schrödinger equation. Employing the new Kudryashov approach, several optical soliton solutions, such as bright and singular solitons, are obtained. The Improved Adomian Decomposition Method is utilized for numerical solutions, offering a systematic analysis of stability and accuracy, corroborated by error tables and graphical illustrations.

* **E-mail address: aalmalki1447.stu@uj.edu.sa (Afrah M. Almalki)**

This research seeks to examine the dynamics of cubic-quartic solitons in birefringent fibers, emphasizing the impacts of chromatic dispersion, self-phase modulation, and birefringence. We utilize the new Kudryashov approach [1, 2] for the analytical derivation of soliton solutions and the Improved Adomian Decomposition Method (IADM) [3, 4] for numerical simulations of the cubic-quartic nonlinear Schrödinger equation (CQ-NLSE). The objective is to attain a deeper comprehension of the stability and propagation properties of solitons in practical environments. Upon making consideration to birefringent fibers under the Kerr law, the CQ-NLSE is given by

$$iM_t + ip_1 M_{xxx} + q_1 M_{xxxx} + \left(r_1|M|^2 + s_1|W|^2\right) M = 0, \tag{4.2.1}$$

$$iW_t + ip_2 W_{xxx} + q_2 W_{xxxx} + \left(r_2|W|^2 + s_2|M|^2\right) W = 0, \tag{4.2.2}$$

with p_j and q_j $(j = 1,\ 2)$ as constant coefficients that respectively represent the third-order and fourth-order dispersions, while the constant r_j $(j = 1,\ 2)$ denotes the respective self-phase modulations, and the constant s_j $(j = 1,\ 2)$ accounts for the respective cross-phase modulation. To analytically treat the system represented by Eqs. (4.2.1)-(4.2.2), one starts by assuming a harmonic-type solution that admits the expression as follows

$$M(x,t) = Z_1(\xi)e^{i\phi(x,t)}, \quad W(x,t) = Z_2(\xi)e^{i\phi(x,t)}, \tag{4.2.3}$$

where i is the imaginary unit. The function $Z_j(\xi)$ $(j = 1, 2)$ represents the amplitude function. The variable ξ is defined as $\xi = x - vt$, where v is the soliton's velocity. The phase function $\phi(x,t)$ is given by $\phi(x,t) = \omega t - kx + \theta_0$, with ω, k, and θ_0 representing the frequency, wave number, and phase term.

Some Results of the Analytical Method : Set-I:

The bright soliton: $M(x,t) = \frac{H_2}{4L^2\ \cosh^2\ (\delta\xi)} e^{i(\omega t - kx + \theta_0)}$, $W(x,t) = \chi \frac{H_2}{4L^2\ \cosh^2\ (\delta\xi)} e^{i(\omega t - kx + \theta_0)}$.

The singular soliton: $M(x,t) = \frac{H_2}{4L^2\ \sinh^2\ (\delta\xi)} e^{i(\omega t - kx + \theta_0)}$, $W(x,t) = \chi \frac{H_2}{4L^2\ \sinh^2\ (\delta\xi)} e^{i(\omega t - kx + \theta_0)}$.

Idea of the Analytical Method: The procedures for applying the new Kudryashov approach to derive specific soliton solutions for the CQ-NLSE are as follows: To begin, we assume that the equation admits a predicted solution of the following form: $Z(\xi) = \sum_{r=0}^{N} H_r F^r(\xi)$, where H_r (with $r = 0, 1, 2, \ldots, N$) are free constants that will be determined, subject to the condition $H_N \neq 0$. The parameter N serves as the balancing constant. Additionally, the function $F(\xi)$ that appears in the subsequent solution expression satisfies the following nonlinear ordinary differential equation (NODE): $[F'(\xi)]^2 = \delta^2 F^2(\xi)\left[1 - \zeta\ F^2(\xi)\right]$. Furthermore, this NODE possesses the following exact solution: $F(\xi) = \frac{4L}{4L^2 e^{\delta\xi} + \zeta e^{-\delta\xi}}$, where δ and ζ are arbitrary nonzero real constants. This solution can also be expressed using hyperbolic functions as follows: $F(\xi) = \frac{4L}{(4L^2+\zeta)\cosh(\delta\xi) + (4L^2-\zeta)\sinh(\delta\xi)}$.

Some Results of the Numerical Method

Table 1: Comparison of errors for the IADM and the bright and singular soliton solutions when $t = 0.5$.

	The bright soliton		The singular soliton	
x	**Error for** $M(x,t)$	**Error for** $W(x,t)$	**Error for** $M(x,t)$	**Error for** $W(x,t)$
-100	$1.4103263940 \times 10^{-12}$	$7.0516291300 \times 10^{-13}$	$1.41032972100 \times 10^{-12}$	$7.0516482490 \times 10^{-13}$
-60	$4.20393165000 \times 10^{-9}$	$2.10196633500 \times 10^{-9}$	$4.20444229000 \times 10^{-9}$	$2.10222016700 \times 10^{-9}$
-20	$1.04526721100 \times 10^{-5}$	$5.80197901300 \times 10^{-6}$	$1.50242864500 \times 10^{-5}$	$8.11078499400 \times 10^{-6}$
20	$3.86725961600 \times 10^{-6}$	$8.46982668800 \times 10^{-7}$	$7.04627313800 \times 10^{-6}$	$2.87214868200 \times 10^{-6}$
60	$1.71246389200 \times 10^{-9}$	$8.5623143340 \times 10^{-10}$	$1.71282922600 \times 10^{-9}$	$8.5641461300 \times 10^{-10}$
100	$5.7452960080 \times 10^{-13}$	$2.8726444010 \times 10^{-13}$	$5.7452771880 \times 10^{-13}$	$2.8726382990 \times 10^{-13}$

Idea of the Numerical Method: The IADM is a numerical method that is efficient for resolving nonlinear differential equations, by decomposing the solution into a sequence of functions. It facilitates an iterative approximation by employing Adomian polynomials to address the nonlinear elements. Using a recursive relation, the method generates a series of successive approximations that converge to the precise solution.

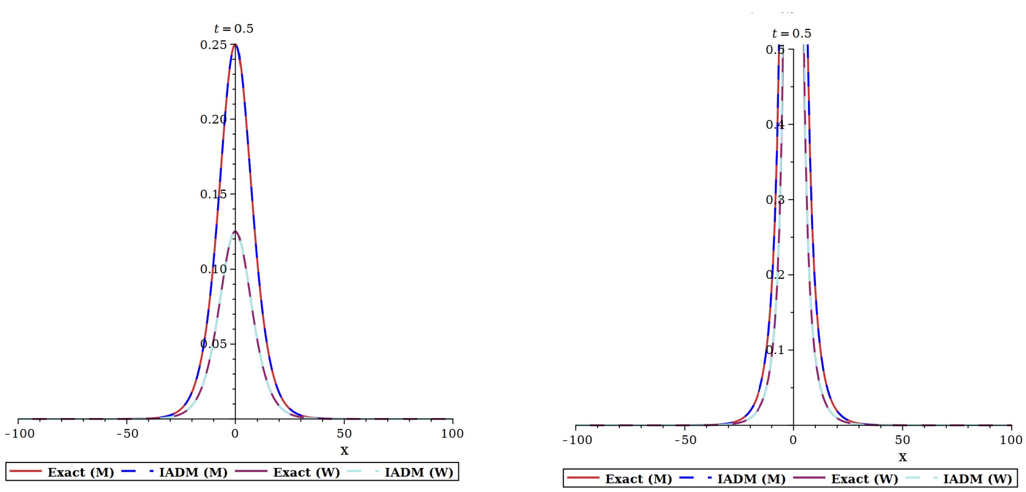

(a) (b)

Figure 1: This figure illustrates: (a) a comparison of the IADM solution with the bright exact solution in Set I for the solution pair $M(x,t)$ and $W(x,t)$ at t=0.5; and (b) a comparison of the IADM solution with the singular exact solution in Set I for the solution pair $M(x,t)$ and $W(x,t)$ at t=0.5.

References

[1] N. A. Kudryashov, Method for finding highly dispersive optical solitons of nonlinear differential equations, *Optik* **206** (2020) 163550.

[2] Ahmad, J., Akram, S., & Ali, A. (2024). Analysis of new soliton type solutions to generalized extended (2+1)-dimensional Kadomtsev-Petviashvili equation via two techniques. *Ain Shams Engineering Journal*, 15(1), 102302.

[3] A. A. AlQarni, A. M. Bodaqah, A. A. Alshaery, H. O. Bakodah, Y. Yildirim, and A. Biswas, Cubic–quartic optical solitons with Fokas–Lenells equation by the improved Adomian decomposition method, *Journal of Optics* (2024) 1-9.

[4] S. Batool, M. Arshad, N. Perveen, and S. Sarwar, Bright optical solution for fractional Lakshmanan–Porsezian–Daniel with spatio-temporal dispersion by improved Adomian decomposition method, *Optical and Quantum Electronics* **56**(7) (2024) 1137.

4.3 Azza Algatheem: β plane magnetohydrodynamic in Kolmogorov flows

Azza Algatheem[1] Hollis williams[2], Velizar Kirkow[3,*]
[1]Department of Mathematics, Faculty of Science, University of Bisha, Bisha 61922, Saudi Arabia
[2]Department of Physics, University of Warwick, Coventry CV4 7AL, United Kingdom
[3]Department of Mathematics and Statistics, University of Exeter, Exeter EX4 4QF, United Kingdom.

Abstract

Our work depends on the kind of fluids -called Kolmogorov flow, first studied [2]. Where Kolmogorov flow has a sinusoidal velocity profile with two-dimensional, unidirectional shear ($\boldsymbol{u} = \sin x$), x is a cross-stream coordinate). This must be maintained by an external force in viscous fluids. It is known that this kind of fluid flow is unstable to large-scale jet motions. This can occur in the presence of the magnetic field and has implications observed in geophysical and astrophysical systems. It is called "Zonostrafic instability" which is recently studied in various settings both numerically and analytically. Many studies suggest that it is responsible for the structure of the astrophysics systems such as Jupiter and the sun tachocline [3, 4].

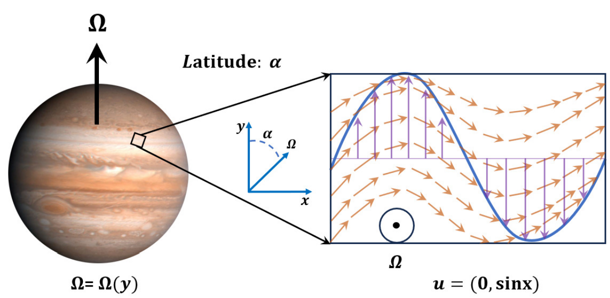

Schematic of the classical approximation of the β-plane, where we keep linear variation with latitude. In an astrophysical body such as Jupiter, the red region represents the zonal flow so that the Cartesian domain represents a small patch in the Jupiter. The rotation vector is inclined by an angle α with respect to the y-direction. The red arrows represent the magnetic field orientation and the wavy blue line represents the fluid flow with sinusoidal velocity field $u = (0, \sin x)$. The Coriolis parameter Ω is orthogonal to the (x, y)-plane.

In this study we consider a 2D Kolmogorov flow with a sinusoidal velocity field $u = (0, \sin x)$ for a magnetic field aligned with possible jet formation. Our system of equations for MHD with incompressible constant density is based on Navier Stokes equations coupled with Lorntz force. Our approach involves setting the essential state of the flow and magnetic field, and then linearizing the system of equations. The Fourier transform uses k as the wave number in the y direction and ℓ as the Bloch wave number in the x direction. After that, the growth rate of instability was determined. We aim to determine the effect of the magnetic field on such instabilities by using the classical linear stability theory as set out in [1], in which the full fluid system is decoupled into a mean flow and waves of one scale. The linear stability problem is truncated to determining the eigenvalues of finite matrices numerically, allowing exploration of the instability growth rate p as a function of the wave number k in the y-direction and a Bloch wave number in the x-direction,with $-\frac{1}{2} < \ell < \frac{1}{2}$. then plan to study non-linear effects. Where the study uses a spectral code of the Dedalus package. Our nonlinear simulations is linked to some linear results presented from our comprehensive linear study [5]. In the longer simulation run, the study aims to probe into some fundamental processes at large-scale structures and generate a possible inverse cascade.

In summary, Linear approximations are developed, valid in the limits $k \to 0, \ell \to 0$ and for $0 < \alpha < \pi/2$, with non zero $\beta \neq 0$, using matrix eigenvalue perturbation theory. Results are presented relevant to understanding the effects of magnetic fields on flows and their implications for the solar system such as Jupiter. This level of abstraction clarifies basic aspects of instability, such as how perturbations are governed. the governing equations for MHD are derived in a general setting using an action principle and Fourier derivatives. The way in which these equations behave as a Fourier series is described. Afterwards, Alfvén waves interacted with Rossby waves to generate the MHD Rossby waves which have no hydrodynamic companion. In high magnetic field strength, these waves return to being Alfvén waves. Eventually, Detailed comparisons are given between theory for small k, ℓ and numerical results.

References

[1] Manfroi, A. J., Young, W. R.(2002). Stability of β-plane Kolmogorov flow. Physica D: Non-linear Phenomena, 162(3-4), 208-232.

[2] Meshalkin,L. ,Sinai,Y. (1961).Investigation of stability for a system of equations describing plane motion of a viscous incompressible fluid.Appl .Math .Mech ,(25),1140-1143.

[3] Durston, S., Gilbert, A. D. (2016). Transport and instability in driven two-dimensional magnetohydrodynamics flows. Journal of Fluid Mechanics, 799 , 541-578.

[4] Hughes, D. W., Steven,T. M. and Patrick, D. H. (2007). β-plane Magnetohydrodynamics turbulence in the solar tachocline. The Astrophysical Journal, 667:113-116.

[5] Algatheem, A. M., Gilbert, A. D. and Hillier, A. S. (2023) 'Zonostrophic instabilities in magnetohydrodynamic Kolmogorov flow', Geophysical & Astrophysical Fluid Dynamics, 117(6), pp. 357–396. doi: 10.1080/03091929.2023.2268817.

4.4 Hadeel Albeladi: Rational Tangle-Oids

Hadeel Albeladi[1,*], **Cenap Ozel**[2] and **Sofia Lambropoulou[3]**
[1]Department of Mathematics, College of Science & Arts, King Abdulaziz University, Rabigh 21911, Saudi Arabia, E-mail: aealbeladi@kau.edu.sa
[2]Department of Mathematics, King Abdulaziz University, Jeddah 21589 Saudi Arabia, E-mail: cozel@kau.edu.sa
[3]Department of Mathematics,National Technical University, GR-15780 Athens, E-mail: sofia@math.ntua.gr

Abstract

In this paper, we introduce a rational tangle-oid, which is a rational tangle with break strands. Rational tangle-oids can be useful models to study broken DNA, and we illustrate them by box invariant.

* **Lead presenter**

4.4.1 Rational Tangle-oids

In this section, we introduce the concept of rational tangle-oids. We work within the framework of the welded tangle-oids category, but without the generator X and excluding the relations $[WT_{13}]$ and $[WT_{13}]$' which correspond to forbidden moves in knotoids. A rational tangle-oid is defined as a subclass of welded tangle-oids that behaves like a rational tangle but allows for strand breaks. In this paper, we restrict our attention to the case where exactly two endpoints lie in the interior of the projection disc.

Definition 4.4.1 *A rational tangle-oid is a tangle-oid that can be decomposed into a finite sequence of twists, analogous to a rational tangle, but adapted to account for broken strands. In this paper, we have just one broken strand.*

In rational tangles, applying twists between neighbouring ends can result in a trivial (unknotted) tangle. However, in rational tangle-oids, this is not always the case–applying similar twists does not necessarily yield an unknotted tangle-oid.

Definition 4.4.2 *We call a rational tangle-oid unknotted if it does not have any positive or negative crossing.*

Definition 4.4.3 *Let T be a rational tangle-oids, we can added (horizontal composition) denoted by '+' or multiplied (vertical composition) denoted by '$*$', by n half twist.*

Theorem 4.4.1 (Existence of Rational Sub-Tangles in a Rational Tangle-oid) *Let T be a rational tangle-oid diagram. Then there exists a rational sub-tangle $T^* \subset T$, obtained by cutting along a simple arc in the projection disc such that: The resulting subdiagram T^* has exactly four ends lying on the boundary of a subdisc.*

Proof A rational tangles obtained by applying a finite number of consecutive twists of neighbouring ends. So by using additive and multiplication operation of rational tangle-oid, we can decompose any rational tangle-oid such that at least one part is a rational tangle.

Conjecture Let T be a rational tangle-oid, assume that:

- The interior endpoints are connected to strands whose boundary ends are adjacent (i.e., neighbouring positions on the boundary of the disc), and
- Twisting the boundary ends of T (those not involved in the broken strand) simplifies the underlying rational tangle-oid structure.

Then the tangle-oid T can be unknotted.

Remark 4.4.1 *The rational tangle-oid is not necessarily equivalent under hflip and vflip as the rational tangle. Here is an example of a rational tangle-oid with a mirror image, horizontal flip and vertical flip*

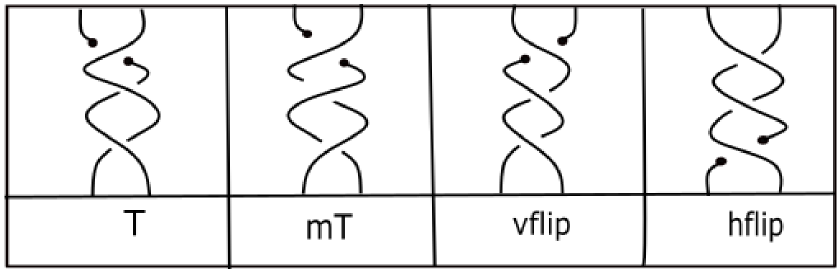

4.4.2 Box Invariant

Lemma 4.4.1 *We can decompose any rational tangle-oid into a finite sequence of twists with respect to the endpoints by using additive and multiplication operations of rational tangle-oid. In this invariant, we enclose segments of the tangle-oid within boxes, ensuring that each box contains either a broken part along with the twists connecting to it, or simply a count representing the number of twists without a broken part. The boxes are then divided into two regions using a diagonal line, either from the top-right to the bottom-left or from the top-left to the bottom-right. The diagonal division allows us to track how the strands interact within each box. We adopt the same notation used for rational tangles to count the twists, both horizontally and vertically, inside each box. Specifically:*

- *Horizontal twists are counted by following the path of the strands parallel to the horizontal direction.*
- *Vertical twists are counted by tracing the strands parallel to the vertical direction.*

Each box contains a number representing the count of twists and whether it is positive or negative crossing, with or without a broken part. By assembling these boxes according to the sequence of broken parts and twist counts, we construct the overall rational tangle-oid. This structure provides a clear method for decomposing and analyzing rational tangle-oids, preserving their combinatorial and topological properties.

References

[1] Hadeel Albeladi. Presentations of strict monoidal categories and Welded tangle-oids. PhD thesis, 2022.

[2] John H Conway. An enumeration of knots and links, and some of their algebraic properties. In Computational problems in abstract algebra, pages 329–358. Elsevier, 1970.

[3] Jay R Goldman and Louis H Kauffman. Rational tangles. Advances in Applied Mathematics, 18(3):300–332, 1997.

[4] Philip J Higgins. Categories and groupoids. Nostrand Reinhold, 1971.

[5] Christian Kassel. Quantum groups, volume 155. Springer Science and Business Media, 2012.

[6] Louis H. Kauffman and Sofia Lambropoulou. On the classification of rational tangles. Adv. Appl. Math., 2004.

[7] Blake Mellor and Sean Nevin. Virtual rational tangles. Journal of Knot Theory and Its Ramifications, 2018

4.5 Mushrifah Al-Malki: Energy Analysis of roughness on the Blasius boundary layer over a heated plate

Mushrifah A. S. Al-Malki
Department of Mathematics and Statistics College of Science Taif University, P.O. Box 11099, Taif 21944, Saudi Arabia.

Abstract

This paper has been designed to analyse the effects of wave roughness on the stability of the Blasius boundary layer flow over a rough plate with a temperature-dependent viscosity flow. We summarised the results of the effects of wave roughness on the boundary layer flow over a heated plate as follows: our theoretical analysis depended on the no-penetration condition approach for formulating the steady boundary-layer flow over a rough, heated plate. The effects of wave roughness show a more steady state of boundary layer flows with decreasing viscosity via setting $\varepsilon > 0$. Our study has revealed that wave roughness acts to reduce energy production of the (T-S) waves of a flow over a heated, wave plate. The conclusions arising from this study are the plate roughness can be useful as an effective passive flow-control mechanism for engineering flows in the (CVD) reactors over waviness of wall. Our results are consistent with the MW model [3].

4.5.1 Formulation

We consider a steady, incompressible, Newtonian fluid flowing with velocity $U = (u^*, v^*)$ over a semi-infinite flat plate, where u^* and v^* are the velocities in the streamwise and plate-normal directions x^* and y^*, respectively. Here T^* is the temperature of the fluid, and the plate heated to a fixed temperature T^*_∞. The system is governed by Navier-Stokes equations. The boundary problem is solved using numerical methods (bv4c) subject to the modified wall boundary conditions which are expressed as: $f(0) = R_1 f'(0)$, $f'(0) = R_2 f''(0)$, and $f'(\eta \to \infty) = 1$, $g(\eta \to \infty) \to 0$. Here primes denote differentiation with respect to η, and the two R_1, R_2 give experimental measures of the roughness in vertical or horizontal directions, respectively, see [1], [2].

4.5.2 Results

Figure 2 (a) shows the velocity profiles of $U(\eta)$ for the case of roughness with vertical grooves, increasing R_2 results in a slight thinning of boundary layer flows and an increase in the jets. Figure 2(b) slightly displays thinning in a decrease in the jets of $U'(\eta)$ towards the surface of plate with increasing groove depth (R_2). Figure 2 displays a similar movement towards the plate surface with increasing R_2 and ε, which is interpreted as a narrowing of the thermal rough boundary layer. Similarly, this is seen as a reduction in the temperature profile gradient similar to that seen in Figure 2 (c).

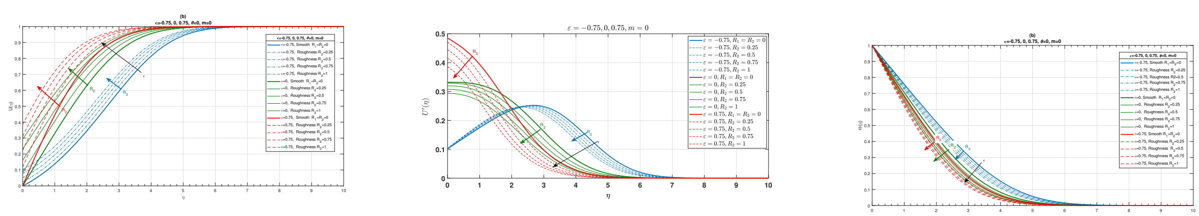

(a) Axial velocity $U(\eta)$ (b) Velocity gradient $U'(\eta)$ (c) Temperature velocity $\Theta(\eta)$

Figure 2: Mean flow profiles, in the cases of various roughness, axial velocity $U(\eta)$, velocity gradient $U'(\eta)$, temperature velocity $\Theta(\eta)$. $R_1 = 0, R_2 > 0$ (waviness wall).

4.5.3 Energy Analysis

The examination of the energetic input and output of disturbance to the mean flow depends on the eigenfunctions. The integrating through the boundary layer results in the integral energy equation. $\frac{dE}{dx} = -\left\{ \int_0^\infty U'\langle \hat{u}\hat{v}\rangle dy \right\}^I + \frac{1}{R}\left\{ \frac{d}{dx}\int_0^\infty \bar{\mu}\langle \hat{v}\hat{q}\rangle dy - \int_0^\infty \bar{\mu}\langle \hat{q}^2\rangle dy \right\}^{II} + \frac{1}{R}\left\{ \frac{d}{dx}\int_0^\infty \bar{\mu}'\langle \hat{u}\hat{v}\rangle + U'\langle \hat{\mu}\hat{v}\rangle dy + \int_0^\infty \bar{\mu}'\langle \hat{u}\hat{q}\rangle - \bar{\mu}''(\langle \hat{e} + \hat{v}^2\rangle) - U'\langle \hat{\mu}\hat{s}\rangle dy \right\}^{III}$. The left-hand- side terms of represent the total mechanic energy (TME) of the system, and here $E = \int_0^\infty U\langle \hat{e}\rangle + \langle \hat{u}\hat{p}\rangle dy$. The integral I represents energy production due to Reynolds stresses (EPRS), the integral II represents energy dissipation due to viscosity (EDV), and terms in III represent additional terms arising from variable viscosity (AVV). Hence the terms in III vanish, when $\varepsilon = 0$.

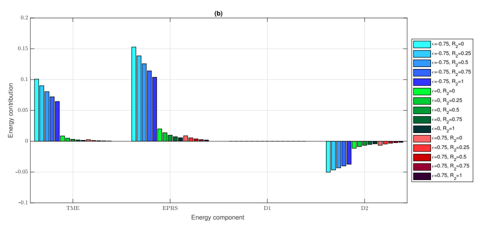

Figure 3: Preliminary results of the energy balance integral showing the contribution of the individual components of the energy balance equation

Note that for the integral energy solved via numerical integration contains the only non-negligible terms (on the left-hand side) are I and the second term of II. However, all the terms in III are consistently negligible. The remaining terms are normalized with respect to $\int_0^\infty U\langle \tilde{e}\rangle + \langle \tilde{u}\tilde{p}\rangle dy$. Figure 3 represents the change in energy contributions for surface roughness generated by vertically roughness combined with values of ε at $R_c(\varepsilon) + 200$. Figure 3 presents the energy balance calculation for a range of temperature-dependent viscosity and wave roughness. This case shows the energy balance calculation for a range of temperature-dependent viscosity and wave grooves. We note that this case leads to a large reduction in energy contribution term, and this means that there is a stabilization effect on the (T-S) waves. Note that the significantly invariant of the energy dissipation of the system (EDV) acts to clearly reduce in the total energy of the system as a result of increasing R_2 and ε.

References

[1] M. A. S. Al-Malki, Z. Hussain, S. J. Garrett, and S. Calabretto. *Phys. Rev. Fluids.*, 6:113902, 2021.

[2] L. Hopf. The measurement of the hydraulic roughness. *(in German) Mathematik und Mechanik*, 3:329–339., 1923.

[3] M. Miklavcic and C. Wang. The flow due to a rough rotating disk. *Z. Angew. Math. Phys.*, 55:235—-246, 2004.

4.6 Eman Alshehery: Numerical treatment for convective Sutterby nanofluid flow with activation energy through intelligent computational technique

Eman Alshehery[1,*], Eman Alaidarous[2], RaniaAlharbey[2], Asif Raja[3]
[1]Department of Mathematics, College of Science, University of Bisha, 8154, Alnamas 67398-5644, Saudi Arabia.
[2]Department of Mathematics, Faculty of Science, King Abdulaziz University, Jeddah 21589, Saudi Arabia.
[3]Future Technology Research Center, National Yunlin University of Science and Technology, Yunlin 64002, Taiwan.

Abstract

Recently, employing artificial intelligence techniques to solve problems in various fields has become more popular. Also, using nanofluids to enhance fluid thermal and mechanical properties, makes nanofluids interesting for various applications, particularly in heat transfer and cooling systems. This work aims to study the flow dynamics in a three-dimensional convective flow of Sutterby nanofluid (3D-CSNFF) across a bidirectional extending surface with the effect of the activation energy and chemical reaction.
* **Eman Fayz A. Alshehery**

The mathematical formulation for the proposed flow model was obtained through non-linear partial differential equations (PDEs). Then the leading PDEs were transmitted into non-linear ordinary differential equations (ODEs) by similarity transformation variables. The solution methodology in this study is implemented in two phases:

- Firstly, the numerical solutions for the mathematical formulation of flow model are found by solving ODEs for different scenarios of physical parameters (by changing the Sutterby fluid parameter (β_1), mixed convection parameter, Brownian motion, thermophoresis, activation energy, and chemical reaction rate through various four cases) through the Lobatto IIIA method by using *bvp4c* package in **MATLAB** platform.

- Secondly, these solutions were used as reference data (target data) through the *nftool* package in the **MATLAB** platform to apply the Levenberg Marquardt back propagation method LMM-TNN to investigate the approximate solution of the flow model by determining the number of neurons, training, testing, and validation data for learning ANN, which uses ten neurons, 80% of the data set for training step, 10% for validation step, and 10% for testing step. A form of an artificial neural network ANN for the flow model is displayed in Figure 4.

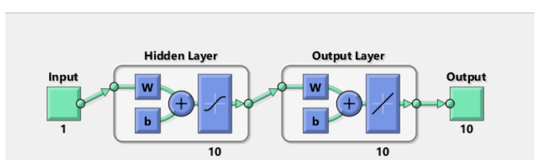

Figure 4: ANNs scheme for 3D-CSNFF.

Result 1: The accuracy of the proposed LMM-TNN is analyzed using the results of error analysis between target data (the solution by Lobatto IIIA) and output data (the solution by LMM-TNN) such as:

- The mean squared error MSE of performance for training, testing, and validation processes. It is about 10^{-9}, as shown in Figure 5(a).

- The error histogram for the different scenarios with different cases is about 10^{-7}, as presented Figure 5(b).

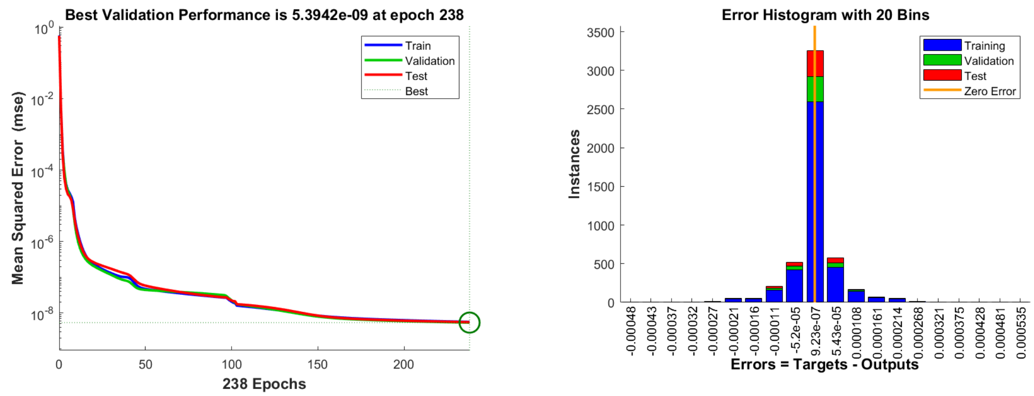

(a) MSE representation.

(b) Error histogram graph.

Figure 5: The analysis of the accuracy and efficiency of the proposed LMM-TNN.

Result 2: The solution of the flow model by LMM-TNN which analyzes the impact of different physical parameters on flow velocities, fluid temperature, and nanoparticle concentration profiles:

- The axial velocity is growing for large values for Sutterby fluid parameter while the tangential velocity decreases.

- For rising rates of thermophoresis and Brownian motion, the fluid temperature is increasing.

- The nanoparticle concentration is rising for large values of activation energy while it is reduced for high rates of chemical reaction rate.

References

[1] Choi, S. U., & Eastman, J. A. (1995). Enhancing thermal conductivity of fluids with nanoparticles (No. ANL/MSD/CP-84938; CONF-951135-29). Argonne National Lab. (ANL), Argonne, IL (United States).

[2] M. Azam, W. A. Khan, M. K. Nayak, and A. Majeed: Three dimensional convective flow of Sutterby nanofluid with activation energy *Case Studies in Thermal Engineering*, **50** (2023), 103446.

[3] J. L. Aljohani, E.S. Alaidarous, M. A. Z. Raja, M. Shoaib, and M. S. Alhothuali: Intelligent computing through neural networks for numerical treatment of non-Newtonian wire coating analysis model *Scientific Reports*, **11(1)** (2021), 1-32.

4.7 Diaa eldin Elgezouli: Greener AI: Fractional Edge Detection for Precision Water Mapping

Diaa eldin Elgezouli
Department of Basic Sciences Common First Year Deanship, King Saud University Saudi Arabia.

Abstract

This study is developing a novel approach to edge detection from satellite imagery using fractional calculus, and specifically the Grünwald-Letnikov (GL) order of fractional derivative, to enhance feature extraction in segmenting water features. Traditional edge detection operators like the Canny operator are compared to a fractional-order derivative model to compare performance in detecting subtle environmental features. A lightweight CNN is learned on conventional and fractional edge-enriched data, and its efficiency is estimated with metrics like mean squared error (MSE), peak signal-to-noise ratio (PSNR), and computational performance. Experiments demonstrate that processing with fractional order refines the maintenance of edges in complex satellite terrain, with valuable implications for sustainable applications like water resource monitoring, ecological surveys, and climatic change mapping. This research links applied mathematics that is fractional calculus to environmental science, providing a mathematically valid tool for high-resolution geospatial analysis in life sciences.

* **Lead presenter**: Diaa eldin Elgezouli, Department of Basic Sciences, King Saud University.

Summary

This paper suggests a **fractional calculus-based edge detection** algorithm for satellite imagery that uses the **Grünwald-Letnikov (GL) derivative** to improve water body segmentation. We compare standard Canny and fractional edge detection pipelines, demonstrating better feature preservation using fractional methods by a lightweight CNN trained on edge-augmented data.

Result 1: Fractional Edge Detection Outperforms Traditional Methods

Key Finding: The GL-based fractional edge detector ($\alpha = 0.8$) achieves **higher PSNR** (∼28.5 dB vs. 25.1 dB for Canny) and **lower MSE** (0.002 vs. 0.003) on satellite water body images, with better retention of fine-scale hydrological features (Fig. 6).

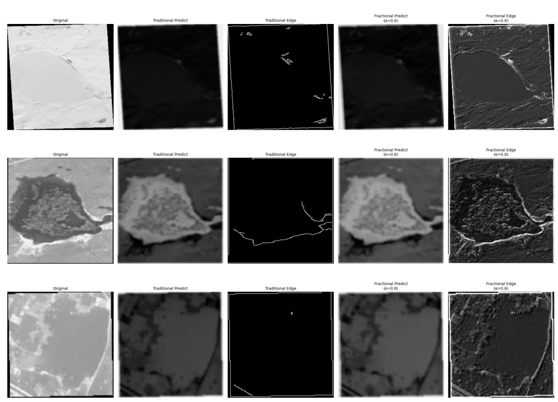

Figure 6: Comparative analysis of edge detection methods.

Idea of the Proof:

1. **Mathematical Foundation:** The GL fractional derivative generalizes integer-order differentiation:
$$D^\alpha f(x) = \lim_{h\to 0} \frac{1}{h^\alpha} \sum_{k=0}^{\infty} (-1)^k \binom{\alpha}{k} f(x-kh) \tag{4.7.1}$$

2. **Implementation:**
   - Bidirectional application preserves edge continuity
   - Adaptive contrast enhancement maintains natural gradients

3. **Validation:**
   - CNN architecture achieves real-time processing (<2ms/image)
   - Quantitative metrics show consistent improvement across 50 test images

Result 2: Computational Efficiency with Fractional Order Adaptability

Key Finding: The method maintains **real-time speeds** (<2 ms/image at 256×256 resolution) despite mathematical complexity, with α tuning ($0.5 \leq \alpha \leq 1.0$) for feature-specific optimization.

Idea of the Proof:

1. **Optimization:**
   - Series truncation at 10 terms
   - Vectorized binomial coefficient computation

2. **Empirical Validation:**
   - Timing: 1.8 ms (GL) vs. 1.2 ms (Canny) per image
   - α-sensitivity: 0.8 optimal for water bodies

3. **CNN Training:**
   - 3-epoch convergence (batch size=16)
   - GL model shows faster loss reduction

Implications and Limitations

- **Applications:** Water resource monitoring, climate adaptation
- **Limitations:** α requires calibration per dataset
- **Future Work:** Scaling to >10k images

Table 2: Performance Comparison ($\alpha = 0.8$)

Metric	Canny	Fractional
PSNR (dB)	25.1	28.5
MSE	0.003	0.002
Time/image (ms)	1.2	1.8

References

[1] D. E. Elgezouli and A. B. M. Alzahrani: Optimizing edge detection efficiency with a Grünwald–Letnikov fractional network, *Electronics*, **13** (2024), 3298.

[2] D. D. E. Elgezouli, M. Abdoon, S. B. Belhaouari and D. K. Almutairi: A novel fractional edge detector based on generalized fractional operator, *European Journal of Pure and Applied Mathematics*, **17** (2024), 1009–1028.

[3] M. E. Tenekeci, S. T. Abdulazeez, K. Karadağ and M. Modanli: Edge detection using the Prewitt operator with fractional order telegraph partial differential equations (PreFOTPDE), *Multimedia Tools and Applications*, (2024), 1–17.

[4] S. Balochian and H. Baloochian: Edge detection on noisy images using Prewitt operator and fractional order differentiation, *Multimedia Tools and Applications*, **81** (2022), 9759–9770.

[5] S. Arora, T. Mathur, S. Agarwal, K. Tiwari and P. Gupta: Applications of fractional calculus in computer vision: a survey, *Neurocomputing*, **489** (2022), 407–428.

[6] S. Balochian and H. Baloochian: Edge detection on noisy images using Prewitt operator and fractional order differentiation, *Multimedia Tools and Applications*, **81** (2022), 9759–9770.

[7] B. Ghanbari and A. Atangana: Some new edge detecting techniques based on fractional derivatives with non-local and non-singular kernels, *Advances in Difference Equations*, **2020** (2020), 435.

[8] J. E. Lavín-Delgado, J. E. Solís-Pérez, J. F. Gómez-Aguilar and R. F. Escobar-Jiménez: A new fractional-order mask for image edge detection based on Caputo–Fabrizio fractional-order derivative without singular kernel, *Circuits, Systems, and Signal Processing*, **39** (2020), 1419–1448.

[9] A. H. Abdel-Gawad, L. A. Said and A. G. Radwan: Optimized edge detection technique for brain tumor detection in MR images, *IEEE Access*, **8** (2020), 136243–136259.

[10] A. Nandal, H. Gamboa-Rosales, A. Dhaka, J. M. Celaya-Padilla, J. I. Galvan-Tejada, C. E. Galvan-Tejada, F. J. Martinez-Ruiz and C. Guzman-Valdivia: Image edge detection using fractional calculus with feature and contrast enhancement, *Circuits, Systems, and Signal Processing*, **37** (2018), 3946–3972.

4.8 Amr R. El-Dhaba: Nonlocal Electromechanical Effects in Anisotropic Dielectric Materials within Simplified Strain Gradient Elasticity

Amr R. El-Dhaba
Department of Mathematics and Statistics, College of Science, King Faisal University
E-mail: aemam@kfu.edu.sa, ORCID ID: - 0000-0002-6123-9002.

Abstract

In this paper, we investigate the effect of non-locality on the flexoelectric effect in dielectric materials using the simplified strain gradient theory of elasticity. Our methodology consists of two main stages. In the first stage, we apply the variational principle to the strain energy functional and virtual work for the external forces. The second stage incorporates the hypothesis introduced by Stratton [1] and later extended by Landau and Lifshitz [2] to derive the field equations and boundary conditions. The non-locality hypothesis states that the variation in any electric quantity includes both the variation of that quantity and the variation in displacement.

This procedure results in a nonlinear system of partial differential equations, where the nonlinearity appears in the equation of motion, while the electrostatic equations governing polarization and its gradient remain linear. As an application of the developed mathematical model, we consider a one-dimensional semi-infinite domain occupied by an elastic dielectric material. The field equations and boundary conditions are formulated in Cartesian coordinates. To obtain hierarchical solutions to the problem, we apply the reductive perturbation method [3]. The results are then plotted and analyzed in detail.

Keywords: Non-local flexoelectric effect, micro-inertia effect; cubic materials; Simplified strain gradient elasticity; Variational techniques; Reductive perturbation technique.

4.8.1 Introduction

The flexoelectric effect is a property of certain materials that allow them to generate electricity despite being non-conductive. This effect discovered by Kogan [4] and takes its name by Indenbom [5]. The flexoelectric effect occurs when the material subjected to non-homogeneous deformation (tension or compression) and the internal structure deformed as in the following:

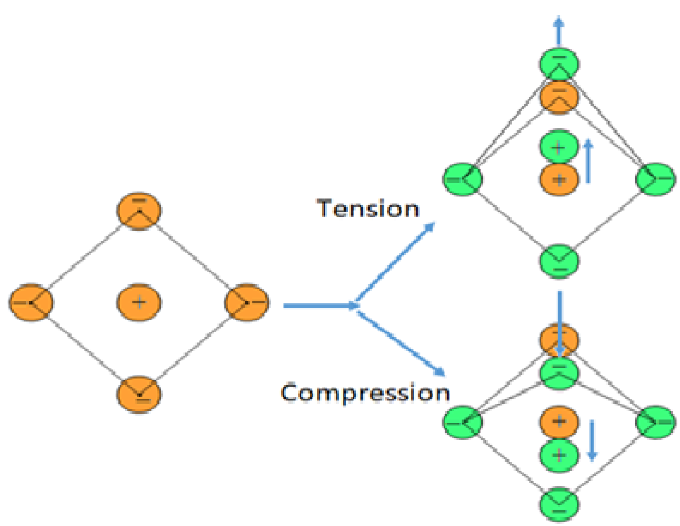

Figure 7: In-homogeneous deformation

Therefore, due to the disruption of the material's internal structure, causing both negative and positive charges to be shifted around their equilibrium positions. As a result, the dipole moment

changes, or a spontaneous polarization induced inside the material.
This effect becomes more noticeable as the material's dimensions decrease, making it a size-dependent phenomenon. At larger scales, strain gradients are typically negligible, making the flexoelectric effect weak or undetectable. However, at the nanoscale, where sharp deformations and high strain gradients are more common, the effect becomes significantly more prominent.

4.8.2 Hamilton's Principle

The variational principle is a widely used technique to obtain field equations and boundary conditions for any continuous system undergoing infinitesimal deformation during two different times.

$$\begin{aligned}\int_{t_0}^{t_1}\Bigg(\int_V\left(\delta W_{\text{Kin}}-\delta H+f_i^{\text{ex}}\delta u_i-\rho_e\delta\phi+E_i^{\text{ex}}\delta P_i+E_{ij}^{\text{ex}}\delta P_{i,j}\right)dV\\+\int_{s_T}\left(t_i^{\text{ex}}\delta u_i+\tau_i^{\text{ex}}n_j\delta u_{i,j}\right)dS-\int_{s_D}\bar{\sigma}_e\delta\phi dS+\int_{\partial S}F_i^{\text{edge}}\delta u_i dL\Bigg)dt=0,\end{aligned} \tag{4.8.1}$$

where $H=H(\varepsilon_{ij},\gamma_{i(jk)},P_i,P_{i,j})$ denotes the electric enthalpy, W^{ex} is the work done by external forces, and W_{Kin} is the kinetic energy. ϕ is the electric potential, P_i is the i-polarization vector, and $P_{i,j}$ is the derivative of the i-polarization vector in the j-direction. ρ_e represents the volume electric charge, and $\bar{\sigma}_e$ is the surface electric charge. E_i^{ex} measures the electric field due to the variation of polarization, while E_{ij}^{ex} measures the electric field due to the variation of the gradient of polarization. t_i^{ex} is the stress vector, τ_i^{ex} is the higher-order stress vector, and F_i^{edge} is the component of the wedge force due to unsmooth domains. Finally, δ represents the variation operator.

As states before, one can write

$$\delta P_i=\delta_P P_i+\delta_u P_i, \tag{4.8.2}$$

where $\delta_P P_i$ is the variation of the polarization due to the polarization, and $\delta_u P_i$ is the variation of the polarization due to the displacement.
But

$$\delta_u P_i=P_{i,j}\delta u_j. \tag{4.8.3}$$

Thus, the total variation in polarization is defined as

$$\delta P_i=\delta_P P_i+P_{i,j}\delta u_j. \tag{4.8.4}$$

Similarly, the total variation in the gradient of polarization is given by

$$\delta P_{i,j}=\delta_P P_{i,j}+\delta_u P_{i,j}=\delta_P P_{i,j}+P_{i,jk}\delta u_k. \tag{4.8.5}$$

The variation of the electric potential is written as

$$\delta\phi=\delta_\phi\phi+\delta_u\phi, \tag{4.8.6}$$

where $\delta_\phi\phi$ is the variation of the electric potential due to the electric potential, and $\delta_u\phi$ is the variation of the electric potential due to the displacement. Then, the total variation of the electric potential is given by

$$\delta\phi=\delta_\phi\phi+\phi_{,j}\delta u_j. \tag{4.8.7}$$

Similarly, the total variation of the gradient of the electric potential is written as

$$\delta\phi_{,i}=\delta_\phi\phi_{,i}+\delta_u\phi_{,i}=\delta_\phi\phi_{,i}+\phi_{,ij}\delta u_j. \tag{4.8.8}$$

By substituting Eqs. (2)–(8) into Eq. (1) and performing some mathematical manipulations, the field equations and boundary conditions are derived.

References

[1] Stratton JA. Electromagnetic Theory. McGraw-Hill, New York; 1941.

[2] Landau LD, Lifshitz EM. Electrodynamics of Continuous Media. 1961.

[3] El-Dhaba, A. R. (2024). Periodic solutions for nonlinear deformation waves based on new Boussinesq-type equation within strain gradient elasticity and reductive perturbation technique. Mechanics of Advanced Materials and Structures, 1–13. https://doi.org/10.1080/15376494.2024.2438905

[4] Kogan SM. Piezoelectric effect during inhomogeneous deformation and acoustic scattering of carriers in crystals. Sov Physics-Solid State 1964;5:2069–70.

[5] Indenbom VL, Loginov EB, Osipov MA. Flexoelectric effect and crystal-structure. Kristallografiya 1981;26:1157–62.

4.9 Ahad Alotaibi: Fixed Point Results Via Multivalued Contractive Type Mappings Involving A Generalized Distance On Metric Type Spaces

Abdul Latif[1], **Ahad Alotaibi[2,*]** and **Maha Noorwali[3]**
[1]Department of Mathematics King Abdulaziz University Jeddah Saudi Arabia,
E-mail address: alatif@kau.edu.sa
[2]Department of Mathematics King Abdulaziz University Rabigh Branch Saudi Arabia
E-mail address: aalotaiby@kau.edu.sa
[3]Department of Mathematics King Abdulaziz University Jeddah Saudi Arabia
E-mail address: mnorwali@kau.edu.sa.

Abstract

In this paper, we present some general results on the existence of fixed points for multivalued contractive type mappings with respect to generalized distance related to metric type spaces. Some common fixed point results for Banach operator pairs are also obtained. Further, examples are provided in the support of our main results. Consequently, our results either improve or generalize many existing results of the metric fixed point theory.

* **Ahad Alotaibi**

Metric fixed point theory is one of the most important and applicable research areas of nonlinear analysis. The well known Banach Contraction Principle (BCP), has been appeared as a powerful tool for solving several scientific problems related to a number of scientific areas. The classical concept of metric (distance) has been extended either by reducing or modifying the metric axioms. One of its generalization, known as a b-metric (metric type). In the literature a number of fixed points results have been established in these both directions. In [3], Kada et al. introduced a notion of generalized distance, namely a w-distance on metric spaces and then improved several known results via this generalized distance, while, metric type version of w-distance introduced by Hussain et al. [1], called it wt-distance (w_b-distance) and proved fixed point and common fixed point results for singlevalued mappings with respect to w_b-distance. For further results in this direction, see [4, 5] and references therein. In this paper, we present some fixed point results for multivalued nonlinear generalized contractions along with supporting examples. In fact, our results either improve or generalize a number of known fixed point results.

In the sequel, we consider (S, D_b) is a complete metric type space otherwise stated and p_b is a w_b-distance on S. Now, we present some of our main fixed point results via multivalued contractive type mappings involving generalized distance p_b.

Theorem 1 Consider a mapping $J : S \to C(S)$ with a b-lower semi-continuous h on S defined by $h(u) = p_b(u, J(u))$. Assume that the following conditions hold:

(a) there exist a constant $c \in (0, 1)$ and a function $\varphi : \mathbb{R}^+ \to [c, 1)$ with $\limsup_{q\to t^+} \varphi(q) < 1$ for every $t \geq 0$,

(b) for u of S, there exits v of $J(u)$ satisfying

$$[\varphi(h(u))]^r \; p_b(u, v) \leq h(u), \text{ where } r \in (0, 1), \tag{4.9.1}$$

and

$$h(v) \leq \varphi(h(u)) \; p_b(u, v). \tag{4.9.2}$$

Then, there exists $u_0 \in S$ such that $p_b(u_0, J(u_0)) = 0$. Further, if $p_b(u_0, u_0) = 0$, then $u_0 \in J(u_0)$.

Now, we observe that the conclusion of Theorem 1 still holds, if we dispense the b-lower semi-continuity of the function h with somewhat another mathematical condition.

Theorem 2 Assume that all the assumptions of Theorem 1 are valid except the b-lower semi-continuity of the function h. Further, if $\inf \{p_b(u,z) + p_b(u, J(u)) : u \in S\} > 0$, for every $z \in S$ with $z \notin J(z)$, then $\mathrm{Fix}(J) \neq \emptyset$.

Now, we present a common fixed point result for Banach operator pairs of metric type spaces.

Theorem 3 Let $g : S \to S$ be a single valued mapping with $\mathrm{Fix}(g)$ is a closed subset of S and let $J : S \to C(S)$ be a multivalued mapping satisfying the conditions (a) and (b) of Theorem 1, where the function h on S defined by $h(u) = p_b(u, J(u))$ is a b-lower semi-continuous and (J, g) is a Banach operator pair. Then, there exists $u_0 \in S$ such that $h(u_0) = 0$. Further, if $p_b(u_0, u_0) = 0$, then $u_0 = g(u_0) \in J(u_0)$.

Now we present some examples in support of our main results.

Example Let $S = [0, \infty)$. Define $D_b(x, y) = (x - y)^2$ for all $x, y \in S$. Then S is a metric type space with $b = 2$. Define a w_b-distance on S by $p_b(x, y) = x^2 + y^2$, for all $x, y \in S$. Now, for any real number $c > 1$, let $J : S \to C(S)$ be defined by

$$J(x) = \left\{ \frac{x}{c} \right\} \cup [1 + 2x, \infty), \quad \forall x \in [0, \infty)$$

Define $g : S \to S$ by $g(x) = x, \forall x \in S$ and define a function $\varphi : [0, \infty) \to (0, 1)$ by $\varphi(t) = \frac{1}{c^2}$. Since $J(x) \subseteq \mathrm{Fix}(g), \forall x \in \mathrm{Fix}(g)$. Then (J, g) is a Banach operator pair. Thus, for each $x \in [0, \infty)$ all the conditions of Theorem 1 and Theorem 3 are satisfied and hence $Fix(J) \neq \emptyset$ and $C(J, g) \neq \emptyset$. Note that $\mathrm{Fix}(J) = \{0\}$ and $C(J, g) = \{0\}$.

References

[1] N. Hussain, R. Saadati and R. P. Agrawal, *On the topology and wt-distance on metric type spaces*, Fixed Point Theory Appl. **2014** (2014), 1–14.

[2] N. Hussain, N. Yasmin and N. Shafqat, Multi-Valued Ćirić Contractions on Metric Spaces with Applications, Filomat, **28** (2014), 1953–1964.

[3] O. Kada, T. Suzuki and W. Takahashi, *Nonconvex minimization theorems and fixed point theorems in complete metric spaces*, Math. Japonicae **44** (1996), 381–391.

[4] A. Latif, R. F. Al Subaie and M.O. Alansari, *Metric fixed points for contractive type mappings and applications*, J. Nonlinear Convex Anal. **23** (2022), 501–511.

[5] A. Latif, A. Alotaibi and M. Noorwali, Multivalued nonlinear contractive type mappings and fixed points, J. Nonlinear Convex Anal. **25** (2024), 2611–2624.

4.10 Bader Saidan: Exotic options in fractal activity time models with the Student distribution of log-returns

Nikolai Leonenko[1], **Andrey Pepelyshev** [2] and **Bader Saidan[3,4,*]**
[1]Cardiff University, School of Mathematics, United Kingdom, leonenkon@cardiff.ac.uk
[2]Cardiff University, School of Mathematics, United Kingdom, pepelyshevan@cardiff.ac.uk
[3]Cardiff University, School of Mathematics, United Kingdom, saidanb@cardiff.ac.uk
[4]Prince Sattam Bin Abdulaziz University, Department of Mathematics, Saudi Arabia.

Abstract

Modeling financial price movements is crucial for both investment strategies and derivative pricing, see the fundamental work of [2]. [3]; [4] introduced supOU and related models incorporating various dependence structure for option pricing and hedging.

Although stochastic models are widely adopted in asset pricing, they face difficulties in accurately capturing the empirical properties of financial returns. These challenges include non-normal, fat-tailed distributions and the dependence structure of squared and absolute returns, commonly referred to as the Taylor effect [2, 10]. To remedy this issue, [8] explored time-changed that use the Lévy processes with Student distribution, normal inverse Gaussian (NIG) distribution and variance-gamma (VG) distributions. It is important to note that while increments of Lévy processes are independent and their marginal distribution is non-Gaussian, but the dependencies of squared returns are not adequately described.

We consider the fractal activity geometric Brownian motion (FATGBM) model proposed by [1]. We focus on the FATGBM with Student marginals because log-returns for real data are well fitted by the location scale Student distribution. This model captures key empirical features of returns; the absence of correlation while preserving dependence, as well as distributions with heavier tails and higher peaks compared to the Gaussian distribution. Specifically, it extends geometric Brownian motion by evaluating standard Brownian motion at a random activity time rather than calendar time.

It is evident that the activity time process is approximately self-similar. Therefore, we need a method that can incorporate both the required distributional and dependence features as well as the property of asymptotic self-similarity. We note that the inverse gamma distribution is infinitely divisible and self-decomposable and based on that we construct the fractal activity time through Ornstein-Uhlenbeck (OU)-type process which has the inverse gamma distribution. After construction of this fractal activity time, we use so-called skew-correcting martingale that imposes parameter restrictions to ensure that $\{e^{-rt}S_t\}$ is a martingale, which relates to the absence of arbitrage.

We derive options pricing formulae for different derivatives which are digital options or cash-or-nothing, power options which are basically the standard European options (vanilla options) with the underlying asset's price raised to a certain power. Finally, barrier options which are considered as exotic options, we use the Girsanov theorem and the joint conditional density to drive pricing formulae for these options. We run numerical simulation to confirm the derived formulae by using the Monte-Carlo method.

The talk is based on the joint work with N. Leonenko and A. Pepelyshev [14].

* **Lead presenter**

References

[1] C. C. Heyde and N. N. Leonenko: Student Processes, *Advances in Applied Probability*, **37** (2005), 342–365.

[2] C. W. J. Granger: The Past and Future of Empirical Finance: Some Personal Comments, *Journal of Econometrics*, **129** (2005), 35–40.

[3] O. E. Barndorff-Nielsen and N. Shepard: Non-Gaussian Ornstein-Uhlenbeck-Based Models and Some of Their Uses in Financial Economics, *Journal of the Royal Statistical Society. Series B: Statistical Methodology*, **63** (2001), 167–241.

[4] O. E. Barndorff-Nielsen and N. N. Leonenko: Spectral Properties of Superpositions of Ornstein-Uhlenbeck Type Processes, *Methodology and Computing in Applied Probability*, **7** (2005), 335–352.

[5] D. B. Madan and A. Cherny: Markets as a Counterparty: An Introduction to Conic Finance, *International Journal of Theoretical and Applied Finance*, **13** (2010), 1149–1177.

[6] E. Seneta: Fitting the Variance-Gamma Model to Financial Data, *Journal of Applied Probability*, (2004), 177–187.

[7] R. Finlay and E. Seneta: A Gamma Activity Time Process With Noninteger Parameter and Self-Similar Limit, *Journal of Applied Probability*, **44** (2007), 950–959.

[8] O. E. Barndorff-Nielsen, T. Mikosch, and S. I. Resnick: *Lévy Processes: Theory and Applications*, Springer Science & Business Media, 2012.

[9] R. Finlay, E. Seneta, and D. Wang: An Inverse Gamma Activity Time Process With Noninteger Parameters and a Self-Similar Limit, *Journal of Applied Probability*, **49** (2012), 441–450.

[10] C. C. Heyde: Scaling Issues for Risky Asset Modelling, *Mathematical Methods of Operations Research*, **69** (2009), 593–603.

[11] O. E. Barndorff-Nielsen: Normal Inverse Gaussian Distributions and Stochastic Volatility Modelling, *Scandinavian Journal of Statistics*, **24** (1997), 1–13.

[12] C. C. Heyde: A Risky Asset Model with Strong Dependence through Fractal Activity Time, *Journal of Applied Probability*, (1999), 1234–1239.

[13] N. N. Leonenko, S. Petherick, and A. Sikorskii: The Student Subordinator Model With Dependence for Risky Asset Returns, *Communications in Statistics - Theory and Methods*, **40** (2011), 3509–3523.

[14] N. Leonenko, A. Pepelyshev, and B. Saidan: Exotic options in fractal activity time models with the Student distribution of log-returns, Submitted, (2025).

4.11 Elsiddig Awadelkarim: Unbiased Parameter Estimation for Partially Observed Diffusion

Elsiddig Awadelkarim
King Abdullah University of Science and Technology, Saudi Arabia. elsiddigawadelkarim.elsiddig@kaust.edu.sa.

Abstract

We consider the problem of estimating static parameters for a partially observed diffusion process X_t with discrete-time noisy observations $\{Y_t\}_{t=1}^{T}$ over a fixed time interval $[0, T]$. The diffusion satisfies the equation

$$dX_t = a_\theta(X_t)dt + \sigma(X_t)dW_t$$

where W_t is a standard Brownian motion, and the goal is to estimate θ. In particular, we assume that one must time-discretize the partially observed diffusion process and work with the model with bias and consider maximizing the resulting log-likelihood of the discrete model. Using a novel double randomization scheme, based upon Markovian stochastic approximation we develop a new method to unbiasedly estimate the static parameters, that is, to obtain the maximum likelihood estimator for the continuous model with no time discretization bias. Under assumptions we prove that our estimator is unbiased and investigate the method in several numerical examples, showing that it can empirically out-perform existing unbiased methodology.

* **Lead presenter**

References

[1] Awadelkarim, E., Jasra, A., Ruzayqat, H. (2024). Unbiased parameter estimation for partially observed diffusions. SIAM Journal on Control and Optimization, 62(5), 2664–2694.

4.12 Fadhah Alanazi: Vine Copula Construction

Fadhah Alanazi
Department of Mathematics and Sciences, Prince Sultan University, Saudi Arabia.

Vine copulas have emerged as a powerful tool for modeling complex multivariate dependencies in various fields, including finance, hydrology, and machine learning. Central to the construction of vine copula models is the choice of bivariate copulas, which serve as building blocks for capturing pairwise dependencies in a hierarchical structure. The type of copula selected, whether Gaussian, Student-t, Clayton, Gumbel, or others, dramatically impacts the construction process and the resulting model's accuracy and interpretability. This talk explores how different copula families influence the flexibility, dependence on the tail, and overall fit of vine copula models. We will discuss the implications of selecting appropriate copulas for capturing diverse dependency structures, particularly in high-dimensional settings, and highlight the trade-offs between model complexity and computational efficiency. Through real-world examples and simulations, we demonstrate how choosing a copula family can lead to significantly different inferences and predictions, emphasizing the importance of thoughtful copula selection in practical applications. At the end of this talk, participants will gain insight into best practices for constructing robust vine copula models tailored to their specific data characteristics and research objectives.

4.13 Fadwa Althrwi: Analysis of Perturbed Gerdjikov-Ivanov Equation Using Traditional and Improved Adomian Decomposition Methods

Fadwa Althrwi[1], **Aisha Farhat**[1], **A. A. AlQarni[2]**, **A. A. Alshaery**[1] and **H. O. Bakodah**[1]
[1] Department of Mathematics and Statistics, College of Science, University of Jeddah, Jeddah 23445, Saudi Arabia.
[2] Department of Mathematics, College of Science, University of Bisha, Bisha 61922, Saudi Arabia.

Abstract

This paper investigates the perturbed Gerdjikov-Ivanov (pGI) equation, a nonlinear partial differential equation (PDE), That describes the evolution of optical solitons, solitons are critical in optical communications. The pGI equation is an extension of the classical Gerdjikov-Ivanov (GI) equation, incorporating perturbation terms that account for external forces or influences on wave dynamics.

The study focuses on solving the pGI equation using two analytical methods: the traditional Adomian Decomposition Method (ADM) and its improved version, The improved Adomian Decomposition Method (IADM). These methods provide approximate solutions without requiring linearization, making them effective for handling nonlinear equations. The pGI equation is expressed as:

$$iu_t + au_{xx} + b|u|^4u + icu^2u_x^* = i[\alpha u_x + \beta((u)^{2m}u)_x + \delta(u^{2m})_x u], \quad m \geq 1. \tag{4.13.1}$$

where $u = u(x,t)$ is a complex-valued wave profile, and the coefficients a, b, and c represent *group-velocity dispersion, quintic nonlinearity, and nonlinear dispersion,* respectively. The exact solution that will be treated in the analysis take place in, see [1]. This paper focuses on the solution from the classical Kudryashov's method, given by

$$u(x,t) = \sqrt{\frac{A_1}{d\exp\left(\eta(x-\nu t)+1\right)}}\exp\left(i(-\kappa x + \frac{1}{4}t(a\eta^2 - 4a\kappa^2 - \alpha\kappa) + \vartheta)\right) \tag{4.13.2}$$

where the solution sets is

$$A_0 = 0, \quad A_1 = A_1, \quad \omega = \frac{1}{4}(a\eta^2 - 4a\kappa^2 - \alpha\kappa) \quad b = -\frac{3a\eta^2}{4A_1^2}, \quad c = \frac{-a\eta^2 - A_1\beta\kappa}{A_1\kappa} \tag{4.13.3}$$

with A_1 and d are any non-zero arbitrary constants.

The study begins by applying the traditional ADM to the pGI equation. ADM decomposes the solution into an infinite series of components [2,3], represented as:

$$u(x,t) = \sum_{n=0}^{\infty} u_n(x,t) \tag{4.13.4}$$

Where the components $u_n, n \geq 0$ will be determined recreantly. ADM and it's modifications uses *Adomian polynomials* to handle nonlinear terms, simplifying the equation into manageable sub-problems according to specific algorithms set by Adomian [4–6].

$$A_n = \frac{1}{n!}\frac{d^n}{d\lambda^n}[A(\sum_{i=0}^{\infty} u(x,t)\lambda^i)]_{\lambda=0}, n = 0,1,2,\ldots \tag{4.13.5}$$

Employ the operator form $L_t = \frac{\partial}{\partial t}$ on equation (4.13.1). Then, define the nonlinear term in equation to be

$$A = -b|u|^4u - icu^2u_x^* + i[\alpha u_x + \beta((u)^{2m}u)_x + \delta(u^{2m})_x u] \tag{4.13.6}$$

Next, apply the inverse operator, $L_t^{-1}(\cdot) = \int_0^t (\cdot)dt$. Thus, we conclude with the recursive relation

$$u_0(x,t) = u(x,0) \tag{4.13.7}$$
$$u_{k+1}(x,t) = -L_t^{-1} a(u_k)_{xx} + L_t^{-1} A_k \tag{4.13.8}$$

where A are Adomian polynomials and each component u is determined recursively.

Forward IADM splits the solution into real and imaginary parts, allowing for a more precise handling of nonlinear and perturbation terms.

First, the function u is presented by

$$u(x,t) = u_1(x,t) + iu_2(x,t) \tag{4.13.9}$$

This will convert equation 4.13.1 into a complex system of two equations. As previous, apply the operator $L_t = \frac{\partial}{\partial t}$. Then, simplify and split the real and the imaginary part. Respectively, define the nonlinear terms by A_1 and A_2, to be the Adomian polynomials,

$$\begin{aligned} A_1 = {} & b[u_1^2 + u_2^2]^2 u_1 + c[(u_1^2 - u_2^2)u_{2x} - 2u_1u_2(u_{1x})] \\ & + \alpha u_{2x} + \beta[(u_1^2 + u_2^2)^m u_2]_x + \delta[((u_1^2 + u_2^2)^m)_x u_2] \end{aligned} \tag{4.13.10}$$
$$\begin{aligned} A_2 = {} & -b[u_1^2 + u_2^2]^2 u_2 - c[(u_1^2 - u_2^2)u_{1x} - 2u_1u_2(u_{2x})] \\ & + \alpha u_{1x} + \beta[(u_1^2 + u_2^2)^m u_1]_x + \delta[(u_1^2 + u_2^2)^m)_x u_1] \end{aligned} \tag{4.13.11}$$

Next, apply the inverse operator $L_t^{-1}(\cdot) = \int_0^t (\cdot)dt$ for both equations, this gives the recursive relation

$$u_{1,0}(x,t) = u_1(x,0) \tag{4.13.12}$$
$$u_{2,0}(x,t) = u_2(x,0) \tag{4.13.13}$$
$$u_{1,k+1}(x,t) = -aL_t^{-1}(u_{2,k}(x,t))_{xx} + L_t^{-1} A_{2,k} \tag{4.13.14}$$
$$u_{2,k+1}(x,t) = aL_t^{-1}(u_{1,k}(x,t))_{xx} + L_t^{-1} A_{1,k}, \qquad k \geq 0, m \geq 1. \tag{4.13.15}$$

where $u_1(x,0) = \mathrm{Re}(u(x,0)), u_2(x,0) = \mathrm{Im}(u(x,0))$ and $A_r, r = 1,2$ are the Adomian polynomials defined as in equation (4.13.5). Pursue with the numerical analysis, consider $m = 1$ and the following parameters in equation(4.21.2) as

$$A_0 = 0, A_1 = 0.0001, \nu = 0.0005, a = 0.002, \vartheta = 0.01, \kappa = 0.01, \tag{4.13.16}$$
$$\eta = 1, d = 1, \alpha = 0.002, \beta = 0.0001, \delta = 0.002 \tag{4.13.17}$$

The results and profiles of the two methods are illustrated in Figure.**??**. This figure present the graphs of the exact solution from equation (4.13.2), along with the approximate solutions from the ADM in equation (4.13.7) and the IADM in equation (4.13.12). Result 1: ADM provides accurate, fast-converging solutions for the pGI equation by decomposing it via Adomian polynomials, simplifying nonlinear terms and enabling efficient computation. but may face convergence and accuracy issues for strong nonlinearity or complex boundaries. IADM enhances this by iteratively reducing errors, offering superior accuracy and stability, particularly in nonlinear or complex scenarios. Result 2: The plots use color-coded markers to distinguish methods clearly illustrating that both ADM and IADM closely follow the exact solution, with IADM maintaining higher accuracy over time due to its iterative refinement. Both methods handle nonlinearity and perturbations well, supporting broader application to nonlinear PDEs.

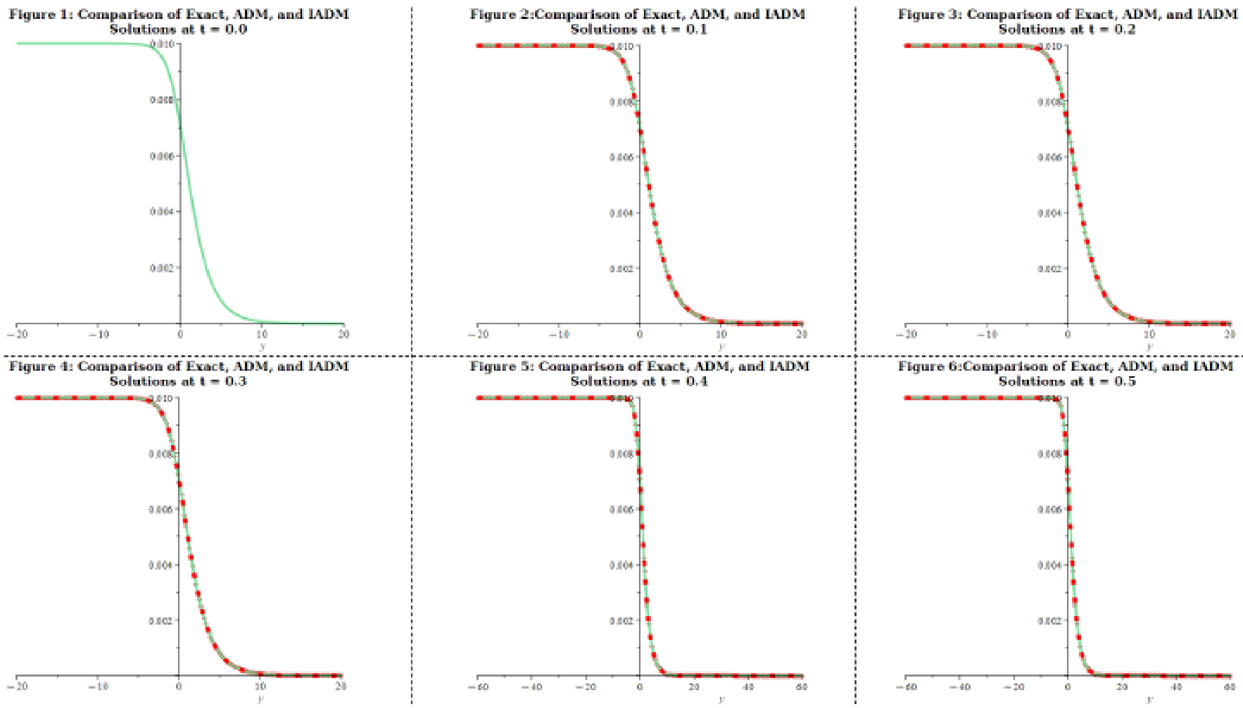

Figure 8: Each graph represent the exact solution (aquamarine line), ADM (orange), and IADM (red) approximations, at $t = 0.$, $t = 0.1$, $t = 0.2$, $t = 0.3$, $t = 0.4$ till $t = 0.5$.

References

[1] Fadwa Althrwi et al., "Supplementary optical solitonic expressions for Gerdjikov-Ivanov equations with three Kudryashov-based methods," *Communications in Theoretical Physics*, vol. 76, no. 12, 2024.

[2] G. Adomian, "Solution of physical problems by decomposition," *Comp. & Math. Appl.*, vol. 27, no. 9-10, pp. 145-154, 1994.

[3] A.A. Qarni, M.A. Banaja, H.O. Bakodah, M. Mirzazadeh, and A. Biswas, "Optical solitons with coupled nonlinear Schrödinger's equation in birefringent nano-fibers by Adomian decomposition method," *Journal of Computational and Theoretical Nanoscience*, vol. 13, no. 8, pp. 5493–5498, 2016.

[4] A.M. Wazwaz, "A new algorithm for calculating Adomian polynomials for nonlinear operators," *Applied Mathematics and Computation*, vol. 111, no. 1, pp. 53–69, 2000.

[5] J. Biazar, E. Bablian, R. Islam, "An alternative algorithm for computing Adomian polynomials in special cases," *Applied Mathematics and Computation*, vol. 138, pp. 523–529, 2003.

[6] A.M. Wazwaz, "A comparison between the Adomian's decomposition method and Taylor series method in the series solutions," *Applied Mathematics and Computation*, vol. 102, pp. 77–86, 1999.

4.14 Jianqing Zhu: Localized Arabic Large Language Model

Jianqing Zhu*, and **Jinchao Xu**
King Abdullah University of Science and Technology, Saudi Arabia.

Abstract

This research presents a comprehensive framework for developing culturally-aligned, linguistically proficient Arabic Large Language Models (LLMs) that address the underrepresentation of Arabic in mainstream LLMs. By integrating targeted Arabic pre-training, progressive vocabulary expansion, supervised fine-tuning with native Arabic instructions, and culturally-sensitive reinforcement learning, the proposed models significantly outperform existing open Arabic LLMs in both accuracy and cultural awareness. Moreover, the introduction of "native alignment"–embedding cultural alignment from the pre-training phase–enhances model stability and safety. This work not only sets a new state-of-the-art for Arabic LLMs but also contributes open-source models to support inclusive and responsible AI development for Arabic-speaking communities.

* **Lead presenter**

This research focuses on developing and democratizing localized Large Language Models (LLMs) specifically tailored for the Arabic language, addressing significant gaps in cultural sensitivity, linguistic appropriateness, and accessibility. Arabic, characterized by distinct linguistic features and rich cultural nuances, remains inadequately supported by mainstream LLMs, which predominantly cater to widely spoken languages such as English and Chinese. Consequently, the Arab world experiences slower progress in benefiting from advanced natural language processing technologies comparable to state-of-the-art models like GPT-4. To bridge this technological divide, this research introduces comprehensive methodologies for developing culturally-aligned, linguistically proficient Arabic LLMs capable of effectively meeting diverse, application-specific needs of Arabic-speaking communities.

Firstly, we introduce a robust and culturally-aware Arabic LLM developed via a multi-stage pipeline designed explicitly for the linguistic and cultural nuances of Arabic. The model undergoes additional pre-training using an extensive Arabic corpus, effectively capturing the language's unique semantic, syntactic, and cultural features. This phase ensures that the model's foundational knowledge aligns closely with Arabic linguistic conventions and cultural sensitivities. Subsequently, we employ Supervised Fine-Tuning (SFT), utilizing native Arabic instructions paired with GPT-4-generated responses in Arabic, significantly enhancing the model's accuracy and coherence in both interpreting and generating Arabic content. Complementing SFT, our model undergoes Reinforcement Learning with AI Feedback (RLAIF), guided by a culturally sensitive reward model. This strategy explicitly integrates local values and cultural expectations into the alignment process, resulting in a model that excels on standard linguistic benchmarks and demonstrates heightened awareness and respect toward cultural contexts. Extensive evaluations across various benchmarks confirm that our model sets a new state-of-the-art standard, notably outperforming existing open Arabic LLMs in both linguistic proficiency and cultural alignment.

Secondly, addressing the practical challenge of tokenizer vocabulary efficiency, this research highlights an innovative method inspired by vocabulary acquisition in human second language learning, specifically targeting Arabic-specific vocabulary constraints. Conventional tokenizers often encounter a high out-of-vocabulary (OOV) rate when dealing with languages like Arabic, resulting in reduced knowledge retention and degraded performance during early training stages. To overcome this limitation, the introduced model employs a Progressive Vocabulary Expansion strategy, utilizing a modified Byte Pair Encoding (BPE) algorithm. This method incrementally expands Arabic subwords within a dynamically adjusted vocabulary throughout training, balancing and steadily reducing the OOV ratio. Through rigorous ablation studies, this progressive expansion approach is empirically validated, demonstrating notable improvements in both training efficiency and overall performance. Consequently, the proposed model achieves comparable, and in some cases superior, performance relative to leading Arabic LLMs across multiple Arabic linguistic benchmarks.

Lastly, this research emphasizes the crucial aspect of alignment in developing reliable and safe Arabic LLMs. Traditional methods often rely heavily on alignment techniques implemented during post-training stages such as instruction tuning and reinforcement learning–approaches collectively termed ”post alignment.” In contrast, this work advocates for the concept of ”native alignment,” where alignment practices are embedded during the initial pre-training phase itself. Native alignment leverages extensively curated and culturally-sensitive pre-training data, proactively preventing the incorporation of unaligned content and biases from the outset. This strategic approach enhances model stability, safety, and effectiveness by reducing reliance on post-hoc interventions. Comprehensive experiments and further ablation studies conducted in this research substantiate the substantial benefits of native alignment. Models trained under the native alignment paradigm exhibit enhanced alignment stability and superior performance across various evaluation metrics. Importantly, this research also provides open-source access to these developed Arabic LLMs, significantly enriching the Arabic LLM community and supporting ongoing research and development efforts.

In conclusion, this research systematically addresses the critical need for culturally-aligned, linguistically proficient, and democratized Arabic Large Language Models (LLMs). Through the integration of targeted Arabic pre-training, progressive vocabulary expansion, supervised fine-tuning with native Arabic instructions, culturally-sensitive reinforcement learning, and native alignment strategies, the proposed models–particularly AceGPT-v2-32B and AceGPT-v2-70B–achieve state-of-the-art performance across a wide range of Arabic benchmarks. As shown in Table 3, AceGPT-v2-70B notably surpasses existing open Arabic models and demonstrates competitive results even when compared to general-purpose models like GPT-3.5 and GPT-4. Furthermore, the implementation of native alignment improves not only cultural sensitivity but also enhances model stability and safety. This comprehensive approach sets new benchmarks for responsible, culturally respectful language technologies and offers powerful open-source tools to advance Arabic NLP research and empower Arabic-speaking communities.

	Arabic								**English**			**Chinese**		
Model	Avg.	MMLU (trans)	MMLU$koto et al.)	ARC	BoolQ	EXAMs	ACVA clean	ACVA all	Avg.	MMLU	RACE	Avg.	CMMLU	CEval
ArabicGPT-8B	66.69	54.45	62.21	72.44	71.65	52.98	76.54	76.55	75.68	67.33	84.02	52.25	51.68	52.82
ArabicGPT-32B	70.63	57.12	68.70	78.07	77.22	52.89	81.36	79.03	82.86	74.43	91.28	77.11	76.10	78.11
ArabicGPT-70B	73.99	64.26	72.50	85.53	82.66	56.99	78.61	77.38	83.69	78.98	88.39	67.56	68.03	67.09
Jais-30B-v3 [1]	57.84	35.68	62.36	51.02	76.30	32.24	73.63	73.66	57.03	59.65	54.40	31.51	25.91	37.10
GPT-3.5 [2]	62.44	46.07	57.72	60.24	76.12	45.63	74.45	76.88	74.70	69.10	80.30	53.20	53.90	52.50
GPT-4 [3]	75.78	65.04	72.50	85.67	85.99	57.76	84.06	79.43	87.00	83.00	91.00	70.45	71.00	69.90

Table 3: Performance comparison of various models across Arabic, English, and Chinese benchmarks.

References

[1] N. Sengupta, et al., Jais and Jais-Chat: Arabic-centric foundation and instruction-tuned open generative large language models, *arXiv preprint*, **arXiv:2308.16149**, (2023).

[2] OpenAI, ChatGPT (3.5): A large language model, *OpenAI*, **https://openai.com/chatgpt**, (2023).

[3] J. Achiam, et al., GPT-4 Technical Report, *arXiv preprint*, **arXiv:2303.08774**, (2023).

4.15 Kais Feki: Bounded Linear Operators and Their Inequalities in Hilbert and Semi-Hilbert Spaces

Kais Feki
Department of Mathematics, College of Science and Arts, Najran University, Najran 66462, Kingdom of Saudi Arabia Email: kfeki@nu.edu.sa.

Abstract

This study explores bounded linear operators and their inequalities in both single and multivariable contexts within Hilbert and semi-Hilbert spaces. The primary focus is on the A-spectral radius of A-bounded operators, its interplay with the A-numerical radius, and the characterization of A-normaloid operators. New inequalities are established for the A-spectral radius and A-numerical radius, providing deeper insights into operator behavior in these spaces.

Keywords: Positive operator, A-numerical radius, A-spectral radius, A-normaloid operator, A-spectrum, operator inequality.

References

[1] K. Feki, Spectral radius of semi-Hilbertian space operators and its applications, *Ann. Funct. Anal.* **11** (2020), 929–946.

[2] K. Feki, Some A-spectral radius inequalities for A-bounded Hilbert space operators, *Banach J. Math. Anal.* **16** (2022), 31.

4.16 Waled Al-Khulaifi: Exponential Decay in a Delayed Wave Equation with Variable Coefficients

Waled Al-Khulaifi[1,2,*], **Manal Alotibi**[1,3] and **Nasser-Eddine Tatar**[1,4]
[1]King Fahd University of Petroleum & Minerals, Department of Mathematics, Dhahran, 31261, Saudi Arabia
[2]Interdisciplinary Research Center for Construction and Building Materials, KFUPM, Dhahran, 31261, Saudi Arabia
[3]Center for Integrative Petroleum Research, KFUPM, Dhahran, 31261, Saudi Arabia
[4]Interdisciplinary Research Center for Intelligent Manufacturing and Robotics, KFUPM, Dhahran, 31261, Saudi Arabia.

Abstract

In this talk, we consider a wave equation that incorporates strong damping and a time delay term, both with weighted coefficients. Previous studies, such as [1], have established exponential stability under the condition that the weight of the damping (or strong damping) dominates that of the delay term. This condition has also been extended to cases involving weighted coefficients, as demonstrated by [2]. Our study introduces a new perspective: we prove that exponential stability can still be achieved, even in scenarios where the delay term is not dominated by the damping term. A numerical example will be presented to validate our result.

* **Lead presenter**

References

[1] S. Nicaise, C. Pignotti, Stability and instability results of the wave equation with a delay term in the boundary or internal feedbacks, SIAM J. Control Optim., 45 (2006), 1561–1585. `https://doi.org/10.1137/060648891`

[2] A. Benaissa, S. Messaoudi, A. Benguessoum, Energy decay of solutions for a wave equation with a constant weak delay and a weak internal feedback, Electron. J. Qual. Theo., 2014, 1–13. `http://dx.doi.org/10.14232/ejqtde.2014.1.11`

4.17 Fawaz Alharbi: Vector Fields on Bifurcation Diagrams of Quasi Singularities

Fawaz Alharbi
Department of Mathematics, College of Sciences, Umm Al-Qura University, Makkah, Saudi Arabia

Abstract

We describe the generators of the vector fields tangent to the bifurcation diagrams and caustics of simple quasi boundary singularities. As an application, submersions on the pair (G, B) which consists of a cuspidal edge G in $\mathbb{R}^3$ that contains a distinguishing regular curve B, are classified. This classification is used as a means to investigate the contact that a general cuspidal edge G equipped with a regular curve $B \subset G$ has with planes. The singularities of the height functions on (G, B) are discussed and they are related to the curvatures and torsions of the distinguished curves on the cuspidal edge. In addition to this, the discriminants of the versal deformations of the submersions that were accomplished are described and they are related to the dual of the cuspidal edge.

* **Lead presenter**

In a series of papers [2, 5], a new non- standard equivalence relation, on a space $\mathbb{R}^n$ equipped with a variety Γ, are studied, and consequently simple classes were obtained. Classification of projections of Lagrangian manifolds endowed with a hypersurface Γ is accomplished through the utilization of these classes. As a result of the classification, the bifurcation diagrams and caustics of versal unfolding of simple classes were described in [1], which conduct in a different manner. In particular, let $G(z, u) = \widetilde{G}(z, u) + u_0$, with $z \in \mathbb{R}^n$ and $u = (u_0, u_1 \ldots, u_s)$ are parameters, be a versal unfolding of the simple $g(z) = G(z, 0)$ with respect the quasi equivalence relation. Then, the respective bifurcation diagram in the space of parameters consists of two components W_0 which is the standard discriminant given by the equations $G = 0$ and $\frac{\partial G}{\partial z} = 0$ and W_1 which is contained in W_0 and it is determined by constraints that define Γ. The caustics is located in the unfolding base $\widetilde{u} = (u_1, \ldots, u_s)$ (which does not include λ_0),and it also consists of two parts Σ_0 which represents the singular set image of W_0 under the projection $\pi : u \to \widetilde{u}$ and $\Sigma_1 = \pi(W_1)$. The preceding construction yields that the bifurcation diagrams is a pair $W = (W_0, W_1)$ where W_0 is a hypersurface in $\mathbb{R}^s_u$ and $W_1 \subset W_0$, while the caustics is the union $\Sigma^* = \Sigma_0 \cup \Sigma_1$ with $dim(\Sigma_0) = dim(\Sigma_1)$.

In the current work, we shall calculate the generators of the vector fields that are parallel to the quasi bifurcation diagrams and caustics, obtained in [1]. This implies that, for the bifurcation diagrams, we seek vector fields that preserve not only W_0 but also the points of W_0, and for the caustics we seek vector fields that preserve both Σ_0 and Σ_1.

Result 1 The stationary algebra of $\mathcal{W}(B_k)$, for $k = 2, 3, 4$, and $\mathcal{W}(F_{2,3})$ is obtained.

Result 2: As application, we consider a cuspidal edge G equipped with a distinguished regular curve$B$ in it. The object appears as a bifurcation diagram of the quasi boundary class B_3. We shall apply the module of vector fields obtained to classify submersions on the pair (G, B). Then we use such classification to study the contact of a general cuspidal edge equipped with a regular curve in it via studying the singularities of height function on (G, B). Mind that, there are two distinguished regular curves Σ_G (the singular set) and B. Finally, we examine the duality of the two curves via describing the versal deformation of the generic submersions that are obtained.

References

[1] F. Alharbi, *Bifurcation diagrams and caustics of simple quasi border singularities,* Topology and its Application, **9** (2012), 381–388.

[2] F. Alharbi, S. Alsaeed, *Quasi Semi-Border Singularities*, Mathematics., **7** (2019), 495.

[3] J. W. Bruce, *Vector fields on discriminants and bifurcation varieties,* Bull. London Math. Soc., **17** (1985), 257-262.

[4] R. Oset Sinha, F. Tari, *On the flat geometry of the cuspidal edge,* Osaka J. Math., **55** (2018), 393–421.

[5] V. M. Zakalyukin, *Quasi singularities,* Geometry and topology of caustics –CAUSTICS '06, Banach Center Publications, Polish Acad. Sci. Inst. Math., Warsaw, **81** (2008), 215-225.

4.18 Maha Alshammari: Specht Modules for the Symmetric Group S_6

Maha Oudah Alshammari[1] and **Faryad Ali**[2]
[1]IMAMU, Department of Mathematics and Statistics, maha-o@outlook.sa
[2]IMAMU, Department of Mathematics and Statistics, faali@imamu.edu.sa.

Abstract

The symmetric group S_6 plays a key role in many areas of research in addition to mathematics and therefore is of great importance. In this paper, we study the irreducible representations of symmetric group S_6 by using the Specht Modules, which are irreducible sub-modules of the permutation modules. We provide a complete description of the construction of irreducible representations via the Frobenius Formula. We describe the construction of Specht Modules S^λ for each partition λ of 6. The group S_6 is symmetric group of order 720 with 11 conjugacy classes of its elements. We compute all the Specht Modules S^λ by applying the Frobenius Formula.

* **Maha Oudah Alshammari**

Let us consider the partition $\lambda = (3, 2, 1)$. We compute the value of the Specht module corresponding to the permutation $(123) \in S_6$, which has cycle type $\mu = (3, 1^3)$. Thus, by the Frobenius Formula, the value of S^λ at $\mu = (3, 1, 1, 1)$ will be the coefficient of $x_1^5 x_2^3 x_3$ in

$$\prod_{1 \leqslant i < j \leqslant 3} (x_i - x_j) \prod_{i=1}^{4} (x_1^{\mu_i} + x_2^{\mu_i} + x_3^{\mu_i})$$

where

$$\prod_{1 \leqslant i < j \leqslant 3} (x_i - x_j) = (x_1 - x_2)(x_1 - x_3)(x_2 - x_3)$$

and

$$\prod_{i=1}^{4} (x_1^{\mu_i} + x_2^{\mu_i} + x_3^{\mu_i}) = (x_1^3 + x_2^3 + x_3^3)(x_1 + x_2 + x_3)^3.$$

On computing the product, we obtain that the coefficient of $x_1^5 x_2^6 x_3$ is -2. Therefore $S^{(3,2,1)} = -2$ corresponding to the permutation $(123) \in S_6$. Similarly, for $\lambda = (5, 1)$ corresponding to the permutation $(1\ 2\ 3)(4\ 5) \in S_6$ will be the coefficient of $x_1^6 x_2^1$ in the expansion of

$$\begin{aligned}\prod_{1 \leqslant i < j \leqslant 2} (x_i - x_j) \prod_{i=1}^{3} (x_1^{\mu_i} + x_2^{\mu_i}) &= (x_1 - x_2)(x_1^3 + x_2^3)(x_1^2 + x_2^2)(x_1^1 + x_2^1) \\ &= x_1^7 + x_1^4 x_2^3 - x_1^3 x_2^4 - x_2^7.\end{aligned}$$

We obtain that the value of $S^{(5,1)}$ corresponding to the conjugacy class with representative $(1\ 2\ 3)(4\ 5) \in S_6$ is zero.

By using a similar technique as in the above cases, the value of $S^{(2,2,2)}$ at the permutation $(1\ 2\ 3)(4\ 5\ 6) \in S_6$ will be equal to the coefficient of $x_1^4 x_2^3 x_3^2$ in

$$\prod_{1 \leqslant i < j \leqslant 3} (x_i - x_j) \prod_{i=1}^{3} (x_1^{\mu_i} + x_2^{\mu_i} + x_3^{\mu_i})$$

In this case, we obtain $S^{(2,2,2)} = 3$ corresponding to the conjugacy class with representative $(123)(456) \in S_6$.

We compute values of S^λ for each partition $\lambda \in S_6$, which we produce in the following table.

Since the Specht Modules are irreducible, we obtain the full character table of S_6.

Table 4: Character Table of S_6

Representative Cycle Type Weight	(1) (1^6) 1	(12) $(2,1^4)$ 15	(123) $(3,1^3)$ 40	(12)(34) $(2^2,1^2)$ 45	(1234) $(4,1^2)$ 90	(123)(45) $(3,2,1)$ 120
χ_1	1	1	1	1	1	1
χ_2	1	-1	1	1	-1	-1
χ_3	5	3	2	1	1	0
χ_4	5	-3	2	1	-1	0
χ_5	10	2	1	-2	0	-1
χ_6	10	-2	1	-2	0	1
χ_7	9	3	0	1	-1	0
χ_8	9	-3	0	1	1	0
χ_9	5	1	-1	1	-1	1
χ_{10}	5	-1	-1	1	1	-1
χ_{11}	16	0	-2	0	0	0

Table 5: Character Table of S_6 (Continued)

Representative Cycle Type Weight	(12345) $(5,1)$ 144	(12)(34)(56) (2^3) 15	(123)(456) (3^2) 40	(1234)(56) $(4,2)$ 90	(123456) (6) 120
χ_1	1	1	1	1	1
χ_2	1	-1	1	1	-1
χ_3	0	-1	-1	-1	-1
χ_4	0	1	-1	-1	1
χ_5	0	-2	1	0	1
χ_6	0	2	1	0	-1
χ_7	-1	3	0	1	0
χ_8	-1	-3	0	1	0
χ_9	0	-3	2	-1	0
χ_{10}	0	3	2	-1	0
χ_{11}	1	0	-2	0	0

References

[1] Fulton, W.: Young Tableaux: with Applications to Representation Theory and Geometry, Cambridge University Press, (1997).

[2] Fulton, W. and Harris, J.: Representation Theory, Springer Science, (2013).

[3] James, G. and Liebeck, M.: Representations and Characters of Groups, Cambridge University Press,(2001).

[4] Saikia, M.: Representations of the Symmetric Group, International Centre for Theoretical Physics, (2015).

[5] Zhao, Y.: Young Tableaux and the Representations of the Symmetric Group, The Harvard College Mathematics Review, Cambridge, (2018).

4.19 Mashael Algoulity: Optimal financial benchmark tracking in a market with a Hull-White interest rate model

Mashael Algoulity[1,*] and **Bujar Gashi**[2]
[1]Department of Mathematics, College of Sciences, King Saud University, P.O. Box 2455, Riyadh 11451, Saudi Arabia. Email: malgoulity@ksu.edu.sa
[2]Department of Mathematical Sciences, The University of Liverpool, Peach Street, Liverpool, L69 7ZL, UK. Email:Bujar.Gashi@liverpool.ac.uk.

Abstract

We consider the problem of optimally tracking a general stochastic financial benchmark in an incomplete market with a *Hull-White* interest rate model. Due to the possibly *unbounded* solution to interest rate equation, and our use of quadratic tracking error as an optimality functional, the resulting optimization problem is an example of a stochastic linear-quadratic control problem with possibly unbounded coefficients. We find the solution to this problem in a explicit closed form as an affine tracking-error feedback control the coefficients of which are determined by a linear backward stochastic differential equation with unbounded coefficients.

* **Lead presenter**

Consider a financial market consisting of a bank account with price S_0 and n stocks with prices S_i, $i = 1, ..., n$, which are solutions to the following equations:

$$dS_0 = r\, S_0\, dt, , \quad S_0(0) > 0; \quad dS_i = S_i(\mu_i dt + \sigma_i' dW), \quad S_i(0) > 0, \quad i = 1, ..., n,$$

Here the interest rate r, the expected rate of return μ_i, and the volatility σ_i, are stochastic processes, whereas W is a standard Brownian motion. The investor's wealth equation in this market is given as:

$$dy = (ry + u'B)\, dt + u'\sigma\, dW, \quad y(0) > 0, \tag{4.19.1}$$

where the elements of vector B are $\mu_i - r$ and the rows of matrix σ are σ_i, $i = 1, ..., n$. The vector u is the investor's trading strategy, with its element u_i representing the amount of wealth in the i'th stock, for $i = 1, ..., n$. A basic problem in *optimal investment* is how to choose the trading strategy u so that the wealth y *tracks* in a certain best possible (optimal) way a desired benchmark trajectory. This is an example of an optimal stochastic control problem. One of its first solutions was given in [4] in the setting of constant coefficients r, B, and σ; a particular benchmark process, such as an exponential growth; and an infinite-horizon cost functional through which the quadratic tracking error is minimised. More recently, in [2] we have considered a more general market model where all coefficients can be random and possibly unbounded. The problem was formulated as a stochastic linear-quadratic (LQ) control problem with possibly unbounded coefficients and its solution was obtained by the completion of squares method. The solution turned out to be an affine tracking-error feedback control law the coefficients of which are determined by a pair of *linear* backward stochastic differential equations (BSDEs). Although our result in [2] is rather general, it does exclude the well-known *Hull-White* interest rate model (and its special cases of the *Vasicek* model, *Ho-Lee* model, and *Merton* model) the equation of which is:

$$dr = (\alpha r + \beta)dt + \gamma' dW, \quad r(0) > 0,$$

where α, β, γ are some given functions.

In this paper, we consider the problem of optimally tracking a general stochastic financial benchmark in the formulated incomplete market with the interest rate process r following the Hull-White model. The financial benchmark process is:

$$dx = x_1\, dt + x_2'\, dW, \quad x(0) > 0, \tag{4.19.2}$$

where x_1 and x_2 are given processes. The optimality criterion that we use is the terminal quadratic tracking error, and this leads to the following *optimal financial benchmark tracking problem*:

$$\begin{cases} \min\limits_{u(\cdot)\in\mathcal{A}} \mathbb{E}\big[(y(T)-x(T))^2\big] \\ \text{s.t. (4.19.1) and (4.19.2),} \end{cases} \tag{4.19.3}$$

for some suitable admissible set of controls $\mathcal{A}$. This renders the formulated optimization problem an example of a stochastic LQ control problem with random and possibly unbounded coefficients. In order to state its solution, consider the BSDE:

$$\begin{cases} dp = p_1 dt + p_2' dW, \ \ p(T) = 0 \quad a.s., \\ p_1 := -\dfrac{p}{h}\big[\dot{h} + hq\beta + \dfrac{1}{2}h\, q^2\gamma'\gamma + hr(\dot{q}+\alpha q)\big] - [2(rx - x_1) + pr] + h\, q\, \gamma'(-2x_2 + p_2) \\ +(B' + q\gamma'\sigma')(\sigma\sigma')^{-1}\big(-2x_2'\sigma' + p_2'\sigma' + p(B' + q\gamma'\sigma')\big), \end{cases} \tag{4.19.4}$$

with h and q being solutions to certain ordinary differential equations. Let the control process u^*, which is of a tracking-error $y-x$ affine feedback form, be defined as:

$$u^*(t) := -\tfrac{1}{2}\big(\sigma\sigma'\big)^{-1}\big[(y-x)\,(2B' + 2q\gamma'\sigma') + \big(-2x_2'\sigma' + p_2'\sigma' + p(B' + q\gamma'\sigma')\big)\big]', \quad t\in[0,T].$$

Result 1 *If $u^*(\cdot)\in\mathcal{A}$, then u^* is the unique solution to problem* (4.19.3).

Idea of the proof: We use the completion of squares-method to find the solution. This involves finding sufficient conditions for the solvability of equation (4.19.4), which is with unbounded coefficients, and the integrability of certain processes. We have drawn ideas from our recent papers [1], [2], [3]. This is an interesting case of a stochastic LQ control problem that does not require Riccati BSDE.

References

[1] M. Algoulity and B. Gashi, Optimal regulator for a class of nonlinear stochastic systems with random coefficients, *E. J. of Control*, (2023) 100844.

[2] M. Algoulity and B. Gashi, Optimal financial benchmark tracking in a market with unbounded random coefficients *Proceedings of the 8th International Conference on Control, Decision, and Information Technologies (CoDIT'23)*, (2023), 2241-2246.

[3] M. Algoulity and B. Gashi, Indefinite optimal regulator for a class of nonlinear stochastic systems with random coefficients, *IFAC-PapersOnLine*, 58 (2024), 139-144

[4] D. Yao, S. Zhang and X. Zhou, Tracking a financial benchmark using a few assets, *Operations Research*, 54 (2006), 232-246.

4.20 Noura Alhouiti: Scalar and Holomorphic Bisectional Curvatures for Pointwise Hemi-slant Submanifolds of Complex Space Forms

Noura Alhouiti
Department of Basic Sciences, University Collage of Haqel, University of Tabuk, Saudi Arabia.

Abstract

In the present article, we examine the scalar and holomorphic bisectional curvatures for pointwise hemi-slant submanifolds of complex space forms. We provide a general example of pointwise hemi-slant submanifold in the Euclidean space. Then, we give these submanifolds a characterization. Moreover, we compute the Ricci tensor, scalar curvature and bisectional curvature.

Introduction

A significant class of submanifolds of almost Hermitian manifold is the class of pointwise slant submanifolds were examined by B.-Y. Chen and O. J. Garay in [1]. Since then, numerous geometers have investigated these submanifolds in different structures such as [2, 3, 5]. After that, the idea of pointwise hemi-slant submanifolds was appeared in [4, 6].

In this paper, we focus on scalar and holomorphic bisectional curvatures for pointwise hemi-slant submanifolds of complex space forms.

Pointwise hemi-slant submanifolds of a complex space form

Let $\tilde{M}(c)$ be a complex space form and M a submanifold of $\tilde{M}(c)$. Then, M is said to be a *pointwise hemi-slant submanifold* if it admits $\mathcal{D}^\theta$ and $\mathcal{D}^\perp$ as orthogonal distributions such that:

(i) The orthogonal direct decomposition $TM = \mathcal{D}^\theta \oplus \mathcal{D}^\perp$ is admissible in the tangent space TM.

(ii) With slant function θ, the distribution $\mathcal{D}^\theta$ is pointwise slant.

(iii) The distribution $\mathcal{D}^\perp$ is a totally real.

Now, we present some findings for this submanifold as follows:

Theorem 1 For any complex space form $\tilde{M}(c)$, let M be a pointwise hemi-slant submanifold of $\tilde{M}(c)$, such that $c \neq 0$. If the second fundamental form h is parallel, then, M is either CR or totally real submanifold of $\tilde{M}$.

Theorem 2 For any complex space form $\tilde{M}(c)$, let M be a pointwise hemi-slant submanifold of $\tilde{M}(c)$, such that $c \neq 0$. If the curvature tensor $R^\perp$ of the normal connection $\nabla^\perp$ vanishes identically and $A_\xi A_{f\xi} = A_{f\xi} A_\xi$, for any $\xi \in \Gamma(T^\perp M)$. Therefore, M is totally real submanifold of $\tilde{M}$.

Theorem 3 For any complex space form $\tilde{M}(c)$, let M be a pointwise hemi-slant submanifold of $\tilde{M}(c)$. Then, we have the Ricci tensor S of M as follows:

$$S(X,W) = \frac{c}{4}\Big\{n + 6\cos^2\theta\Big\}\, g(X,W) + n\, g(\sigma(X,W), \vec{H}) - \sum_{r=1}^{n} g(\sigma(X,e_r), \sigma(e_r,W)),$$

for every $X, W \in \Gamma(TM)$, where $n = 2p + q$ for $2p = dim(\mathcal{D}^\theta)$ and $q = dim(\mathcal{D}^\perp)$.

From this theorem, we conclude the following corollary.

Corollary 4 For any complex space form $\tilde{M}(c)$, let M be a totally umbilical pointwise hemi-slant submanifold of $\tilde{M}(c)$. Then, the Ricci tensor S of M satisfies

$$S(X,W)=\frac{c}{4}\Big\{n+6\cos^2\theta\Big\}\,g(X,W),$$

for every $X,W\in\Gamma(TM)$.

Theorem 5 For any complex space form $\tilde{M}(c)$, let M be a pointwise hemi-slant submanifold of $\tilde{M}(c)$. Then, the scalar curvature τ of M is given by

$$\tau=\frac{c}{4}\,n(n+6\cos^2\theta)+n^2\|\vec{H}\|^2-\|\sigma\|^2.$$

The above theorem immediately leads to the following corollary.

Corollary 6 For any complex space form $\tilde{M}(c)$, let M be a totally umbilical pointwise hemi-slant submanifold of $\tilde{M}(c)$. Subsequently, M, the scalar curvature τ of M fulfills

$$\tau=\frac{c}{4}\,n(n+6\cos^2\theta).$$

Theorem 7 For any complex space form $\tilde{M}(c)$, let M be a pointwise hemi-slant submanifold of $\tilde{M}(c)$. Then, for any unit vectors $X\in\Gamma(D^\theta)$ and $Z\in\Gamma(D^\perp)$, the holomorphic bisectional curvature $H_B(X,Z)$ of (X,Z) on M is given by

$$H_B(X,Z)=-2\Big(\|h(X,Z)\|^2+g(J\nabla_{JX}Z,\nabla_XZ)\Big).$$

References

[1] B.-Y. Chen and O. J. Garay: Pointwise slant submanifolds in almost Hermitian manifolds, *Turk. J. Math*, **36** (2012), 630-640.

[2] M. Gulbahar, E. Kilic, S.S. Celik: Special proper pointwise slant surfaces of a locally product Riemannian manifold, *Turk. J. Math*, **39** (2015), 884-899.

[3] S. Kumar and R. Prasad: Pointwise slant submersions from Sasakian manifolds, *J. Math. Comput . Sci*, **8** (2018), 454-466.

[4] M. F. Naghi, M. S. Stankovic and F. Alghamdi: Chen's improved inequality for pointwise hemi-slant warped products in Kaehler manifolds, *Filomat* , **34** (2020), 807–814.

[5] S. Uddin and A. H. Alkhaldi: Pointwise slant submanifolds and their warped products in Sasakian manifolds, *Filomat* , **32** (2018), 4131-4142.

[6] S. Uddin and M.S. Stankovic: Warped product submanifolds of Kaehler manifolds with pointwise slant fiber, *Filomat*, **32** (2018), 35-44.

4.21 Nuha Alasmi: Optimal investment in a multi-stock market with borrowing and unbounded random coefficients

Nuha Alasmi[1,2,*] and **Bujar Gashi**[1]

[1]Department of Mathematical Sciences, The University of Liverpool, UK
[2]Department of Mathematics, The University of Jeddah, Jeddah, KSA
Emails:N.Alasmi@liverpool.ac.uk; Bujar.Gashi@liverpool.ac.uk.

Abstract

We consider the problem of optimal investment in a multi-stock market with borrowing, unbounded random coefficients, and the power utility from terminal wealth. The resulting optimization problem, is a multi-input stochastic optimal control problem with a nonlinear system dynamics and unbounded random coefficients. A certain multi-dimensional *piece-wise* completion of squares method and a linear backward stochastic differential equation are used to find an explicit closed-form solution as a linear state-feedback control, the gain of which can have up to *five* different regimes.

* **Lead presenter**

Consider a market of a bond with price B and n stocks with prices $S_i, \ \ i = 1, ..., n$, that are solutions to following equations:

$$dB = Brdt, \quad B(0) > 0; \quad dS_i = S_i(\mu_i dt + \sigma_i' dW), \quad S_i(0) > 0, \quad i = 1, ..., n.$$

Here r is the bond interest rate, μ_i and σ_i are the appreciation rate and volatility of the i'th stock, and W is a d-dimensional standard Brownian motion. If R is the borrowing interest rate, then the wealth equation of an investor in this market is given as:

$$dy = \left(ry + u'a - b[u'\mathbf{1} - y]^+\right) dt + u'\sigma dW, \quad y(0) > 0, \tag{4.21.1}$$

where $a := [\mu_1 - r, ..., \mu_n - r]'$, $b := R - r$, $\mathbf{1}$ is an n-dimensional vector of ones, u is the trading strategy with its i'th element representing the amount of wealth in the i'th stock, $[u'\mathbf{1} - y]^+ := \max[0, u'\mathbf{1} - y]$, and σ is the volatility matrix with σ_i' as its i'th row. The market coefficients r, a, b, and σ are stochastic processes in general and possibly *unbounded*. The *optimal investment problem* in this market with *power* utility from terminal wealth is the following optimal stochastic control problem:

$$\begin{cases} \min\limits_{u(\cdot)\in\mathcal{A}} -\dfrac{1}{\gamma}\mathbb{E}\left[y^\gamma(T)\right], \\ \\ \text{s.t. } (4.21.1). \end{cases} \tag{4.21.2}$$

where $\gamma \in (0, 1)$, and $\mathcal{A}$ is a suitable admissible set of controls. The first solution to problem (4.21.2) was given in [6] under the assumption of complete market, i. e. $n = d$, and deterministic coefficients. More recently, there has been an increasing interest in the more realistic case of markets with random and possibly unbounded coefficients (see, e. g., our recent works [1]- [5], and the references therein). These recent works have focused exclusively in the market with a single stock, i.e. the case with $n = 1$, and have left open the problem in multi-stock market .

In this paper, we derive an explicit closed-form solution to the problem (4.21.2) for a class of multi-stock markets. The derivation now is more involved and it turns out to be of a linear state-feedback form with up to *five* different regimes (as compared to only three different regimes when $n = 1$). In order to state this solution, we first introduce the following processes: $\xi := (1-\gamma)\sigma\sigma'$, $\bar{f} := \alpha_1'\xi\alpha_1$, $\underline{f} := (\alpha_1' a - \alpha_1'\xi\alpha_0)$, where $\alpha_0' := [1 \quad 0 \quad \ldots \quad 0]$ is n-dimensional, and $\alpha_1' := [-\mathbf{1}_{n-1} \quad I_{n-1}]$ with $\mathbf{1}_{n-1}$ being an $(n-1)$-dimensional vector of ones and I_{n-1} an $(n-1)$-dimensional identity matrix. Further let: $g_1 := -0.5a'\xi^{-1}a$; $g_2 := -0.5(a-b\mathbf{1})'\xi^{-1}(a-b\mathbf{1}) - b$; $h_1 := (\xi^{-1}a)'\mathbf{1}$; $h_2 := (\xi^{-1}a - \xi^{-1}b)'\mathbf{1}$; $k_1 := \xi^{-1}a$; $k_2 := \xi^{-1}(a-b\mathbf{1})$, $k_3 := \alpha_0 + \bar{f}^{-1}\underline{f}'$, and

$$\Gamma := \begin{cases} k_1 & \text{if } h_1 \leq 1 \text{ and } h_2 \leq 1, \\ k_1 & \text{if } g_1 \leq g_2,\ \ h_1 \leq 1 \text{ and } h_2 > 1, \\ k_2 & \text{if } g_1 > g_2,\ h_1 \leq 1, \text{ and } h_2 > 1, \\ k_2 & \text{if } h_1 > 1, \text{ and } h_2 > 1, \\ k_3 & \text{if } h_1 > 1 \text{ and } h_2 \leq 1, \end{cases}$$

Result 1 *If $u^* := \Gamma y$ is an element of $\mathcal{A}$, then u^* is the unique solution to problem (4.21.2).*

Idea of the proof: We develop a certain multi-dimensional piece-wise completion of squares method, combined with the theory of linear backward stochastic differential equations with unbounded coefficients, to prove Result 1. Our approach borrows several ideas from [1]- [5], which require a considerable generalisation.

References

[1] N. Alasmi and B. Gashi, Optimal investment in a market with borrowing and combined interest rate, *Proceedings of the 9th International Conference on Control, Decision, and Information Technologies (CoDIT'23)*, (2023), 2550-2555.

[2] N. Alasmi and B. Gashi, Optimal investment in a market with borrowing, unbounded random coefficients, and a random time-horizon, *Proceedings of the 2024 UKACC 14th International Conference on Control (CONTROL)*, (2024), 248-253.

[3] N. Alasmi and B. Gashi, Optimal investment in a market with borrowing and the Heston volatility model, *Proceedings of the 9th International Conference on Control, Decision, and Information Technologies (CoDIT'24)*, (2024), 848-853.

[4] N. Alasmi and B. Gashi, Optimal investment in a market with borrowing, quadratic-affine interest rates, and Heston stochastic volatility, *Memorias del Congreso Nacional de Control Automático*, 7 (2024), 262-267.

[5] N. Alasmi and B. Gashi, Optimal Investment in a Market with Borrowing, the CIR Interest Rate Model, and the Heston Volatility Model, *IFAC-PapersOnLine*, 58 (2024), 55-60.

[6] J. Cvitanić and I. Karatzas, Convex duality in constrained portfolio optimization, *The Annals of Applied Probability*, 2 (1992), 767-818.

4.22 Rahaf Al-Zammam: Sequential Tests Based on F-Distribution for Detecting Active Effects in Unreplicated Two-Level Factorial Designs

A.A.Al-Shiha[1] and **R.A.Al-Zammam**[2]
[1]Department of Mathematics and Sciences, Prince Sultan University, Saudi Arabia
[2]Department of Statistics and O.R ,King Saud University, Saudi Arabia

Abstract

This paper presents a novel methodology in the field of non-replicated factor analysis for detecting active effects, which are of great importance in various scientific and practical applications. Factorial experiments play a crucial role in many research areas, as they allow researchers to determine which factors significantly influence outcomes. However, in unreplicated designs, distinguishing between active and inactive effects is a challenging task, particularly when error variance estimation is required. Traditional methods, such as Lenth's approach, have been widely used to detect active effects, relying heavily on the assumption that most effects are inactive and can be used to estimate the experimental error variance(Sparsity Assumption) However, these assumptions may not always hold, leading to inaccuracies in detecting significant effects.

The primary objective of this paper is to introduce a more reliable, systematic, and effective methodology that outperforms Lenth's well-established approach. The proposed method eliminates the need for error variance estimation, which is a key limitation in existing methods. Instead, it leverages the F-distribution for significance testing, ensuring robustness and increased accuracy in identifying active effects under various experimental conditions. The method is particularly useful in scenarios where the assumption of rare active effects does not hold, making it a valuable tool for researchers working with non-recursive factor experiments This paper aims to achieve several key objectives.

1. Independence from the Sparsity Assumption making it suitable for handling dense or complex data. This contrasts with traditional models, which heavily depend on this assumption.

2. Straightforward and uncomplicated implementation mechanisms, making it easy to understand and apply even for non-specialists.

3. The test does not require the estimation of error variance, which reduces computational complexities associated with data analysis and enhances efficiency and speed.

4. The test is built on the statistical F-distribution, which improves result accuracy and facilitates its application in practical statistics.

5. The test can utilize existing traditional tables for critical values of the F-distribution, eliminating the need to create new tables and providing additional ease of application.

To validate the proposed methodology, an extensive Monte Carlo simulation study was conducted using the R programming language. This simulation evaluated test size and statistical power, comparing the accuracy and effectiveness of the proposed method against Lenth's approach. Various scenarios were analyzed, including different significance levels, varying sample sizes, and diverse active effect values, to ensure a comprehensive evaluation. The results, presented through figures clearly illustrate the superiority of the proposed method in all tested conditions. Additionally, three applications were analyzed to assess the practical relevance of the proposed method. In each case, both the proposed method and Lenth's method were applied to detect active effects, and the results were compared. The findings demonstrated that the proposed method consistently provided more accurate and reliable results, confirming its potential for use in diverse research and industrial settings. The conclusion of this paper summarizes the key findings from the theoretical analysis, simulation study, and practical applications. The results strongly support the effectiveness of the proposed methodology and its advantages over existing techniques. By eliminating the need for error variance estimation, the proposed method simplifies factorial analysis while maintaining statistical rigor and accuracy. this research contributes to the advancement of statistical methodologies in experimental analysis, offering a more reliable and robust alternative to traditional methods for detecting active effects in non-recursive factorial experiments.

Result (1)
Suppose that $y_1, y_2, \ldots, y_m$ are independent, and $y_i \sim N(\mu_i, \tau^2)$; $i = 1, 2, \ldots, m$, in other words:

$$\boldsymbol{y} = \begin{pmatrix} y_1 \\ \vdots \\ y_m \end{pmatrix} \sim MVN(\boldsymbol{\mu}, \tau^2 I) \quad \text{where} \quad \boldsymbol{\mu} = \begin{pmatrix} \mu_1 \\ \vdots \\ \mu_m \end{pmatrix}$$

then:

1. $Q_j = \frac{(y_j - \mu_j)^2}{\tau^2} \sim \chi^2_{(1)}, \quad j = 1, 2, \ldots, m \quad \big(Q_j = Q_j(\boldsymbol{y})\big)$
2. $Q_j^* = \sum_{\substack{i=1 \\ i \neq j}}^{m} Q_i \sim \chi^2_{(m-1)}, \quad j = 1, 2, \ldots, m \quad \big(Q_j^* = Q_j(\boldsymbol{y})\big)$
3. Q_j and Q_j^* are independent
4. $F_j = \frac{Q_j}{Q_j^*/(m-1)} \sim F(1, m-1)$

Result (2)
Consider the random variables mentioned in Result (1), we need to test the following null hypothesis and alternative hypothesis:

$$H_0\colon \mu_1 = \mu_2 = \cdots = \mu_m = 0 \quad \Leftrightarrow \quad \boldsymbol{\mu} = \mathbf{0}$$

$$H_1\colon \mu_k \neq 0, \text{ for some } i \quad \Leftrightarrow \quad \boldsymbol{\mu} \neq \mathbf{0}$$

Under H_0, we have $\mathbf{y} \sim MVN(\mathbf{0}, \tau^2 I)$, and hence we have the following:

1. $Q_j = \frac{y_j^2}{\tau^2} \sim \chi^2_{(1)}$.
2. $Q_j^* \sim \chi^2_{(m-1)}$.
3. Q_j and Q_j^* are independent.
4. $F_j = \frac{Q_j}{Q_j^*/(m-1)} \sim F(1, m-1)$.

Therefore, we reject H_0 at a significance level α if:

$$F_j > F_{\alpha/2}(1, m-1) \quad \text{or} \quad F_j < F_{1-\alpha/2}(1, m-1)$$

for at least one j.
For example, for $j = 1$ and under H_0, we have:

$$F_1 = \frac{y_1^2}{\sum_{i=2}^{m} y_i^2/(m-1)} \sim F(1, m-1).$$

The proofs of Result (1) and Result (2) are straightforward.

References

[1] G. E. P. Box and R. D. Meyer: An analysis for unreplicated fractional factorials, *Technometrics*, **28** (1986), 11-18.

[2] M. Hamada and N. Balakrishnan: Analyzing unreplicated factorial experiments: A review with some new proposal, *Statistica Sinica*, **8** (1998), 1-41.

[3] R. V. Lenth: Quick and easy analysis of unreplicated factorials, *Technometrics*, **31** (1989), 469-473.

[4] T. M. Loughin and W. Noble: A permutation test for effects in an unreplicated factorial design, *Technometrics*, **39** (1997), 180-190.

[5] P. D. Haaland and M. A. O'Connell: Inference for effect-saturated fractional factorials, *Technometrics*, **37** (1995), 82-93.

[6] A. A. Al-Shiha and S. S. Yang: A multistage procedure for detecting significant effects in unreplicated factorial designs, *Biometrical Journal*, **41** (1999), 659-670.

[7] M. A. F. Aboukalam and A. A. Al-Shiha: A robust analysis for unreplicated factorial experiments, *Computational Statistics and Data Analysis*, **36** (2001), 31-46.

[8] F. Aboukalam: More on quick analysis of unreplicated factorial designs avoiding shrinkage and inflation deficiencies, *International Journal of Reliability and Applications*, **7** (2006), 167-175.

[9] D. C. Montgomery: *Design and Analysis of Experiments*, 9th Edition, Wiley, 2017, pp. 1, 12-40.

[10] A. A. Al-Shiha and M. A. F. Aboukalam: Quick and easy analysis of unreplicated factorial designs avoiding shrinkage deficiency, *Journal of Statistical Theory and Applications*, **6** (2007), 35-43.

[11] F. Aboukalam, M. Alharbi, and M. Ishaq Bhatti: Improved approximation scales for unreplicated factorial experiments, *Journal of Statistical Theory and Applications*, **21** (2022), 200-216.

4.23 Shreen El-Sapa: Effect of slippage on a translational motion of two interacting non-concentric spheres squeezed by couple stress fluid

Shreen El-Sapa[1] Noura S. Alsedais [2]

[1]Department of Mathematics and Computer Science, Faculty of Science, Damanhour University, Damanhour, Egypt
[2]Department of Mathematical Sciences, College of Science, Princess Nourah bint Abdulrahman University, 11671 Riyadh, Saudi Arabia.

Abstract

This study investigates the behavior of couple stress fluid that occupies the space between two non-concentric spheres under slippage conditions. The research is innovative in its application of velocity slip conditions to the sphere surfaces. Additionally, the spheres translate axially at various linear speeds. The solutions are derived semi-analytically using a superposition method combined with a numerical collocation approach, specifically at low Reynolds numbers. This paper also examines the hydrodynamic drag force that the fluid exerts on the internal particle.

4.23.1 Introduction

The paper addresses the limitations of traditional nonpolar fluids in modeling fluid dynamics with suspended particles, leading to increased interest in polar fluids, particularly Stokes' couple stress fluid. This type of fluid is significant for various industrial applications, such as crude oil extraction and cooling processes, due to its unique length-dependent properties. Previous research has investigated different flow scenarios involving couple stress fluids and highlighted the importance of slip conditions, which challenge the conventional no-slip boundary assumption [1]- [3].

4.23.2 Field equations and mathematical formulation

The steady motion of an incompressible couple stress liquid are dictated by [1]:

$$u_{i,j} = 0,\ \mu u_{i,jj} - \eta u_{i,jjkk} - p_{,i} = 0, \tag{1}$$

$$\omega_i = \frac{1}{2} e_{ijk} u_{k,j}. \tag{2}$$

Here, the constant μ is the fluid viscosity, η is the viscosity of 1st couple stress, u_i is the velocity of the fluid, and p is the fluid pressure. Furthermore, boundary conditions on the surfaces of the spheres $r_j = a_j,\ j = 1, 2$:

1. **Slippage restriction**: $\beta_j \left(u_{r_j} - U_j \cos\theta_j\right) = 0,\ \beta_j \left(u_{\theta_j} + U_j \sin\theta_j\right) = \tau_{r_j\theta_j}$,
   where β_j is the slippage parameter changing its values from zero to infinity.

2. **No couple stresses**: $m_{ij} n_i = 0$ on
   where n_i is the unit normal to the surface of the solid sphere.

In addition, the vorticity and velocity vectors are shown by $\vec{u} = (u_r(r,\theta), u_\theta(r,\theta), 0), \vec{\omega} = (0, 0, \omega_\phi(r,\theta))$. Eliminating the pressure from (1) leads to the partial differential equation:

$$E^4 \left(E^2 - \kappa^2\right) \psi = 0, \tag{3}$$

where the material constant is defined as $\kappa = \sqrt{\frac{a^2\mu}{\eta}}$. The solution of (3) obtained as:

$$\psi = \sum_{n=2}^{\infty} \left[A_n r^{-n+1} + B_n r^{-n+1/3} + C_n \sqrt{r} K_{n-\frac{1}{2}}(kr) \right] \operatorname*{Im}_n(\zeta), \tag{4}$$

where $K_n(.)$ is the modified Bessel function of the second kind, and $\mathrm{Im}_n(\zeta)$ denotes the Gagenbauer functions. We get the velocity components from this relations $u_r = -\frac{1}{r^2 \sin\theta}\frac{\partial\psi}{\partial\theta}, u_\theta = \frac{1}{r\sin\theta}\frac{\partial\psi}{\partial r}$.
The tangential stress can be obtained from this relation:

$$\tau_{r\theta} = \mu \left[\frac{1}{r}\frac{\partial u_r}{\partial r} - \frac{u_\theta}{r} + \frac{\partial u_\theta}{\partial r} \right] - 2\eta \left[\frac{\partial^2 \omega_\phi}{\partial r^2} + \frac{2}{r}\frac{\partial \omega_\phi}{\partial r} + \left(\frac{1}{r^2}\frac{\partial^2}{\partial \theta^2} + \cot\theta \frac{\partial}{\partial\theta} - \csc^2\theta \right) \omega_\phi \right] \tag{5}$$

4.23.3 Results

Slippage parameters: Perfect and partial slippage increase the normalized drag force compared to no-slip conditions [3], especially as interatomic forces between solid and liquid rise.

Size ratio: As the size ratio $\frac{a_1}{a_2}$ approaches 0.99, the normalized drag force increases, indicating that larger size discrepancies enhance drag, with convergence of drag values observed at higher ratios.

Size ratio: As the size ratio $\frac{a_1}{a_2}$ approaches 0.99, the normalized drag force increases, indicating that larger size discrepancies enhance drag, with convergence of drag values observed at higher ratios.

Velocity ratio: Increasing the velocity ratio $\frac{U_2}{U_1}$ generally decreases the normalized drag force, highlighting the importance of relative speeds in fluid dynamics between the spheres.

Couple Stress Parameters: Increasing the first couple stress parameter significantly raises the drag force, indicating its strong influence on fluid behavior. In contrast, an increase in the second couple stress parameter tends to lower the drag force.

References

[1] V.K. Stokes: Couple stresses in fluid. *Physics of Fluids*, 1966, 9: p. 1709-1715.

[2] H. Ramkissoon: Drag in couple stress fluids, *ZAMP*, 29, 341–346 (1978).

[3] N. S. Alsudais, S. El-Sapa, and E. A. Ashmawy: "Stokes flow of an incompressible couple stress fluid confined between two eccentric spheres", *Eur. J. Mech. B. Fluids*, 91, 244–252 (2021).

4.24 Maha Helmi: Approximate model for the propagation of surface waves on a coated cylindrical half-space with imperfect interface and Winkler-Fuss load

Maha M. Helmi

Department of Mathematics and Statistics, College of Science, Taif University, P.O. Box 11099, Taif 21944, Saudi Arabia. Email: m.hlmi@tu.edu.sa

Abstract

In the present communication, we show how elastic surface waves propagate on a coated cylindrical half-space by deriving an approximate equation of anti-plane motion through the application of the asymptotic approximation method; the untapped asymptotic approximation techniques that derive the consequential effective boundary conditions have been deployed. The coated structure was assumed to have generalized imperfect conditions on its interface of the coating and half-space layers, while at the same time endowed with a Winkler-Fuss elastic foundation on the coating medium, serving as a shearing mechanical loading. Comparatively, the derived approximate results have been noted to agree with the corresponding analytical results, which comprise both the displacements, stresses and the resultant dispersion relations. Moreover, some realistic contrast setups have been analyzed in the end.

Keywords: Anti-plane shear motion, coated half-space, cylindrical composites, imperfect interface, elastic foundations, asymptotic analysis.

4.24.1 Introduction

Propagation of surface waves on elastic structures and composites is an important phenomenon of contemporary interest. The recent development in modern structures and materials has triggered vast interest from the research community to propose optimal models and methods for perfect implementation and analysis, respectively. Mathematically, various researchers have both recently and long ago modeled the propagation of surface waves in composite and multilayered media [1, 2], including the interaction of multilayered media with the imposed mechanical loads that are exerted externally [3, 4], and the on the other hand, the vast relevance of siding contact conditions presumed on the interfaces of the multilayered structures, the so-called imperfect interfacial conditions [5]. Certainly, these two phenomena of elastic foundations and imperfect interface between layers have been extensively examined in relation to elastic structures that appear mostly in rectangular coordinate systems, with a few studies concerning structures in cylindrical and spherical coordinate settings. Moreover, the importance of elastic foundations in supporting the geometrical configuration of elastic structures can never be overemphasized. For this season, the literature is full of various considerations and proposals of several elastic foundations, with the view to attaining perfect structural dynamics.

4.24.2 Problem formulation

This study considers the anti-plane shear motion in a cylindrical coordinate system such as the displacement fields take the following setting: $u_r = 0$, $u_\theta = u(r, z, t)$ and $u_z = 0$, where r is the radius of the cylinder, z is the azimuthal variable, while t is the temporal variable. Further, with the consideration of a coated cylindrical half-space, see Figure 1, the equation of anti-plane shear motion in the respective layers is presided over by the following out-of-plane displacement field.

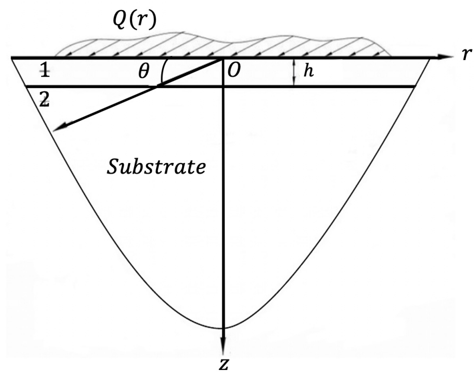

$$\tau^p_{r\theta,r} + \tau^p_{\theta z,z} + \frac{2}{r}\tau^p_{r\theta} = \rho_p \frac{\partial^2 u_p}{\partial t^2}, \qquad p = 1, 2, \tag{4.24.1}$$

where u_p are the out-of-plane displacement fields in the coating $(0 \leq z \leq h)$ when $p = 1$, and the half-space $(h \leq z < \infty)$ when $p = 2$; h is a finite thickness. In addition, $\tau_{r\theta}$ and $\tau^p_{\theta z}$ are the related shear stresses expressed as follows

$$\tau^p_{r\theta} = \mu_p \left(\frac{\partial u_p}{\partial r} - \frac{u_p}{r} \right), \qquad \text{and} \qquad \tau^p_{\theta z} = \mu_p \frac{\partial u_p}{\partial z}, \qquad p = 1, 2, \tag{4.24.2}$$

where μ_p for $p = 1, 2$ are the material constants in the layers of the coated cylinder, while ρ_p are the corresponding densities in the layers.
Boundary conditions: At $z = 0$, we have a mechanical load P as follows $\tau^1_{\theta z} = -P, \quad \text{at} \quad z = 0.$ Certainly, upon considering the load to be due to Winkler-Fuss elastic foundation, P then takes the following expression [4] $P = \chi u_1$, where χ is the rigidity of the Winkler-Fuss elastic foundation. Moreover, when $\chi = 0$, the loading reduces to that of the known case of traction-free surface condition. Moreover, as $z \to \infty$, we imposed a boundedness condition at infinity as follows: $u_2 \to 0, \quad \text{as} \quad z \to \infty.$
Imperfect interfacial conditions: The interface between the coating and the half-space is at $z = h$. Thus, the following generalized sliding contact conditions are considered [5]

$$u_1 - u_2 = \psi \tau^2_{\theta z}, \qquad \tau^1_{\theta z} = \tau^2_{\theta z}, \qquad \text{at} \quad z = h, \tag{4.24.3}$$

where $\psi \neq 0$ is the imperfect interface (sliding contact) parameter; besides, one gets perfect interface when $\psi = 0$.

To solve the governing model, one first re-write (4.24.1) using the constitutive relations in (4.24.2) as follows

$$\frac{\partial^2 u_p}{\partial r^2} + \frac{1}{r}\frac{\partial u_p}{\partial r} - \frac{u_p}{r^2} + \frac{\partial^2 u_p}{\partial z^2} = \frac{1}{c_p^2}\frac{\partial^2 u_p}{\partial t^2}, \qquad p = 1, 2 \tag{4.24.4}$$

where $c_p = \sqrt{\frac{\mu_p}{\rho_p}}$ for $p = 1, 2$, are the shear speeds in the respective layers.

Next, Eq. (4.24.4) features the Bessel differential equation of order one in the radial r, a harmonic wave solution of the following form:

$$u_p(r, z, t) = V_p(z) J_1(kr) e^{i\omega t}, \qquad p = 1, 2 \tag{4.24.5}$$

where k is the dimensional wavenumber, $J_1(.)$ is the Bessel function of the first kind of order one, ω is the angular frequency, while i is the imaginary unit.

Accordingly upon utilizing Eq. (4.24.5) in Eq. (4.24.4), the following reduced differential equations are thus obtained

$$\frac{d^2V_p}{dz^2} - \alpha_p^2 V_p = 0, \qquad \alpha_p = \sqrt{k^2 - \frac{\omega^2}{c_p^2}}, \qquad p = 1, 2 \tag{4.24.6}$$

which then yield the following respective displacement fields in the governing layers of the coated body

$$\begin{aligned} u_1(r, z, t) =& (A_1 \cosh(\alpha_1 z) + B_1 \sinh(\alpha_1 z)) J_1(kr) e^{i\omega t}, \quad 0 \leq z \leq h, \\ u_2(r, z, t) =& A_2 J_1(kr) e^{-\alpha_2 z + i\omega t}, \qquad\qquad\qquad\qquad h \leq z < \infty, \end{aligned} \tag{4.24.7}$$

where A_1, B_1 and A_2 are constants to be determined, while $B_2 \to 0$ as $z \to \infty$.

Accordingly, with the utilization of the imposed boundary and interfacial conditions in Eqs. (**??**)-(4.24.3), the respective exact solutions in Eq. (4.24.7) thus yields the following exact dimensionless dispersion relation

$$\left(\mu \left(\xi_2 \Psi - 1\right) \xi_1^2 + \xi_2 X\right) \tanh\left(\xi_1\right) = \xi_1 \left(\left(\mu X \Psi + 1\right)\xi_2 - \mu X\right), \tag{4.24.8}$$

where

$$\xi_1 = \sqrt{K^2 - \Omega^2}, \quad \xi_2 = \sqrt{K^2 - \mho^2 \Omega^2}, \tag{4.24.9}$$

with

$$K = kh, \quad \Omega = \frac{\omega h}{c_1}, \quad \mho = \frac{c_1}{c_2}, \quad \Psi = \frac{\psi \mu_2}{h}, \quad X = \frac{\chi h}{\mu_1}, \tag{4.24.10}$$

where K is the dimensionless wavenumber, Ω is the dimensionless frequency, $\mho$ is the dimensionless speed ratio, Ψ is the dimensionless sliding or imperfect contact parameter, while X is the dimensionless stiffness of the Winkler-Fuss load; moreover, the rigidity ratio and density ratio are expressed as follows $\mu = \frac{\mu_1}{\mu_2}$, and $\rho = \frac{\rho_1}{\rho_2}$, respectively.

References

[1] M.H. Helmi, S. Althobaiti, A.M. Mubaraki, G.A. Rogerson. Asymptotic formulations of anti-plane problems in pre-stressed compressible elastic laminates. *Open Phys.* **21**, 20220265 (2023).

[2] A.M. Mubaraki, F.M. Almalki. Surface waves on a coated homogeneous half-space under the effects of external forces. *Symmetry*, **14**, 2241 (2022).

[3] F. Ebrahimi, A. Seyfi. A wave propagation study for porous metal foam beams resting on an elastic foundation. Waves Random *Complex Media.* **31** (2021) 1-15.

[4] B. Erbas, J. Kaplunov, A. Nobili, G. Kilic. Dispersion of elastic waves in a layer interacting with a Winkler foundation. *J. Acoust Soc. Am.* **144** (2018), 2918–2925.

[5] R.I. Nuruddeen, A.M. Mubaraki. Propagation of damped SH waves on nonhomogeneous elastic composites involving viscoelasticity, generalized interface, rotation and mechanical loading. *Ain Shams Eng. J.* **15** (2024), 103053

4.25 Ibrahim Shaaban: Fractional Differential-Integral Inequalities and Their Applications in Medicine: A Mathematical Model for Cancer Treatment

Ibrahim Mohammed Shaaban
Department of Basic Sciences Common, First Year Deanship, King Saud University, Saudi Arabia.

Abstract

Fractional differential-integral inequalities provide a framework for modeling complex biological systems characterized by memory and hereditary properties. This research addresses their application in medicine, focusing on cancer dynamics. We propose a model based on a fractional inequality to describe tumor growth and treatment, incorporating immune response and therapeutic interventions. The stability of the model is analyzed theoretically, and numerical simulations confirm its effectiveness, highlighting the advantages of fractional calculus in understanding and optimizing cancer therapies.
* **Lead presenter**

4.25.1 Introduction

Mathematical models play a crucial role in understanding biological systems and designing effective treatments. Traditional differential equations often fail to capture the complexities of biological processes involving memory effects. Fractional calculus, with its nonlocal derivatives and integrals, offers a powerful alternative. This study explores fractional differential-integral inequalities and their applications in modeling cancer dynamics, aiming to provide deeper insights into tumor growth and therapeutic strategies.

4.25.2 Fundamental Concepts

Fractional Calculus Fractional calculus extends the concept of derivatives and integrals to non-integer orders, enabling the modeling of systems with memory and hereditary properties. The two primary definitions used in this study are:

Caputo Derivative:

$$D_t^{\alpha} f(t) = \frac{1}{\Gamma(n-\alpha)} \int_0^t \frac{f^{(n)}(\tau)}{(t-\tau)^{\alpha-n+1}} d\tau, \qquad n-1 < \alpha \leq n. \tag{4.25.1}$$

Riemann-Liouville Derivative:

$${}_0D_t^{\alpha} f(t) = \frac{1}{\Gamma(n-\alpha)} \frac{d^n}{dt^n} \int_0^t \frac{f(\tau)}{(t-\tau)^{\alpha-n+1}} d\tau, \qquad n-1 < \alpha \leq n. \tag{4.25.2}$$

4.25.3 Fractional Differential-Integral Inequalities

Fractional differential-integral inequalities involve fractional derivatives and integrals, providing a versatile tool for analyzing dynamic systems. These inequalities describe relationships between various states of a system, often capturing intricate dependencies more accurately than classical counterparts. A general form of such inequalities can be expressed as:

$$D_t^{\alpha} x(t) \leq f\left(t, x(t), D_t^{\beta} x(t)\right), \qquad 0 < \alpha, \beta \leq 1. \tag{4.25.3}$$

where f is a given function that encapsulates the system's dynamics. These inequalities are particularly useful in ensuring boundedness, stability, and convergence of solutions in complex systems.

4.25.4 Application to Cancer Dynamics

Model Formulation The proposed model represents tumor growth, immune response, and treatment effects using a fractional differential-integral inequality:

$$D_t^{\alpha} x(t) \leq -ax(t) + bx^n(t) - cu(t). \tag{4.25.4}$$

- D_t^{α} : Fractional derivative of order α.
- $x(t)$: Tumor size at time t.
- $u(t)$: Treatment effect (e.g., chemotherapy, immunotherapy).
- Constants a, b, c : Represent biological interactions.
- n : Exponent reflecting tumor growth dynamics.

This inequality ensures that the tumor size dynamics remain bounded under specific treatment protocols, reflecting realistic biological constraints.

4.25.5 Results

- Graphical Analysis: The results demonstrate tumor dynamics under different treatment scenarios, constrained by a fractional inequality.
- Effect of Fractional Order: The parameter α significantly influences the system's memory and response properties, while the inequality ensures realistic bounds on tumor growth.
- Numerical Results: Simulations show that the proposed model accurately predicts tumor size chang over time, particularly when initial conditions and biological parameters are adjusted.
- Therapeutic Effectiveness: Results confirm that therapeutic interventions, such as chemotherapy an immunotherapy, substantially reduce tumor growth rates, especially when parameters a, b, c are carefully chosen.
- Parameter Effects: The model reveals that increasing b reflects nonlinear interactions among canceı cells, while decreasing a lowers initial growth rates.
  Practical Application: The model can be used to design personalized treatment protocols based on patient-specific biological characteristics.

References

[1] Podlubny, I.: Fractional Differential Equations, *Academic Press*, 1999.

[2] Magin, R. L.: Fractional Calculus in Bioengineering, *Begell House*, 2006.

[3] Mainardi, F.: Fractional Calculus and Waves in Linear Viscoelasticity House, *Imperial College Press*, 2010.

[4] George A.: Anastassiou Fractional Differentiation Inequalities, *University of Memphis*.

4.26 Reemah Alhuzally: On a Two–Dimensional Dirichlet Type Problem for a Linear Hyperbolic Equation of Fourth Order

Tariel Kiguradze [1] and **Reemah Alhuzally**[2,*]
[1]Florida Institute of Technology, Melbourne, USA, e-mail: tkigurad@fit.edu
[2]Department of Mathematics, Faculty of Science, Al-Baha University, Al-Baha, Saudi Arabia; ralhothali@bu.edu.sa

Abstract

A linear hyperbolic equation of fourth order a Dirichlet type boundary problem in an orthogonally convex domain is investigated. Sharp sufficient conditions guaranteeing solvability and well–posedness of the problem under consideration are established.

* **Lead presenter**

4.27 Sami Alabiad: Full classification of a class of finite local rings of length 5

Sami Alabiad and **Alhanouf Ali Alhomaidhi**
Department of Mathematics, College of Science, King Saud University

Abstract

This talk aims to explore finite local rings characterized by the established invariants p, n, m, l, and k, where p denotes a prime number. We offer a detailed characterization of Frobenius local rings with length $l = 5$ and $t = 3, 5$, where t denotes the index of nilpotency of the maximal ideal. The significance of Frobenius rings is evident in coding theory, as it has been shown that two famous theorems by MacWilliams–the Extension Theorem and the MacWilliams identities–are relevant not only to finite fields but also to finite Frobenius rings. Consequently, we categorize and enumerate Frobenius local rings of order p^{5m} for $t = 3, 5$, delineating their characteristics in relation to diverse values of n.

*__Lead Presenter__

Result 1: The number of Frobenius local rings of length 5 with invariants p, n, m, k and index of nilpotency $t = 5$ is given in the following table:

Table 6: Numbers of chain rings of length 5 and of order p^{5m}.

Char (R) $= p^n$	**Number of Non-Isomorphic Classes**
$n = 1$	1
$n = 2$ and $i_p = 3$	$\begin{cases} \begin{cases} 3, & \text{if } p \equiv 1 \pmod 3, \\ 1, & \text{if } p \not\equiv 1 \pmod 3, \ (p \neq 3), \end{cases} \\ \frac{1}{m} \sum_{i=0}^{m-1} 3^{(i,m)}, \quad \text{if } p = 3 \end{cases}$
$n = 2$ and $i_p = 4$	$\begin{cases} \begin{cases} \frac{2(2m-1)}{m}, & \text{if } p^m \equiv 3 \pmod 4, \\ \frac{4}{m} \sum_{i=0}^{m-1} (p^i - 1, 4), & \text{if } p^m \equiv 1 \pmod 4, \ (p \neq 2), \end{cases} \\ 1, \quad \text{if } p = 2 \end{cases}$
$n = 3$	$\begin{cases} 2, & \text{if } p \neq 2, \\ \frac{1}{m} \sum_{i=0}^{m-1} 2^{(i,m)}, & \text{if } p = 2 \end{cases}$
$n = 4$	0
$n = 5$	1

Idea of the proof: The proof is executed by examining all possible relationships among the elements of the minimal generating set of the maximal ideal over the primary subring for $n = 1, 2, 3, 4$, and 5.

Result 2: The number of Frobenius local rings of length 5 with invariants p, n, m, k and index of nilpotency $t = 3$ is

$$N = \begin{cases} 16, & \text{if } p = 2, \\ 17, & \text{if } p \neq 2. \end{cases}$$

Idea of the proof: The result is demonstrated by examining two cases: (i) $p = 2$; (ii) $p \neq 2$. We identify all potential relationships between the generators of the maximal ideal over the coefficient subring where $n = 1, 2$, and 3.

References

[1] S. Alabiad, A.A. Alhomaidhi, N.A. Alsarori: MacWilliams identities and generator matrices for linear codes over $\frac{\mathbb{Z}_{p^4}[u]}{\langle u^2 - p^3\beta, pu\rangle}$, *Axioms*, **13** (2024), 552.

[2] S. Alabiad, A.A. Alhomaidhi, N.A. Alsarori: On linear codes over finite singleton local rings, *Mathematics*, **12** (2024), 1099.

[3] S. Alabiad, Y. Alkhamees: On classification of finite commutative chain rings, *AIMS Mathematics*, **7** (2021), 1742–1757.

[4] B. Corbas, G. Williams: Rings of order p^5 Part II. *Local Rings J. Algebra*, **231** (2000), 691–704.

4.28 Sarah Aljohani: New Developments in $\mathscr{F}_c$-Contractions and Fixed-Circle Theorems in Metric-Like Spaces

Sarah Aljohani Department of Mathematics and Sciences Prince Sultan University Saudi Arabia
sjohani@psu.edu.sa

Abstract

This study investigates fixed-circle theorems within the context of metric-like spaces, utilizing methods developed by Cirić-type, Hardy-Rogers, Reich, and Chatterjea. We introduce a novel class of $\mathscr{F}_c$-contractions, providing a deeper understanding of circular symmetries in metric-like spaces. Through practical examples, we demonstrate the versatility and potential applications of these contractions. Furthermore, we explore the role of discontinuous self-mappings that maintain fixed circles, offering new insights into mappings with discontinuities. This work not only advances theoretical understanding but also lays the groundwork for future applications in fields such as robotics and economic modeling, where such mathematical structures can be utilized for optimization and stability analysis.

* **Lead presenter**

Let (Y, δ) be a metric space and S be an $\mathscr{F}_c$ with $w_0 \in Y$. Define the number σ by

$\sigma = \min\{\delta(w, Sw) : w \neq Sw\}(1)$

If there exist $t > 0$, $F \in \mathbb{F}$, and $w_0 \in Y$, such that for all $w \in Y$:

$$\delta(w, Sw) > 0 \Rightarrow t + F(\delta(w, Sw)) \leq F(m(w, w_0)),$$

where

$$\begin{aligned} m(w, w_0) \;\; = \;\; \max \Big\{ & |\delta(w, w_0) - \delta(w_0, w_0)|, \delta(w, Sw), \delta(w_0, Sw_0), \\ & \frac{1}{2}\left[|\delta(w, Sw_0) - \delta(w_0, w_0)| + |\delta(w_0, Sw) - \delta(w_0, w_0)|\right] \Big\}. \end{aligned}$$

then S is said to be a **C-type $\mathscr{F}_c$-contraction**.

If there exist $t > 0$, $F \in \mathscr{F}$, and $w_0 \in Y$, such that for all $w \in Y$, the following holds: $\delta(w, Sw) > 0$, implies

$$\begin{aligned} t + F(\delta(w, Sw)) \leq F \Bigg(& \alpha|\delta(w, w_0) - \delta(w_0, w_0)| + \beta\delta(w, Sw) + \gamma\delta(w_0, Sw_0) \\ & + \zeta|\delta(w, Sw_0) - \delta(w_0, w_0)| + \eta|\delta(w_0, Sw) - \delta(w_0, w_0)| \Bigg), \end{aligned}$$

where

$$\alpha + \beta + \gamma + \zeta + \eta = 1, \quad \alpha, \beta, \gamma, \zeta, \eta \geq 0, \quad \alpha \neq 0,$$

then S is said to be a Hardy-Rogers type (H-R-type) $\mathscr{F}_c$-contraction on Y.

If there exist $t > 0$, $F \in \mathscr{F}$, and $w_0 \in Y$, such that for all $w \in Y$ the following holds: $\delta(w, Sw) > 0$, implies

$$t + F(\delta(w, Sw)) \leq F\left(\alpha|\delta(w, w_0) - \delta(w_0, w_0)| + \beta\delta(w, Sw) + \gamma\delta(w_0, Sw_0)\right),$$

where

$$\alpha + \beta + \gamma < 1 \quad \text{and} \quad \alpha, \beta, \gamma \geq 0,$$

then S is said to be a R- type $\mathscr{F}_c$-contraction on Y.

Result 1 If $\delta(w_0, w_0) \leq \sigma$, then $C_{w_0,\sigma}$ is a fixed circle of S. In particular, S fixes every disc $D_{w_0,\sigma}$.

Result 2 If S is a C-type $\mathscr{F} - c$-contraction on a metric-like space (Y, δ) with $w_0 \in Y$ and $\delta(w_0, w_0) \leq \sigma$, where σ is defined as in (1), then S fixes the point w_0.

Result 3 If S is a H-R-type F_c-contraction with $w_0 \in Y$ and $\delta(w_0, w_0) \leq \sigma$, then we have $Sw_0 = w_0$.

Result 4 If a self-mapping S on Y is a R-type $\mathscr{F}_c$-contraction with $w_0 \in Y$, σ is defined as in (1) and $\delta(w_0, w_0) \leq \sigma$, then we have $Sw_0 = w_0$.

References

[1] Özgür, N.Y., Taş, N. Some Fixed-Circle Theorems on Metric Spaces. Bull. Malays. Math. Sci. Soc. 42, 1433–1449 (2019).

[2] Taş N, Özgür NY, Mlaiki N. New Types of Fc-Contractions and the Fixed-Circle Problem. Mathematics. 2018; 6(10):188.

[3] Mlaiki, Nabil, Özgür, Nihal ,Tas, Nihal. (2021). New fixed-circle results related to Fc-contractive and Fc-expanding mappings on metric spaces. 10.48550/arXiv.2101.10770.

[4] Taş, N. Özgür, N. Y. (2024). Application to Activation Functions through Fixed-Circle Results with Symmetric Contractions. Symmetry, 16(1), 69.

[5] Mlaiki, N., Özgür, N. Y., Taş, N. (2023). On the Fixed Circle Problem on Metric Spaces and Related Results. Axioms, 12(4), 401.

[6] Saipara, P., Khammahawong, K.,Kumam, P. (2019). Fixed-point theorem for a generalized almost Hardy-Rogers-type F contraction on metric-like spaces. Mathematical Methods in the Applied Sciences, 42(17), 5898–5919.

[7] Tomar, A., Joshi, M., Padaliya, S. K. (2022). Relation theoretic contractions and their applications in b-metric like spaces. Journal of Applied Analysis, 28(2), 295–309.

4.29 Abdessatar Souissi: Matrix Product States as Observations of Entangled Hidden Markov Models

Abdessatar Souissi University of Monastir, Tunisia, s.abdessattar.souissi@ipest.rnu.tn.

Abstract

This paper reveals the intrinsic structure of Matrix Product States (MPS) by establishing their deep connection to entangled hidden Markov models (EHMMs). It is demonstrated that a significant class of MPS can be derived as the outcomes of EHMMs, showcasing their underlying quantum correlations. Additionally, a lower bound is derived for the relative entropy between the EHMM-observation process and the corresponding MPS, providing a quantitative measure of their informational divergence. Conversely, it is shown that every MPS is naturally associated with an EHMM, further highlighting the interplay between these frameworks. These results are supported by illustrative examples from quantum information, emphasizing their importance in understanding entanglement, quantum correlations, and tensor network representations.

This paper [1] establishes a fundamental connection between Matrix Product States (MPS) [6, 7] and Entangled Hidden Markov Models (EHMMs) [5], a subclass of Hidden Quantum Markov Models (HQMMs) [2–4]. EHMMs describe entangled stochastic processes, where MPS arise as partial observations of an underlying entangled Markov chain. This connection is formalized through the following results.

Theorem 4.29.1 *Let an EHMM be defined by the triplet $(\pi_1, (V_H^{[n]})_n, (V_O^{[n]})_n)$, where π_1 is the initial state, $V_H^{[n]}$ are unistochastic hidden partial isometries, and $V_O^{[n]}$ are observation partial isometries.*

For any $N \in \mathbb{N}$, the MPS generated by matrices $A_k^{[n]} = (a_{k;ij}^{[n]})$ with entries

$$a_{k;ij}^{[n]} = U_{ij}^{[n]} \chi_i^{[n]}(k) \tag{4.29.1}$$

can be expressed as a partial measurement of the EHMM state $|\Psi_{H,O;n}\rangle$ with respect to the vector $E_{N,n}$:

$$\left\langle \Psi_{H,O;n} \mid E_{N,n} \right\rangle = \sum_{k_1,\dots,k_N} \mathrm{Tr}(A_{k_1}^{[1]} \cdots A_{k_N}^{[N]})\, |k_1 k_2 \cdots k_N\rangle, \quad \forall n \geq N. \tag{4.29.2}$$

Additionally, the MPS tensors satisfy the gauge condition:

$$\sum_k A_k^{[n]} A_k^{[n]\,\dagger} = 1\!\!1_m. \tag{4.29.3}$$

This result establishes that a broad class of MPS with periodic boundary conditions can be rigorously derived from EHMMs, revealing a structured relationship between tensor network states and entangled quantum processes.

Theorem 4.29.2 *Under the notations and assumptions of Theorem 4.29.1, let $\rho_N = \frac{1}{m}|\psi_N\rangle\langle\psi_N|$ represent the density operators of the MPS and $\rho_{O;N}$ denote the observation density matrix. The relative entropy between these density operators satisfies the following inequality:*

$$S(\rho_N \| \rho_{O;N}) \geq \frac{1}{m} \sum_{k_1,\dots,k_N} \left| \mathrm{Tr}\left(A_{k_1}^{[1]} \cdots A_{k_N}^{[N]}\right) \right|^2 \log \left(\frac{\left| \mathrm{Tr}\left(A_{k_1}^{[1]} \cdots A_{k_N}^{[N]}\right)\right|^2}{m^{3/2} \pi^\dagger \left(\prod_{\ell=1}^N \left| A_{k_\ell}^{[\ell]} \right|_\diamond^2 \right) e} \right) \tag{4.29.4}$$

Here, $|A_{k_\ell}^{[\ell]}|_\diamond^2 = A_{k_\ell}^{[\ell]} \diamond \overline{A_{k_\ell}^{[\ell]}}$, $\pi^\dagger$ is an initial state and $e = \frac{1}{\sqrt{m}} \sum_j e_j$, and the summation spans all possible sequences $k_1, \dots, k_N$.

Theorem 4.29.2 establishes a lower bound on the relative entropy between the MPS and its corresponding observation state and provides a measure of their distinguishability and entanglement.

These results highlight the deep interplay between HQMMs and tensor network states, offering new insights into quantum correlations and their applications in quantum information theory.

References

[1] Souissi, A., 2025. Matrix Product States as Observations of Entangled Hidden Markov Models. arXiv preprint arXiv:2502.12641.

[2] Accardi L., Souissi A., Soueidy E. G., Quantum Markov chains: A unification approach, *Inf. Dim. Analysis, Quantum Probab. Related Topics* **23**(2020), 2050016.

[3] Accardi L, Soueidi EG, Lu YG, Souissi A. Algebraic Hidden Processes and Hidden Markov Processes. Infin Dimens Anal Quantum Probab Relat Top 2024.

[4] Accardi L, Soueidi EG, Lu YG, Souissi A. Hidden Quantum Markov processes. Infin Dimens Anal Quantum Probab Relat Top 2024.

[5] Souissi, A., 2023. Entangled Hidden Markov Models. Chaos, Solitons & Fractals, 174, p.113804.

[6] Movassagh, R., Schenker, J. An Ergodic Theorem for Quantum Processes with Applications to Matrix Product States. Commun. Math. Phys. 395, 1175–1196 (2022).

[7] Verstraete F, Murg V and Cirac J I 2008 Matrix product states, projected entangled pair states, and variational renormalization group methods for quantum spin systems, Advances in physics 57(2) 143-224

4.30 Sumayyah Alabdulhadi: Numerical investigation of thermal radiation, slip and chemical reaction effects on MHD mixed convection stagnation point flow through porous medium past an inclined plate

Sumayyah Alabdulhadi[1], **Anuar Ishak**[2] and **Iskandar Waini[3]**
[1]Department of Mathematics,
Faculty of Science, Qassim University,
Qassim 52571, Saudi Arabia
[2]Department of Mathematical Sciences,
Faculty of Science and Technology, Universiti Kebangsaan Malaysia, 43600 UKM Bangi, Selangor, Malaysia
[3]Fakulti Teknologi Kejuruteraan Mekanikal dan Pembuatan, Universiti Teknikal Malaysia Melaka, Hang Tuah Jaya, Durian Tunggal 76100, Melaka, Malaysia.

Abstract

This paper investigates the thermal radiation effects, slip as well as chemical reactions with respect to the magnetohydrodynamic (MHD) mixed convection flow of a viscous fluid as an outcome of an inclined plate in a porous medium. The effects of various parameters with respect to the temperature, velocity, as well as concentration profiles together with the local Nusselt number, skin friction coefficient and local Sherwood number are illustrated. The results illustrated that the rise in the thermal radiation parameter and the heat generation/absorption parameter raise the temperature profile. Meanwhile, the rise in the chemical reaction parameter and Schmidt number reduces the concentration profile. Furthermore, it is revealed that the temperature and concentration profiles rise with a rise in the value of the inclination angle parameter. Apart from that, an opposite trend is noticed concerning the velocity profile. The findings also indicated that the skin friction coefficient and local Sherwood and Nusselt numbers in the assisting flow region are noticeably reduced by the increment in the inclination angle parameter. We contrasted our results to previously published research to assess their validity and discovered a substantial agreement.

* **Lead presenter**

Numerous research studies have employed flat plates in both horizontal and vertical positions. In contrast, there has been little attention on the inclined flat plate. However, no study has so far been reported about the analysis of the MHD mixed convection stagnation point flow towards an inclined plate with slip, chemical reaction, and radiation effects. Therefore, we have demonstrated our interest in this work to make an effort to discuss this new case. The current study aims to expand the paper conducted by Niranjan et al. [1] and Alabdulhadi et al. [2],by considering the inclination angle. By using the proper similarity transformations, a set of nonlinear ordinary differential equations (ODEs) is isolated from the governing system of partial differential equations (PDEs). The resulting system of equations is computed numerically using the MATLAB software's bvp4c boundary value problem solver. Examined and discussed are the effects of various physical variables on the skin friction coefficient, local Nusselt and Sherwood numbers, velocity, temperature, and concentration profiles.

The magnetohydrodynamic (MHD) mixed convection stagnation point flow, heat, as well as mass transfer produced by an inclined plate in a porous medium with consideration of slip, radiation, as well as chemical reaction are studied. With the aid of MATLAB software's bvp4c solver, the numerical findings were achieved. Thus, the major findings of the present research are as below:
Result 1 The velocity profile $f'(\eta)$ rises for greater values of R_d and Q. Nevertheless, it displays the opposite attitude for different values of Cr and Sc.

Result 2 The $\theta(\eta)$ and $\phi(\eta)$ increase while the $f'(\eta)$ decreases by increasing the inclination angle parameter ω, whereas a totally different trend is observed for the case of K.

Result 3 Both skin friction coefficient and mass transfer experience an increment with the rise in Q, while the heat transfer acts in the opposite behavior.

Result 4 The enhancement in the inclination angle parameter ω remarkably reduces the values of $Re_x^{1/2}C_f$, $Re_x^{-1/2}Nu_x$ and $Re_x^{-1/2}Sh_x$ in the assisting flow region.

References

[1] Niranjan, H.; Sivasankaran, S.; Bhuvaneswari, M. Chemical reaction, Soret and Dufour effects on MHD mixed convection stagnation point flow with radiation and slip condition., *Sci. Iran.*, 2017, 24, 698–706.

[2] Alabdulhadi, S.; Waini, I.; Ahmed, S.E.; Ishak, A. Hybrid Nanofluid Flow and Heat Transfer Past an Inclined Surface. *Mathematics*, 2021, 9, 3176.

4.31 Suraiya Mahmood: Addition of Endomorphisms

Suraiya J. Mahmood
Retired, United Kingdom

Background

It is a well known fact that pointwise addition is not defined on the endomorphisms of a non abelian group. H. Neuman [5], gave an example of a non abelian group with a special addition $\oplus$ defined on its semigroup of endomorphisms, which is different from pointwise addition. But even though the maps are written on the left of the argument, it becomes a left nearring and the group is its left module.

Inspired by this example, Frolich [2] developed a method of defining a special addition on special subsets of $End(G)$, for non abelian groups using a generating subset of G. He called the generating set a basis and addition a free addition. He proved the following result:

Let $(G, +)$ be a non abelian group. Then

1. If a non empty subset $\mathcal{H}$ of $End(G)$ has a basis B an addition $\oplus_B$is defined on $\mathcal{H}$ as $(\alpha \oplus_B \beta)(x) = \alpha(x) + \beta(x)$, $\forall\ \alpha, \beta \in \mathcal{H}$ and $\forall\ x \in B$. He called $\oplus_B$free addition.
2. If $\mathcal{H}$ is a subsemigroup of $(End(G), \circ)$ with basis B then $(\mathcal{H}\ ,\oplus_B, \circ)$ is a nearring and G is a $\mathcal{H}-$module.

Grainger [3] generalized this concept further. He used a subset X of G, not necessarily a generating set and defined an addition on a special subset $\mathcal{H}$ of $End(G)$, denoted by $\oplus_X$. He called this subset X a support system for $\mathcal{H}$. He also generalized results of Frolich for this concept.

The following is an interesting and useful result by Grainger.

If $\mathcal{H}$ is a subsemigroup of $(End(G), \circ)$, for a group $(G, +)$, with support system X, then $(\mathcal{H},\oplus_X, \circ)$ is a left nearring and G is a left $\mathcal{H}-$ comodule.

If the free addition coincides with point wise addition then $(\mathcal{H},\oplus_X, \circ)$ is a ring and $(G, +)$ is a left $\mathcal{H}-$ nearmodule.

Anyhow he did not give any example of a non abelian group to support his results. But he suggested to look for some better examples than the example he gave of a cyclic group.

This article

In this article we study $(End(S_3), \circ)$ and $(End(D_8), \circ)$ in detail.
$S_3 = \langle a, b|3a, 2b, 2(a + b)\rangle$ and $End(S_3) = \{0, I, \alpha, \alpha^2, \beta, \alpha\beta, \alpha^2\beta, \theta_i, i = 0, 1, 2\}$.
$D_8 = \langle a, b|4a, 2b, 2(a + b)\rangle$,
$End(D_8) = \{0, I, \alpha^i, \beta, \alpha^i\beta, (i = 1, 2, 3), \theta_j, \tau_j, (j = 0, 1, 2, 3, \phi, \psi, \rho, \mu_k, \tau_k, \zeta_k, \delta_k, \nu_k, (k = 1, 2, 3, 4)\}$

Idea of Proofs

Using the action of the endomorphism on the group elements and some results, we prove the following results:

Theorem 1

Let H be a subsemigroup of $(End(S_3), \circ)$
If $\theta_i, \theta_j \in H, i \neq j, i, j \in \{0, 1, 2\}$ then H has no support system.

Theorem 2

1. The subsemigroups $\{0\}\,\{I\}\,, \{\theta_i\}\,, 0 \leq i \leq 2$,have support system $S = \{0\}$.
   $\oplus_S$ is the same as pointwise addition for $\{0\}$ and is a zero ring.

$\oplus_S$ for $\{I\}$ and $\{\theta_i\}$ is not not pointwise addition.

2. The subsemigroups $\{0, \theta_i\}, i \in \{0,1,2\}$ have support system $S = \{b\}$.

   $\oplus_S$ is the same as pointwise addition and each near ring is a field isomorphic to $\mathbb{Z}_2$.

3. The subsemigroups $\{\theta_0, I, \beta\}, \{\theta_1, I, \alpha^2\beta\}, \{\theta_2, I, \alpha\beta\}$ have support system $S = \{a\}$.

   The zeros for $\oplus_S$ is $\theta_0, \theta_1, \theta_2$ respectively and the nearring is isomorphic to $\mathbb{Z}_3$.

4. The subsemigroups $\{0, I, \alpha^i\beta\}, i \in \{0,1,2\}$ have support system $S = \{a\}$.

   $\oplus_S$ is not pointwise addition in each case but the near ring is isomorphic to $\mathbb{Z}_3$.

Remarks

1. S_3 is left nearmodule only in the case where $\oplus_S$coincides with pointwise addition. In all other cases it is a comodule.

2. As seen above the other subsemigroups do not have support system. Anyhow for $i \in \{1,2\}$,each subsemigroup $\{\theta_i, \theta_0\}$ is in 1-1 correspondence with $\mathbb{Z}_2$ with same multiplication table. This induces an addition on it $\boxplus$ making it a field and S_3 a $\mathbb{Z}_2-$ comodule.

<u>$(End(D_8), \circ)$</u>

We study $(End(D_8), \circ)$ in the same way and come up with more interseting results.
Considering the length we mention only one result. The detail will be given in the paper.

Theorem 3

The subsemigroup $H = \{0, I, \alpha^2, \beta, \alpha^2\beta, \phi, \psi, \rho\}$ of $(End(D_8), \circ)$ has a basis $B = \{a, b\}$, $\oplus_B$is not pointwise addition but it is a ring. Moreover
$(\{0, I, \alpha^2, \beta, \alpha^2\beta, \phi, \psi, \rho\}, \oplus_B) = \langle I \rangle \oplus_B \langle \rho \rangle \cong \mathbb{Z}_4 \oplus \mathbb{Z}_2$.

For easy reference we record all the findings in the form of tables.

1. Tables of action of $End(S_3)$ on $(S_3, +)$ and of $End(D_8)$ on $(D_8, +)$
2. Caley tables of $(End(S_3), \circ)$ and $(End(D_8), \circ)$
3. Detail of additions on all subsemigroup of $(End(S_3), \circ)$ and nearrings and modules we get.
4. Detail of additions on all subsemigroups of $(End(D_8), \circ)$ and nearrings and modules we get.

References

[1] Clay,J.R. Nearrings - Geneses and Applications, Oxford University Press, Oxford, 1992.

[2] Frolich, A. On groups over a d.g. nearring (I. Sum constructions and Free R-groups). Quart. J. Math. Oxford (2)(11) 1960.

[3] Granger,G. Left modules for left nearrings, Doctoral Thesis, Univ. of Arizona, 1988.

[4] Hungerford, T.W. Algebra, Springer-Verlag, New York, 1974.

[5] Neumann,H. On Varieties of groups and their associated nearrings, Math.Z.65 (1956).

4.32 Tong Mao: Integral Representations of Barron and Sobolev Spaces Via ReLU^k Activation Function and Applications

Xinliang Liu, **Tong Mao*** and **Jinchao Xu**
King Abdullah University of Science and Technology, Thuwal 23955, Saudi Arabia

Abstract

This paper establishes that nonlinear shallow neural networks with ReLU^k activation functions can achieve their optimal approximation rates even when simplified to linearized networks with fixed, preselected weights and biases. This key result challenges the prevailing belief that the flexibility of trainable parameters in neural networks is essential for superior approximation performance. Since the non-convexity of neural networks stems from the dependence on trainable weights and biases, our result allows shallow network training to be reformulated as a linear, convex problem, significantly simplifying the optimization process.

By analyzing both Sobolev and Barron function classes, we show that linearized shallow networks achieve approximation rates comparable to their nonlinear counterparts. Notably, we show that the approximation rates for Barron spaces remain intact when restricted to a Sobolev subspace of comparable complexity in terms of metric entropy.

* **Lead presenter**

In the context of shallow ReLU^k networks, a strong connection exists between Barron spaces $\mathcal{B}^k(\Omega) = \mathcal{B}^{\sigma_k}(\Omega)$ and the class of shallow networks:

1. A function f can be approximated by neural network classes $\{\Sigma_{n,M}^k\}_{n=1}^{\infty}$ if and only if $f \in \mathcal{B}^k(\Omega)$ [2].

2. The Barron space $\mathcal{B}^k(\Omega)$ has an integration form [2]

$$\mathcal{B}^k(\Omega) = \left\{ \int_{\mathbb{S}^d} \sigma_k(\theta \cdot \tilde{x}) d\mu(\theta) : \ \mu \in \mathcal{M}(\mathbb{S}^d) \right\}. \tag{4.32.1}$$

   Moreover,

$$\|f\|_{\mathcal{B}^k(\Omega)} \simeq \inf_{\mu \in \mathcal{M}(\mathbb{S}^d)} \left\{ |\mu|(\mathbb{S}^d) : \ f(x) = \int_{\mathbb{S}^d} \sigma_k(\theta \cdot \tilde{x}) d\mu(\theta) \right\}. \tag{4.32.2}$$

3. Shallow ReLU^k networks achieve the optimal approximation rate in $\mathcal{B}^k(\Omega)$ [1]:

$$\inf_{f_n \in \Sigma_{n,M}^k} \|f - f_n\|_{\mathcal{L}^2(\Omega)} = \mathcal{O}(n^{-\frac{1}{2} - \frac{2k+1}{2d}}), \tag{4.32.3}$$

   where $M \simeq \|f\|_{\mathcal{B}^k(\Omega)}$.

Given a predetermined set of parameters $\left\{\theta_j^*\right\}_{j=1}^n \subset \mathbb{S}^d$, we define the corresponding basis functions

$$\phi_j(x) = \sigma_k(\theta_j^* \cdot \tilde{x}) = \sigma_k(w_j^* \cdot x + b_j^*), \quad j = 1, \ldots, n,$$

and the finite neuron space as $L_n^k = L_n^k(\left\{\theta_j^*\right\}_{j=1}^n) = \operatorname{span}\{\phi_1, \ldots, \phi_n\}$. Define the constrained version of L_n^k as $L_{n,M}^k = \left\{ \sum_{j=1}^n a_j \phi_j : \ \left(n \sum_{j=1}^n a_j^2\right)^{\frac{1}{2}} \leq M \right\}$. By applying the Cauchy–Schwarz inequality, it follows that $L_{n,M}^k \subset \Sigma_{n,M}^k$. A key advantage of the linear spaces L_n^k and $L_{n,M}^k$ lies in their structural simplicity, which enables more efficient analysis and computation. Notably, optimization over $L_{n,M}^k$ reduces to a convex least squares problem, whereas training in $\Sigma_{n,M}^k$ generally involves solving a highly nonconvex optimization problem.

Similar to the results on ReLU^k neural networks $\Sigma_{n,M}^k$, this paper presents a novel perspective on characterizing the finite neuron space L_n^k and its constrained counterpart $L_{n,M}^k$. Under the assumption that the parameters $\{\theta_j^*\}_{j=1}^n$ form a quasi-uniform mesh over $\mathbb{S}^d$, we establish the following results:

1. A function f can be approximated by FNS $\{L_{n,M}^k\}_{n=1}^{\infty}$ if and only if $f \in \mathcal{H}^{\frac{d+2k+1}{2}}(\Omega)$;

2. The Sobolev space $\mathcal{H}^{\frac{d+2k+1}{2}}(\Omega)$ has an integration form

$$\mathcal{H}^{\frac{d+2k+1}{2}}(\Omega) = \left\{ \int_{\mathbb{S}^d} \sigma_k(\theta \cdot \tilde{x})\psi(\theta)d\theta : \ \psi \in \mathcal{L}^2(\mathbb{S}^d) \right\}.$$

   Moreover,

$$\|f\|_{\mathcal{H}^{\frac{d+2k+1}{2}}(\Omega)} \simeq \inf_{\psi \in \mathcal{L}^2(\mathbb{S}^d)} \Big\{ \|\psi\|_{\mathcal{L}^2(\mathbb{S}^d)} : f(x) = \int_{\mathbb{S}^d} \sigma_k(\theta \cdot \tilde{x})\psi(\theta)d\theta \Big\},$$

3. The FNS achieves the optimal approximation rate in $\mathcal{H}^{\frac{d+2k+1}{2}}(\Omega)$: $\inf_{f_n \in L_{n,M}^k} \|f - f_n\|_{\mathcal{L}^2(\Omega)} = \mathcal{O}(n^{-\frac{1}{2} - \frac{2k+1}{2d}})$, where $M \simeq \|f\|_{\mathcal{H}^{\frac{d+2k+1}{2}}(\Omega)}$.

Result 1 Let $d, n \in \mathbb{N}$, $k \in \mathbb{N}_0$, $\Omega \subset \mathbb{R}^d$ be a bounded domain, and $\{\theta_j^*\}_{j=1}^n = \left\{ \begin{pmatrix} w_j^* \\ b_j^* \end{pmatrix} \right\}_{j=1}^n \subset \mathbb{S}^d$ be a set of quasi-uniform points. Then for any f in the Sobolev space $\mathcal{H}^{\frac{d+2k+1}{2}}(\Omega)$, there exists $a_1, \ldots, a_n \in \mathbb{B}$ such that f can be approximated by a shallow ReLU^k neural network with these predetermined parameters as $\left\| f(x) - \sum_{j=1}^n a_j \sigma_k(w_j^* \cdot x + b_j^*) \right\|_{\mathcal{L}^2(\Omega)} \lesssim n^{-\frac{1}{2} - \frac{2k+1}{2d}} \|f\|_{\mathcal{H}^{\frac{d+2k+1}{2}}(\Omega)}$. Moreover, the parameters satisfy $\left(n \sum_{j=1}^n a_j^2 \right)^{\frac{1}{2}} \lesssim \|f\|_{\mathcal{H}^{\frac{d+2k+1}{2}}(\Omega)}$. The corresponding constants are independent of n, $\{\theta_j^*\}_{j=1}^n$, and f.

Idea of the proof: The work is still in progress. We expect to finish the whole paper before April 15.

Result 2 The Sobolev norm can be equivalently written as

$$\|f\|_{\mathcal{H}^{\frac{d+2k+1}{2}}(\Omega)} \simeq \inf_{\psi \in \mathcal{L}^2(\mathbb{S}^d)} \left\{ \|\psi\|_{\mathcal{L}^2(\mathbb{S}^d)} : \ f(x) = \int_{\mathbb{S}^d} \sigma_k(\theta \cdot \tilde{x})\psi(\theta)d\theta \right\}. \tag{4.32.4}$$

Idea of the proof: The work is still in progress. We expect to finish the whole paper before April 15.

References

[1] Jonathan W. Siegel and Jinchao Xu. Sharp bounds on the approximation rates, metric entropy, and n-widths of shallow neural networks. *Foundations of Computational Mathematics*, pages 1–57, 2022.

[2] Jonathan W. Siegel and Jinchao Xu. Characterization of the variation spaces corresponding to shallow neural networks. *Constructive Approximation*, **57**(3):1109–1132, 2023.

4.33 Muhanna A. H Alrashdi: A model for viscoelastic fluids based on logarithmic strains

Muhanna A. H Alrashdi[1] and **Giulio G. Giusteri**[2]
[1]Department of Mathematics, University of Hail, Hail 2440, Saudi Arabia
[2]Dipartimento di Matematica “Tullio Levi-Civita”, Università degli Studi di Padova, via Trieste 63, 35131, Padova, Italy.

Abstract

Viscoelastic materials are ubiquitous in industrial processes involving polymers and mixtures of macromolecules with various suspending fluids. An interest in these materials dates back to the very origin of rheological studies. We present a model for viscoelastic materials based on the observation that the microscopic arrangement of molecules determines the state at which the system would converge in the absence of applied forces. Differently from what happens for solids, this state can evolve in time as a result of deformations and stresses. We incorporate concepts originated in the theory of solid plasticity and introduce an elastically-relaxed deformation tensor. The modeling effort focuses on the evolution of the relaxed state. We take as a basic request that, if we keep the material in a static configuration, then the relaxed deformation tensor should converge to the current deformation tensor.

Within this class of models, even the simple case with constant material parameters is able to qualitatively reproduce a number of experimental observations in both simple shear and extensional flows, including linear viscoelastic properties, the rate dependence of steady-state material functions, the stress overshoot in incipient shear flows, and the difference in shear and extensional rheological curves. Furthermore, by allowing the relaxation time of the model to depend on the total strain, we can reproduce some experimental observations of the non-attainability of steady flows in uniaxial extension, and link this to a concept of polymeric jamming or effective solidification. Our framework is quite effective in reproducing experimental data of wormlike micellar solutions.

Another distinctive feature of our approach is the fundamental use of logarithmic strains, that leads to a proper generalisation to finite elastic deformations of the Maxwell model. Indeed, we can recover the upper-convected Maxwell model and the Giesekus model for the elastic stress evolution as different truncations for small elastic strains of the stress evolution implied by our model.

* **Dr. Muhanna Ali H Alrashdi**

We introduced a class of tensorial models aimed at describing viscoelastic materials [1]. The cornerstones of this framework are an elastic stress that depends logarithmically on a suitable measure of strain and the choice of letting the elastic strain evolution emerge from two distinct evolution equations, one for the current deformation and the other for a tensorial descriptor of the elastically-relaxed state. While the former is a necessary kinematic relation between velocity and deformation, the latter involves constitutive choices that are based on arguments borrowed from solid plasticity. Our line of thought differs considerably from the classical Oldroyd's approach [2,3]. Even though we can derive an equation for a quantity akin to a conformation tensor, the objective rate entering its evolution is not a matter of choice, as it descends directly from the kinematic evolution of the current deformation gradient. We stress that, in our framework, viscoelastic fluids emerge as an interpolation between purely viscous fluids and solids, controlled by a relaxation time parameter ranging from zero (viscous fluid) to infinity (viscoelastic solid).

We have shown that a simple model with constant material parameters performs very well in reproducing the behavior of viscoelastic fluids observed in rheometric experiments. Moreover, it helps understanding the origin of the difference in extensional and shear rheology and the relative importance of viscous, elastic, and plastic effects. Another important feature of this model is that it avoids the erroneous prediction of an exponential growth of the elastic stress in extensional flows that sometimes arises in connection with elastic models of neo-Hookean type.

To approach the modelling of real fluids, it is important to consider the presence of multiple relaxation times. This can be done within our framework by letting the relaxation time parameter depend on other relevant quantities. We provide a first example of what can be achieved in this way by addressing a situation in which an abrupt change in the elastic response during uniaxial extension prevents the attainment of steady flows. Our findings suggest the presence of a phenomenon that can be described as a progressive polymeric jamming, in which the relaxation time diverges due to the experiment geometry. We have also shown how to capture the rheological behaviour of wormlike micellar solutions [4] by means of a rate-dependent relaxation time. Meanwhile, we can indicate as the presence of multiple relaxation modes a challenging aspect of real fluids that may require important generalisations of our model.

References

[1] M. A. Alrashdi and G. G. Giusteri, Evolution of local relaxed states and the modelling of viscoelastic fluids, Physics of Fluids, vol. 36, no. 9, 2024.

[2] Oldroyd, J. G., On the formulation of rheological equations of state, Proceedings of the Royal Society of London. Series A. Mathematical and Physical Sciences 200, 523–541 (1950).

[3] Oldroyd, J. G., Non-Newtonian effects in steady motion of some idealized elastico- viscous liquids, Proceedings of the Royal Society of London. Series A. Mathematical and Physical Sciences 245, 278–297 (1958).

[4] Varchanis, S., Haward, S. J., Hopkins, C. C., Tsamopoulos, J. and Shen, A. Q., Evaluation of constitutive models for shear-banding wormlike micellar solutions in simple and complex flows, Journal of Non-Newtonian Fluid Mechanics 307, 104855 (2022).

4.34 Huda Al-Malki: Strong GP-continuity and weakly GP-closed functions on GPT spaces

Hanan Al-Saadi[1] and **Huda Al-Malki**[2,⋆]

[1] Department of Mathematics, Faculty of Sciences, Umm Al-Qura University, Makkah 21955, Saudi Arabia E-mail address: hsssaadi@uqu.edu.sa

[2] Department of Mathematics, Adham University College, Umm Al-Qura University, Saudi Arabia E-mail address: hmmalki@uqu.edu.sa

Abstract

In this research article, we present the procedure for generating GPT spaces in two different ways: using the generalized neighborhood system and the monotonic operator. Then, we introduce several types of generalized primal continuous functions. Some characteristics have been dissected, and the relationships among them have been studied. We use the technique of Császár, which changes the "generalized topology" to other "generalized topologies" weaker than it, to show some important results. Furthermore, we show that the notion of "strong GP-continuity" coincides with the notion of "GP-continuity" under some conditions. We present these results in a simple graph to make it easier for the reader. Finally, we study the preservation of the notions of "GP-connected" and "GP-hyperconnected" by different types of generalized primal continuous functions.

* **Lead presenter:**

Continuity has been a fundamental concept in pure mathematics, particularly in topology. A function between two topological spaces is continuous if the preimage of every open set is open. To determine whether a function is continuous, we must analyze the structure of the spaces involved. Such functions are crucial because they preserve the topological structure of the domain space within the codomain space.

This study focuses on generalized continuity under the influence of the primal set. Continuity is one of the central topics in topology, and, therefore, we explore various types of continuous functions in depth. These types have already been examined in the context of generalization theory. Here, we investigate them from the perspective of primal collection. Additionally, we examine the relationships between these functions and establish the necessary conditions for transforming weaker forms into stronger ones. The significance of continuous functions in topology lies in their essential role in preserving topological properties.

This article consists of four sections. Section 1 is divided into two parts: the first part summarizes previous studies related to this research, while the second part revisits basic definitions and fundamental theorems. In Section 2, we introduce three types of continuous functions in GPT spaces. First, we construct GPT spaces in two different ways: one using the generalized neighborhood system and the other using the monotonic operator. Then, we define GPN-continuous, GP-θ-continuous, and almost GP-continuous functions, discussing their properties and characteristics. We also examine the relationships among them and provide counterexamples. In Section 3, we introduce the concepts of "strong GP-continuous function," "strongly GP-θ-continuous function," and "super GP-continuous function" and study the relationships among them. Additionally, we present the notions of "weakly GP-closed function" and "GP-regular space," analyzing their characteristics. In Section 4, we explore the notions of "GP-connected" and "GP-hyperconnected" spaces. We then examine how different types of generalized primal continuous functions preserve these properties. **Main Results:**

Theorem: Every GPN-continuous function is GP-continuous, where $\mathfrak{g}$ is generated by the neighborhood system.

The idea of the proof relies on the fact that $\mathfrak{g}$ is generated by the neighborhood system. However, there exists a GP-continuous function induced by the neighborhood system that is not GPN-continuous. An example illustrating this is provided in the paper.

Theorem: Let $(T, \mathfrak{g}, \mathcal{P})$ and $(T^\backprime, \mathfrak{g}^\backprime, \mathcal{P}^\backprime)$ be two GPT spaces. Consider $p : T \to T^\backprime$. If $T^\backprime$ is GP-regular and strong, then the next are identical:
(i) p is a strong GP-continuous;
(ii) p is a strongly GP-θ-continuous;
(iii) p is a GP-continuous.

The proof follows consequently from the construction of minor results in the paper.

Theorem: Let $p : (T, \mathfrak{g}, \mathcal{P}) \to (T^\backprime, \mathfrak{g}^\backprime, \mathcal{P}^\backprime)$ be a contra GP-α-continuous onto function. Consider T as GP-α-connected space. Then, $T^\backprime$ is GP-connected space.

The proof shows that a contra GP-α-continuous onto function preserves GP-connectedness. That is, there do not exist non-empty disjoint $(\mathfrak{g}, \mathcal{P})$-open sets G and H such that $T = G \cup H$.

Theorem: Let $(T, \mathfrak{g}, \mathcal{P})$ be a GPT space. Then, we have:
(i) T is GP-β-connected $\Rightarrow$ GP-semi-connected $\Rightarrow$ GP-α-connected $\Rightarrow$ GP-connected.
(ii) T is GP-β-connected $\Rightarrow$ GP-pre-connected $\Rightarrow$ GP-α-connected.

The proof depends on the relationships between certain weak types of open sets that are given throughout the paper.

References

[1] S. Acharjee, M. Özkoç, and F. Issaka: Primal topological spaces, *ArXiv* 2022.

[2] A. AL-Omari, S. Acharjee, and M. Özkoç: A new operator of primal topological spaces, *ArXiv* 2022.

[3] H. Al-Saadi and H. Al-Malki: Generalized primal topological spaces, *AIMS Math.,* **8** (2023), 24162–24175.

[4] H. Al-Saadi and H. Al-Malki: Categories of open sets in generalized primal topological spaces, *Mathematics,* **12** (2024), 207.

[5] D. Jayanthi: Contra continuity on generalized topological spaces, *Acta Math. Hungar.,* **137** (2012), 263–271.